Hyperglycaemia in Experimental Glaucoma

Andreas Johannes Anton Ebneter, MD

School of Medicine

Discipline of Ophthalmology & Visual Sciences

A thesis submitted to the University of Adelaide in fulfilment of the requirements for the degree of Doctor of Philosophy

May 2011

Papers produced during the candidature (included in this thesis)

Microglial Activation in the Visual Pathway in Experimental Glaucoma: Spatiotemporal Characterization and Correlation with Axonal Injury
Ebneter A, Casson RJ, Wood JP, Chidlow G.
Investigative Ophthalmology & Visual Science. 2010 Dec;51(12):6448-60.
Impact factor*: 3.466

The optic nerve head is the site of axonal transport disruption, axonal cytoskeleton damage and putative axonal regeneration failure in a rat model of glaucoma
Chidlow G, Ebneter A, Wood JP, Casson RJ.
Acta Neuropathologica. 2011 Jun;121(6):737-51.
Impact factor*: 7.695

Protection of Retinal Ganglion Cells and the Optic Nerve During Short-term Hyperglycemia in Experimental Glaucoma
Ebneter A, Chidlow G, Wood JP, Casson RJ.
Archives of Ophthalmology. 2011 Oct; 129(10)
Impact factor*: 3.516

Comparison of fixed-pattern sampling with targeted sampling for estimation of axon counts in a rat model of glaucoma
Ebneter A, Casson RJ, Wood JP, Chidlow G.
Clinical & Experimental Ophthalmology (accepted)
Impact factor*: 1.755

Paper Presentations

Retinal Neuronal Protection Via the Crabtree Effect
RANZCO Annual General Meeting and Scientific Congress 2008 - Melbourne

Microglial Activation in the Optic Nerve and Tract in Experimental Glaucoma
RANZCO Annual General Meeting and Scientific Congress 2009 – Brisbane

Hyperglycemia is Neuroprotective in a Rat Model of Experimental Glaucoma
RANZCO Annual General Meeting and Scientific Congress 2010 – Adelaide

Posters

Microglial Activation in the Optic Nerve and Tract in a Rat Model of Experimental Glaucoma
ARVO Annual Meeting 2009 – Fort Lauderdale (FL)

Hyperglycemia is Neuroprotective in a Rat Model of Experimental Glaucoma
ARVO Annual Meeting 2010 – Fort Lauderdale (FL)

Evaluation of Axonal Regeneration in a Rat Model of Experimental Glaucoma
ARVO Annual Meeting 2011 – Fort Lauderdale (FL)

Lab Talks

Quantification of optic nerve injury
Center for Molecular Ophthalmology & Neuroscience (Jeffrey Goldberg's Lab) – May 2010
Bascom Palmer Eye Institute – Fort Lauderdale (FL)

---

* As per THOMSON REUTERS Journal Citation Reports®, Science Edition 2010

TABLE OF CONTENTS

ABSTRACT

Glaucoma refers to a family of optic neuropathies with multi-factorial aetiology. The pathogenesis of glaucoma remains unclear, but there is good evidence that the optic nerve head is involved early in the pathogenesis of the disease. Inadequate blood supply to the optic nerve head may play a role, at least in some types of glaucoma. Given that vasculopathy is a hallmark of diabetes, one would expect that diabetes might exacerbate glaucoma; however, in large epidemiological studies no clear association was found. The Ocular Hypertension Treatment Study even suggested that diabetes protected against the conversion of ocular hypertension to glaucoma. In this thesis, I attempted to investigate the effect of short-term hyperglycaemia on retinal ganglion cell death and optic nerve damage in an experimental rat model of chronic ocular hypertension, which consisted of laser photocoagulation of the trabecular meshwork.

The thesis is made up of four papers. The first paper characterises the rat model for our laboratory and validates the laser parameters used, which, in comparison to the original publication describing the model, have been slightly modified to minimise the ocular complications. A combination of histology, immunohistochemistry, Western blotting and real-time polymerase chain reaction was used to portray the spatial and temporal nature of retinal ganglion cell pathology. The data provides robust support for the hypothesis that the optic nerve head is the pivotal site of retinal ganglion cell injury, with resulting anterograde degeneration of axons and retrograde injury and death of perikarya. It was found that disruption of axonal transport occurs very soon after ocular hypertension, prior to structural damage, substantiating the hypothesis that axonal dysfunction may be an important cause of retinal ganglion cell degeneration. Moreover, as a novel finding, restricted axonal regeneration were observed at the optic nerve head.

The second and third papers address the issue of damage quantification in the optic nerve. Axon counting on semi-thin optic nerve cross-sections represents the gold standard to evaluate the extent of axonal injury. However, this method is very laborious and time consuming. In search for alternatives, I investigated the accuracy of different sampling methods to estimate optic nerve axon numbers on cross sections and the usefulness of immunohistochemical markers on longitudinal optic nerve sections. Random sampling of pictures for automated axon counting was sufficiently accurate and the microglial response proved very valuable and effective for quantification of optic nerve damage.

The thesis culminates in the fourth paper, which presents a limited reproduction of the Ocular Hypertension Treatment Study in a laboratory environment. Unilateral ocular hypertension was induced in two groups (n=26 per group) of Sprague-Dawley rats. One group remained normoglycaemic; the other was rendered hyperglycaemic by intraperitoneal injection of streptozotocin. After two weeks of elevated intraocular pressure, axonal and retinal damage were compared using the quantification methods introduced in the previous papers. There was convincing evidence for delayed axonal degeneration and retinal ganglion cell death in the hyperglycaemic rats. Axonal loss was reduced by about 50%. Survival of retinal ganglion cell somata was increased to a similar extent in hyperglycaemic rats. Hence, energy substrate availability may play a role in glaucomatous optic neuropathy. Targeted manipulation of neuronal energy metabolism may delay optic nerve degeneration and may represent a novel neuroprotective strategy for neurodegenerative diseases of the visual system such as glaucoma.

DECLARATION OF ORIGINALITY AND COPYRIGHT

This work contains no material which has been accepted for the award of any other degree or diploma in any university or other tertiary institution and, to the best of my knowledge and belief, contains no material previously published or written by another person, except where due reference has been made in the text.

I give consent to this copy of my thesis when deposited in the University Library, being made available for loan and photocopying, subject to the provisions of the Copyright Act 1968.

The author acknowledges that copyright of published works contained within this thesis (as listed below) resides with the copyright holders of those works.

I also give permission for the digital version of my thesis to be made available on the web, via the University's digital research repository, the Library catalogue, the Australasian Digital Theses Program (ADTP) and also through web search engines, unless permission has been granted by the University to restricted access for a period of time.

Andreas Ebneter
Adelaide, October 2011

The optic nerve head is the site of axonal transport disruption, axonal cytoskeleton damage and putative axonal regeneration failure in a rat model of glaucoma
Acta Neuropathologica. 2011 Jun;121(6):737-51.
Copyright holder Springer-Verlag GmbH
Rights and Permissions
Tiergartenstr. 17
D - 69121 Heidelberg, Germany
Fax: +49 6221 487 8223

Microglial Activation in the Visual Pathway in Experimental Glaucoma: Spatiotemporal Characterization and Correlation with Axonal Injury
Investigative Ophthalmology & Visual Science. 2010 Dec;51(12):6448-60.
Copyright holder The Association for Research in Vision and Ophthalmology (ARVO)
1801 Rockville Pike, Suite 400
Rockville, MD 20852-5622
Phone: +1 240 221 2900 Fax +1 240 221 0370

Protection of Retinal Ganglion Cells and the Optic Nerve During Short-term Hyperglycemia in Experimental Glaucoma
Archives of Ophthalmology. 2011 Oct
Copyright holder American Medical Association
515 North State St
Chicago, IL 60654
Phone: +1 312 464 2513 Fax: +1 312 464 5834

Comparison of fixed-pattern sampling with targeted sampling for estimation of axon counts in a rat model of glaucoma
Clinical & Experimental Ophthalmology
Copyright holder John Wiley & Sons, Ltd.
Permissions Department
The Atrium, Southern Gate
Chichester, West Sussex, PO19 8SQ
Phone: +44 1243 843356 Fax: +44 1243 770620

ACKNOWLEDGMENTS

This study was partially supported by a grant from the foundation OPOS, Switzerland. This research was also supported by funds from ORIA and NHMRC.

First and foremost I would sincerely like to thank Prof Robert Casson and Prof Dinesh Selva for allowing me to undertake my PhD in the Ophthalmic Research Laboratories of the South Australian Institute of Ophthalmology. I am deeply grateful to Prof Robert Casson, an outstanding mentor in clinical and experimental ophthalmology, for his constant support as my principal supervisor throughout the last 3 years.

To Dr. Glyn Chidlow I say thank you for his support, his honest, thorough and constructive criticism, and for sharing his outstanding knowledge in the field of experimental ophthalmology. It has been a privilege to work with you. Thank you for your expert guidance and for finding answers to so many, at first glance, puzzling observations. Unfortunately we have not yet got a chance to test our skills on the downhill run on a snowfield. To Dr. John Wood I say thank you not just for expert supervision or teaching me many valuable technical and scientific skills but also friendship.

Mark Daymon contributed incredibly to this work through his creative input and exceptional expertise in theory and practice of histological techniques. Also, you were always prepared to give me a hand with immunostaining or cutting when I was short of time. Not to forget about his worldly wisdom and the after-work beers at the Elephant Pub.

Teresa Mammone brought the laboratory back to life after a transient quiet period. I thank you for continuing the work I started and wish you the best of luck in developing it further. I am certain that you have the necessary skills and attitude to succeed.

To the entire Neuropathology Laboratory including Kathy, Cai, Bernice, Sven, Serg, Yvonne and Sophie. You made my life easier with helpful advise and the occasional chat in the tearoom. In particular I would like to thank Kathy and Cai for introducing me to the resin processing.

Special thanks go to Jim Manavis for giving me access to his fantastic range of antibodies and for letting me use the laboratory facilities, which he manages so smoothly.

I would like to offer a big thank you to all the animal house staff for looking my rats during the experiments. In particular I would like to mention Briony, Brian and Brigit who taught me a lot about animal handling and gave me invaluable insight into the behaviour of laboratory rats.

Special thank you also to Dr. Tim Kuchel, who helped us to improve the experimental procedures and supported our research team with his knowledge when we encountered difficulties.

I am very grateful to my friend Martin for his forward-looking, anticipatory and creative thinking and his invaluable mental support during the long experiments.

Levon enriched the everyday laboratory routine with his philosophical and open-minded thoughts on life and science.

Lenny. We crossed our ways on a plane between Los Angeles and Miami in difficult times.

Last but certainly not least I wish to thank my parents and brothers for their support, appreciation and inspiring guidance during all these years on this long and eventful journey.

ABBREVIATIONS

ATP	adenosine triphosphate
GLUT	glucose transport protein
HIF	hypoxia inducible factor
IOP	intraocular pressure
NMDA	N-methyl-D-aspartate
NO	nitric oxide
pO_2	oxygen partial pressure
POAG	primary open-angle glaucoma
RGC	retinal ganglion cell
ROS	reactive oxygen species
STZ	streptozotocin

1. Contextual statement and review of literature

1.1. Glaucoma and its significance

Glaucoma is a progressive neuropathy of the retinal ganglion cells (RGC) and their axons, resulting in a distinct appearance of the optic disc, characterised by cupping, and a specific pattern of visual field loss.[1] Visual loss in glaucoma is usually slow and may take decades to develop, but is irreversible. The pathophysiology and the site of the primary insult are not yet known in full detail. Nevertheless, there is consensus that glaucoma is a neurodegenerative disease[2] and RGC death occurs by apoptosis.[3] It is likely that the character of the primary insult varies because there are morphologically different types of glaucomas.[4] Nevertheless, currently, the only modifiable contributing factor is the intraocular pressure (IOP), and reduction of eye pressures remains the mainstay of treatment. The risk of progression of glaucomatous optic nerve damage increases with increasing IOP.[5, 6] However, the vulnerability to IOP-related damage varies between individuals and and a large proportion of patients with ocular hypertension never suffer loss of neuronal fibres.

1.1.1. Formal classification of glaucoma[7]

The glaucomas are classified as primary and secondary forms. Leaving aside the congenital forms of glaucoma, which present with angle dysgenesis, the primary glaucomas are further categorized as open-angle or angle-closure glaucomas, depending on the gonioscopic appearance of the angle. By far the most common type is primary open-angle glaucoma (POAG). By definition, the appearance of the angle is normal and any secondary form of glaucoma has been ruled out. The resistance to aqueous humour drainage is found at the level of the trabecular meshwork or beyond.[8] Based on their IOP level, POAG can be further subdivided into high-pressure or low-pressure. The second most common type is primary angle-closure glaucoma, which can present as acute, intermittent or chronic. Here, the peripheral iris obstructs the trabecular meshwork through apposition of the iris or peripheral anterior synechiae. The secondary glaucomas can present in a wide variety of forms, are associated with specific ophthalmological, extraocular or systemic conditions and can, based on the appearance of the angle, again be sub-classified as open- or closed-angle.

1.1.2. Optic nerve head morphology

Characteristic optic disc changes in glaucoma are as follows: thinning of neuroretinal rim, progressive cupping, asymmetric cupping, optic disc haemorrhage, retinal nerve fibre layer loss, acquired pit of the optic disc or notching.[1]

As the disease progresses, the thickness of the neuroretinal rim diminishes and the diameter of the cup increases. In many patients, thinning of the rim is most pronounced and progresses faster in the superior and inferior parts of the optic nerve, producing vertical enlargement of the cup.[9] Whereas pallor of the optic nerve head is seen in most optic neuropathies, this thinning of the neuroretinal rim, cupping, is very characteristic of glaucoma and rarely occurs in other optic nerve pathologies.

1.1.3. Field defects

Generally, glaucoma is a bilateral, but often asymmetrical, condition.[1] Only late in the disease the visual acuity is affected by glaucomatous damage and nerve fibre loss first becomes manifest in the peripheral field of vision. The regional glaucoma injury produces a specific pattern of visual field loss. Characteristic visual field changes are as follows[10]: nasal step, arcuate scotoma, paracentral scotoma, generalised depression. Paracentral scotomas are more frequent in low-tension glaucoma whereas nasal step and arcuate field defects are primarily encountered with high-pressure glaucoma.

Standard automated perimetry is most commonly used for diagnosing glaucoma and for monitoring progression;[11] however, this method is insensitive at the initial stages of glaucoma.[12] Selective perimetry, which tests specific RGC populations, identifies neuronal damage earlier.[13] A blue stimulus is presented on a yellow background in short-wavelength automated perimetry to test RGCs that target the koniocellular layer.[14] Frequency doubling perimetry is equally effective in detecting early glaucoma and tests ganglion cells that target the magnocellular layer.[15]

1.1.4. Significance of glaucoma

Glaucoma affects more than 66 million people worldwide and is the cause for bilateral blindness in at least 6.8 million individuals,[16] which makes it the second leading cause of vision loss in the world. Close to 80 million people worldwide will be affected by 2020.[17] The prevalence of glaucoma correlates with age and is approximately 0.2% in whites between 40 and 60 years of age,[18] and over 10% in Black people at 80 years of age.[5] The diagnosis of glaucoma resides on evidence of nerve fibre layer loss, which is not always easy to document and evident only relatively late in the disease, after a significant amount of neural tissue has been irreversibly damaged.[19] Hence, the number of individuals suspected of having glaucoma is far higher than the number of diagnosed cases.

1.1.5. Risk factors for POAG

The strongest recognised risk factors for the progression of POAG are IOP[6, 20, 21] and age.[18, 22-24] To date, IOP is the only modifiable risk factor.[20, 25-27] Ethnicity is another, non-modifiable risk factor.[28, 29] High myopia, thin corneas and a family history of glaucoma are significantly associated with glaucomatous optic neuropathy as well.[30-32] Another set of risk factors seems to be linked to perfusion abnormalities: systemic hypertension, cardiovascular disease, peripheral vasospasm and migraine headache.[1] However, the association of these vascular factors with development or progression of glaucoma is weaker.

Genetically, POAG is mostly of multifactorial aetiology. However, it has been estimated that in 3-4% of POAG patients the disease is associated with mutations at the GLC1A locus (myocilin gene), for which more than 43 mutations have been described.[33]

1.2. Current treatment of glaucoma

1.2.1. General Principles

The goal of glaucoma care is to preserve visual function and quality of life without causing unwanted side effects and morbidity.[7] At present, this means lowering IOP, which is the only modifiable risk factor. IOP reduction significantly improves the prognosis, but does not avoid damage in all patients.[34] Treatment modalities include topical and systemic drug therapy, laser, and incisional surgery, in order of priority. In most cases of POAG the treatment goals can be achieved with the available topical glaucoma drugs.

Management and interventions are guided by the target IOP. The target pressure is chosen arbitrarily for each patient and should be modified according to the observed progression. Following the general consensus, the initial aim is to reduce the IOP at which damage occurred by 20-50%; but target IOP and treatment should be individualised based on age, stage of glaucoma, estimated progression and life expectancy of the patient.[7] As mentioned, the target IOP is not a fixed IOP reading but should be continuously modified, based on hints for progression at the optic nerve head or in the visual fields.

The challenge for the clinician is to achieve the target IOP with the least number of substances and minimal side-effects.[7] Clinically, progression is monitored based on optic disc photographs, nerve fibre layer measurements and visual fields. Initial therapy is usually a monotherapy with a first-choice agent, commonly a prostaglandin analogue. If IOP reduction is ≥ 20% from baseline, the treatment is considered effective. If the drug is not effective, the substance should be switched within or outside the agent class. If the drug is effective but IOP reduction is not sufficient to reach the target, another substance is added. Combinations of three drugs are judged maximum medical therapy. Using a fourth topical agent has been shown not to lower IOP further and is not warranted. Aside from the option of laser treatment, incisional surgery is in general the only remaining treatment choice.[35]

1.2.2. First-choice glaucoma drug classes

The equilibrium between secretion and drainage of aqueous humour determines IOP. Aqueous is produced by the non-pigmented epithelium of the ciliary body. Interestingly, there is no such thing as hypersecretion glaucoma and aqueous humour secretion is fairly constant.[36] Without medical topical or systemic influence, equilibrium pressure is determined by the global outflow resistance. Aqueous outflow is composed of trabecular and uveoscleral outflow. Physiologically, 85-90% of drainage is via the trabecular pathway and 10-15% via the uveoscleral pathway.[37] The different substance classes of drugs act to variable extents via one or several of these mechanisms.

Prostaglandin analogues, prostamides and decosanoids reduce IOP by increasing the uveoscleral outflow. These agents supposedly activate matrix metalloproteinases which remodel the extracellular matrix of the ciliary body and reduce outflow resistance.[38] This class of drugs is generally used as the first line treatment. Application is only once a day and the systemic side-effects are minimal with great IOP lowering effect.[39]

Alpha2-adrenergic agonists diminish secretion of aqueous humour and enhance uveoscleral outflow.[40] Interestingly, brimonidine tartrate has been shown to have neuroprotective properties in animal models[41] and human clinical trials.[42] The main drawback of this drug class is an association with allergic conjunctivitis.[43]

Carbonic anhydrase inhibitors lower aqueous secretion and are the only drug class for which systemic agents are available.[44] The use of these substances in eyes with a compromised corneal endothelium can result in further deterioration of the corneal endothelium function.[45]

Beta-adrenoceptor antagonists were among the first topical agents available and are therefore still widely used. They also reduce aqueous humour secretion.[46] Their systemic absorption can cause significant cardiovascular and respiratory side effects. However, this risk is lower for the newer, more selective substances such as betaxolol. One fifth of first time beta-blockers users are non-responders.[8] Also, after long-term use of beta-blockers, reduced efficacy (tachyphylaxis)[47] can occur. Topical beta-adrenoceptor antagonists are, understandably, less effective in patients taking systemic beta-blockers.[48]

1.2.3. Second-choice drug classes

These drugs are not used as first-line agents, but may be of benefit under special circumstances. This group includes parasympatheticomimetics, non-selective adrenoceptor agonists and systemic carbonic anhydrase inhibitors.[8]

1.2.4. Laser procedures and surgical interventions

The most widely used laser treatment for glaucoma is laser trabeculoplasty.[49] Trabeculoplasty increases the aqueous humour outflow by remodelling of the trabecular meshwork resulting in decreased outflow resistance.[50] Different wavelengths have been used with similar effectiveness.[51] Initially argon laser trabeculoplasty was the most commonly used modality. Here, an argon laser beam with 50 μm spot size is aimed at the trabecular meshwork. Use of this argon laser trabeculoplasty is recommended only once because it results in significant scarring. Selective laser trabeculoplasty specifically targets pigmented cells of the trabecular meshwork, is less damaging and histologically does not result in scar formation. Selective laser trabeculoplasty can therefore be repeated.[52] Both argon laser trabeculoplasty and selective laser trabeculoplasty have good initial response rates and the magnitude of the effect corresponds approximately to that of a prostaglandin analogue.[53] Unfortunately, the effect gradually decreases over time.

If drug treatment in combination with laser treatment fails to adequately control IOP in eyes with useful visual function, surgical intervention is indicated. A filtering procedure is considered the treatment of choice in most cases. The next step after failure of this approach is tube implantation.[54]

Laser diode cyclophotocoagulation results in destruction of the ciliary body and reduction of aqueous humour secretion. Because of the risk of phthisis, it represents a last resort of treatment and is only used when medical and surgical treatment has failed.[55]

1.3. Injury hypothesis in glaucoma

There are two major hypotheses for the pathogenesis of glaucomatous optic neuropathy: a mechanical and a vascular theory.[2] However, this separation is most likely artificial and, in reality, mechanical and vascular mechanisms are intimately interconnected.[56] IOP-related mechanics determine the biomechanical situation which influences blood flow and cellular responses. Reciprocally, biomechanics are determined by the anatomy and tissue properties, both of which are in turn affected by remodelling and compositional changes.[57] Despite many decades of research, there remain many unanswered questions and the exact mechanisms have not yet been elucidated. It is likely that a multitude of insults at the optic nerve head with the same downstream effects can result in glaucomatous optic neuropathy, and the clinical picture of glaucoma represents the morphological end result of a number of distinct, different optic nerve head injuries. Hence, the mechanics behind the initial insult would differ between individuals, and so would the contribution of the mechanical and vascular component in each individual case. There might well exist other, as yet unknown, contributors to the injury.

1.3.1. Mechanical hypothesis

Glaucomatous excavation is a morphological hallmark of glaucomatous optic neuropathy. The biomechanical paradigm proposes that the phenotype of glaucomatous axon damage is determined by the configuration of IOP-related stress and strain, independent of the exact axonal injury mechanism and level of IOP.[57] From several forms of glaucomas, which are always associated with raised IOP, such as angle-closure glaucoma or secondary glaucoma, we know that increased IOP is sufficient to cause glaucomatous optic neuropathy. IOP-related forces are significant in the connective tissue of the optic nerve head, even at low IOP[58] and, according to the mechanical hypothesis, are thought to underly both optic nerve head aging and the pathophysiology of glaucomatous damage. The mechanical paradigm postulates that the primary site of IOP-related axonal damage is within the lamina cribrosa and peripapillary sclera.[59] Of note, the optic nerve head represents a discontinuity in the corneo-scleral shell[58] and discontinuities commonly cause stress concentrations in mechanical systems. IOP-induced stress, deformation and strain in these tissues eventually lead to a multitude of cellular events, which result in degeneration of RGC axons.

The stress in the corneo-scleral shell is determined by the IOP, which is slowly fluctuating diurnally,[60] and by the ocular pulse amplitude, a rapidly pulsatile component produced by the ocular, mainly choroidal, blood flow.[61] In particular the pulsating component of the wall stress carries the potential to cause fatigue with direct failure of connective tissue fibres as well as changes in connective tissue composition. Currently, data suggest that the optic nerve head of glaucomatous eyes experiences more mechanical stress than the optic nerve head of non-glaucomatous eyes.[62] Both the ocular pulse amplitude[63] and the magnitude of diurnal IOP variation are increased in glaucoma patients.[64] Changes in the biomechanical properties of the sclera will affect the forces at the optic nerve head and likely have an effect on development and progression of glaucomatous optic neuropathy.

1.3.1.1. Structure of the optic nerve head

Connective tissues, and in particular the sclera, serve as the load-bearing structure of the eye. The sclera is composed of multiple layered dense sheets of collagen.[65] The scleral structure is specially organised in a well-circumscribed area at the back of the globe, the lamina cribrosa, to provide support for the axons as they pass through the connective tissues.[66] Importantly, the

extracellular matrix structures are covered by astrocytes, which provide axons with neurotrophic factors.[67]

The principal constituents of the sclera are collagen, elastin, and glycosaminoglycans. Collagens I and III provide tensile strength to the sclera.[68] Elastin confers elastic properties as deformation and recovery,[69] which seem to be crucial given the variable character of ocular wall stress. Both human research and laboratory work in primates has found altered elastin in glaucomatous eyes,[70-75] which suggests that alterations of the surrounding connective tissues caused by elastin degradation are of relevance in the pathogenesis of glaucoma. However, it is not clear whether these changes are a result of glaucoma or actually a reason for the development of glaucoma. Of note, exfoliation syndrome is associated with polymorphisms in the lysyl oxidase-like 1 gene and the protein coded contributes to the properties of elastin.[76] In the mouse, the density of the elastin fibres has been shown to be highest in the peripapillary area where they surround the optic nerve head like a ring. With increasing distance from the optic nerve head the content of elastin in the sclera diminishes.[68] The distribution of elastin is similar in human eyes. Elastin has a very slow turnover rate and lasts many decades, but shows degenerative changes.

1.3.1.2. Biomechanics at the optic nerve head

Given the assumed significance of the optic nerve head in glaucoma, study of the biomechanics of this anatomical region, and the lamina cribrosa in particular, seems important and has attracted a lot of attention in recent years. The biomechanical properties of the peripapillary sclera and the microarchitecture of the laminar beams strongly determine the mechanical stress the cells in the lamina cribrosa are exposed to.[62] Since this region of the eye is not easily accessible in vivo for measurement of forces and deformations, modelling techniques[77, 78] have been used in combination with data from in vivo studies in primates.[57, 79, 80]

Some studies have used the displacement of the vitreoretinal interface as a surrogate marker for lamina cribrosa movement.[81, 82] However, IOP-induced movement of the optic nerve head surface may not be an appropriate parameter to measure actual lamina cribrosa deformation because of the plasticity of the overlying neural tissues. Therefore, it is of interest to quantify deformations of the connective tissues directly. However, this was hitherto not possible, because appropriate non-invasive imaging technologies were not available and the lamina cribrosa inaccessible. Modelling has therefore become an important tool for studying optic nerve head biomechanics. Analytical and numerical modelling approaches can be distinguished. For analytical models, the stresses and strains need to be represented as mathematical expressions, which requires substantial simplification. Analytical models have been used to describe and investigate ocular rigidity.[83, 84] However, because of the complexity of the geometry and the variety of tissue-determined mechanical constants, they are not suitable for the study of the optic nerve head. Numerical models have proven to be more helpful. The most popular numerical methods for tissue biomechanics are finite element analyses. They permit the computation of the response of complex structures to mechanical loading if the material properties and the geometry of the objects are established. The more complex eye-specific models were mostly determined using three-dimensional reconstructions of human and monkey eyes. Material properties were derived from human donor eyes and laboratory animals.[78, 80, 85, 86] The most important determinants of optic nerve head biomechanics are as follows: compliance of the sclera, size of the eye, IOP, compliance of the lamina cribrosa, and the thickness of the sclera.[87]

Of relevance for lamina cribrosa deformation is the translaminar pressure gradient,[88, 89] not IOP per se. The translaminar pressure gradient is equal to the difference between retrolaminar pressure and IOP. The cerebrospinal fluid pressure is supposed to be a good surrogate marker for the retrolaminar pressure.[90]

1.3.1.3. Configuration of the lamina and explanation for sectoral damage

Visual field loss in glaucoma usually manifests as a nasal step, which then progresses into an arcuate scotoma and later a complete hemi field defect. This pattern of visual field loss, together with corresponding defects of the neural rim, is pathognomonic for glaucoma.[91] Glaucomatous is the term to describe this unique pattern of optic nerve head damage involving characteristic neural and connective tissue changes. Mechanical failure and backward bowing of the lamina cribrosa is characteristic at later stages of glaucomatous optic neuropathy.[92] It is hypothesized that the explanation of the highly predictable pattern of axonal loss outlined above is explained by the structure of the lamina cribrosa and the resulting pattern of mechanical failure, independent of the level of IOP.[93] The stress distribution in load-bearing structures can be predicted. Deformation and progressive mechanical failure is ultimately dictated by the material properties. Once a portion of the lamina cribrosa mechanically fails, the forces that this portion was resisting are transferred to nearby trabeculae, which increases their load despite an unchanged level of IOP. Hence, even at a steady IOP, neighbouring trabeculae may gradually fail if the local load redistribution results in supra-threshold stress.[57] As mechanical failure progresses, the same overall IOP-induced mechanical load needs to be born by a permanently diminishing cross-sectional area. Therefore, cup progression can take place at stable or even lower IOP levels.

The morphological study of human optic nerve head cross sections has disclosed regional anatomical variations of the lamina cribrosa pores.[94] The size of the pores is larger in the superior and inferior parts of the lamina cribrosa. It has been postulated that the larger pores and less mechanical support by the connective tissue in these regions renders these areas of the lamina cribrosa more susceptible to deformation and failure secondary to mechanical stress.[95, 96] In fact, as glaucoma progresses, the normally almost round pores become more elongated and elongated pores have been related to visual field deterioration.[97, 98] Hence, the mechanical properties and susceptibility to stress of the lamina cribrosa can explain the specific patterns of visual field loss and neural rim changes in human glaucoma.[91] This finding provides strong evidence that the optic nerve head, and more specifically the lamina cribrosa, is the site of the primary axonal insult and that mechanical factors are significant contributors.

1.3.1.4. Glia and extracellular matrix

A key point to consider in the understanding of how ocular biomechanics are transduced into pathological changes are the biological pathways activated. Ultimately, several principal mechanisms might cause axon damage:[99] (1) axonal ischemia (vascular hypothesis), (2) physical compression of axons caused by the deformation of the lamina cribrosa (mechanical hypothesis), and (3) spontaneous compression mediated by tissue pressure differences through the uncompromised lamina cribrosa.[100] Regardless of the mechanism of the insult, astrocytes and glia may mediate the effects.[99]

Mechanical and other stress can influence cellular behaviour in many ways. Mechanosensitivity is common in many cell types.[101] In primary human lamina cribrosa cells subjected to cyclic stretch, a plethora of genes have been shown to be up- or downregulated,[102] including genes coding for proteins that form or modify the extracellular matrix. The stiffness of the substrate on which the cells reside has been shown to affect cell migration, proliferation and apoptosis.[103, 104] Cells continually probe the stiffness of the surrounding matrix and react to changes.[105] The composition of the extracellular matrix of the lamina cribrosa has been shown to change in glaucoma,[72, 74, 75, 106] which influences the stiffness and potentially affects the behaviour of resident lamina cribrosa cells. Active remodelling of the lamina cribrosa and peripapillary sclera has been demonstrated in experimental primate glaucoma models and illustrates that the connective tissue at the optic nerve is mechanically important.[107-109] Unconnected to these events, IOP-related strain may

compromise capillary blood flow by compression. Axonal nutrition relies on diffusion of nutrients through the basement membrane of endothelial calls and pericytes, extracellular matrix and across the basement membranes of the astrocytes, which then supply the nutrients to the axons via their processes. Age- or stress-related cellular changes and basement membrane alterations may affect diffusion even independently of capillary flow.

In summary, mechanical changes at the optic nerve head potentially trigger substantial cascades of cellular events which affect the local environment: blockage of pro-survival factors,[110] glial (astrocytes and microglia) reactivity[67, 111] with compositional changes in the extracellular matrix, and death of oligodendrocytes.[112]

1.3.2. Vascular hypothesis

Increased IOP is clearly sufficient for the development of glaucoma. However, normal pressure glaucoma represents more than 70% of cases with POAG in certain populations.[22] Moreover, ocular hypertension, that is chronically elevated IOP without evidence of optic nerve damage, is more frequent than frank glaucoma.[25] Therefore, other factors than IOP and mechanical failure must be involved in the pathogenesis of glaucomatous optic neuropathy. The vascular theory proposes that glaucomatous optic neuropathy results from insufficient perfusion secondary to either increased IOP or other pathologic changes which compromise blood supply.[2] Normal pressure glaucoma is a clinical example of a glaucomatous optic neuropathy where perfusion plays a major role in the pathogenesis. Nevertheless, lowering IOP can still be of benefit and reduce the risk of progression and optic damage.[25] These observations substantiate the concept of glaucoma as a IOP-sensitive disease, potentially influenced by many other, mostly yet unknown variables.[113]

Multiple lines of evidence suggest that ischemia-reperfusion injury at the optic nerve head due to compromised vascular circulation is a component of glaucomatous optic neuropathy.[114] To characterise blood supply, the optic nerve head is best divided into 4 zones: (1) Superficial nerve fibre layer, (2) Prelaminar portion, (3) Lamina cribrosa, and (4) Retrolaminar portion. The superficial layer of the optic nerve head receives blood supply from small branches of the central retinal artery. The prelaminar region, just anterior to the lamina cribrosa, is supplied by branches from the choroidal arterioles and the short posterior ciliary arteries.[115] The retrolaminar portion receives blood from pial vessels of the optic nerve. Venous drainage is through the central retinal vein. Interestingly, the capillaries of the optic nerve head lack blood-brain barrier properties.[116]

Retinal blood flow is characterised by auto-regulated low-flow and high extraction. Autoregulation occurs through local factors, since there is no autonomic innervation. The choroid, fed by the posterior ciliary arteries, is a non-autoregulated high-flow system with low oxygen extraction.[117] The extent of auto-regulation in the optic nerve head remains unclear. It seems to be less efficient than in the retina but better than in the choroid.[118]

Risk factors for arteriosclerosis are not closely associated with open-angle glaucoma, and arteriosclerosis does not seem to be a major contributor to perfusion disturbances at the optic nerve head. Rather, there is evidence that vascular dysregulation and insufficient autoregulation is the main pathology.[119] Increased levels of circulating endothelin-1 go along with increased sensitivity to IOP-mediated damage at the optic nerve head due to impaired autoregulation.[120-126] Also, it has been shown that progression in patients with vasospastic syndrome is more closely related to IOP than in non-vasospastic glaucoma patients.[127]

1.4. Animal models of glaucoma

Glaucoma is a difficult disease to research in humans because of the inaccessibility of the optic nerve and the lack of sensitive clinical techniques to detect early glaucomatous changes. Hence, animal models have always played an important role in glaucoma research, particularly with regards to the pathophysiology. In an ideal animal model one would wish to see focal axonal injury at the optic nerve head and corresponding regional RGC loss in the retina. A multitude of animal models have been developed and used over the last few decades. Each of the models has advantages and disadvantages. A single model, in general, cannot faithfully replicate all aspects of a disease. Hence, a wise choice of the appropriate model for the question to be answered is crucial, depending on the mechanism of the condition to be investigated.

Primate models have the advantage that these animals are genetically very close to humans, possess a lamina cribrosa structurally similar to humans, and the disease kinetics are similar. They have proven to be helpful for the development and testing of IOP-lowering treatments. However, since much effort has and is being put into finding neuroprotective agents, rodent models have gained greater importance. Such studies require large numbers of experimental animals because, to date, determining RGC survival is terminal for the individual animal. Rodent models are attractive because of their short life span, low cost and relatively low ethical cost. Mouse models offer the opportunity of genetic engineering, but are less suitable for surgical manipulations due to the small size of the animal and the eye. Rats are more suitable for surgical interventions and even though there is no lamina cribrosa *per se*, they do have cellular structures that resemble a lamina cribrosa.

A model can be characterised by the success rate of the manipulation to achieve satisfactory IOP elevation, as well as the kinetics of onset and the sustainability of the IOP elevation. Furthermore, models differ in their technical difficulty and their training requirements. Another issue that needs to be considered when choosing a model is the availability of the equipment required.

Interventional models possess certain advantages over spontaneous models. Foremost, unilateral intervention gives the opportunity to use the fellow eye as a control to correct for inter-animal variability. Second, the predictable onset of the injury allows the study of sequential events.

1.4.1. Acute models

Acute and subacute angle-closure is characterized by a fairly sudden, very substantial and sometimes repeated rise in IOP. If the IOP surpasses the intraluminal pressure of the capillaries, transient disruption of blood flow ensues. Hence, ischemia of the inner retinal layers is a substantial part of the injury mechanism and RGC undergo ischemia stress-mediated apoptosis. This type of injury is reproduced in the laboratory by experimental elevation of the IOP by cannulating the anterior chamber and connecting the intraocular space to an infusion which can be raised to a certain level above the eye.[128] Typically, the IOP is elevated above systolic blood pressure for variable time periods.[129] This model has been used in mice and rats. Swelling of RGC with disruption of mitochondria and neurotubular degeneration is observed on histological examination.[130] Although there is some early necrosis, most cells die by apoptosis in delayed cell death and protein p53[131] and caspase[132, 133] levels are elevated. The injury is also accompanied by elevated glutamate levels and increased inducible nitric oxide synthase (iNOS) messenger ribonucleic acid expression.[134, 135]

1.4.2. Chronic models

Since elevated IOP is the most prominent risk factor for glaucoma, and in some patients probably the only cause for glaucomatous optic neuropathy, experimental models based on chronic elevation of IOP have always been regarded as highly suitable to study the disease. Most animal models employ experimental elevation of IOP. An ideal glaucoma model would exhibit the following characteristics:[136] (1) Prompt, and chronically-maintained, increase in IOP; (2) Lack of complications; (3) Selective death of RGC; (4) Ease and low cost of implementation.

Primates possess a solid lamina cribrosa that is structurally very similar to humans; unlike rodents which *sensu stricto* do not have a lamina cribrosa. Primate models involving argon laser photocoagulation of the trabecular meshwork are hence very representative of glaucomatous optic neuropathy in humans and have been used for the development of many pressure-lowering agents on the market today. However, as mentioned previously, they are expensive, both financially and ethically. Therefore, various methods to raise the IOP in rat eyes have subsequently been developed and used to study pathophysiological mechanisms in the retina and optic nerve. All these techniques aim to elevate IOP by obstructing the aqueous outflow. Manipulations that have been used comprise cauterization of the episcleral veins, injection of hypertonic saline into the episcleral veins, laser photocoagulation of the trabecular meshwork, and injection of particles into the anterior chamber. Mouse models based on chronic experimental elevation of the IOP have only recently been introduced.

1.4.2.1. Laser photocoagulation of the trabecular meshwork

This technique is generally only used in nonpigmented animals. In pigmented eyes the energy uptake is too high, producing significant inflammation, which influences the cellular response in the retina and the optic nerve head. Argon laser photocoagulation models have been successfully applied in mice and rats since the late 1990s. Laser techniques have been used to damage the trabecular meshwork and elevate IOP in primates for a quarter of a century.[137]The first published techniques in rodents utilized injections of India ink into the anterior chamber prior to the laser application to enhance energy absorption and localize scar formation at the trabecular meshwork.[138] Despite weekly laser treatment, IOP elevation was only moderate, although it could be maintained for 12 weeks. The use of pigment has subsequently been abandoned and more energy has been used for the laser burns. In general, the results from the laser photocoagulation methods have been consistent and the models are considered to be reproducible, reliable and efficient. The animals can be lasered by a single technician, no surgical instruments are needed and the intervention does not need to be performed under sterile conditions. However, access to a suitable continuous wave laser is necessary.

Essentially two techniques of laser application have been described in the literature. One approach consists of lasering the limbal vessels. Alternatively, investigators aim the laser burns at the trabecular meshwork itself in a tangential manner. None of the methods has been shown to be noticeably superior, and as Morrison has argued, the two techniques quite possibly work via the same principle, namely damage to the anterior chamber angle.[139] Laser application directed at the limbal vasculature certainly does cause 'collateral damage' at the level of the trabecular meshwork due to the proximity of the two anatomical structures.

In the limbal vessels approach the laser beam is aimed perpendicularly at the limbal vessels. 130-150 laser burns (spot size 50-100 μm, power 1W, exposure 0.2 sec) were applied to the limbal episcleral veins within 0.5-0.8 mm from the limbus. The treatment was repeated after 1 week. This resulted in a mean IOP elevation of 10-17 mmHg for at least 2 months. The

corresponding ganglion cell loss was progressive, 6.1% after 4 days, 19.4% after 10 days, 26.5% after 15 days and 44.2% after 60 days.[140]

Levkovitch-Verbin[141] modified the laser application by increasing the intensity and aiming the laser beam directly at the anterior chamber angle. Different settings were compared. It was found that 360 degree lasering of the trabecular meshwork with 60-80 spots (spot size 50 μm, power 0.6W, exposure 0.5 sec) combined with 4-7 laser burns (spot size 100 μm, power 0.6W, exposure 0.5 sec) to each of the three radial episcleral veins each yielded the best result and was most suitable to mimic chronic ocular hypertension. IOP elevation was maintained for up to 3 weeks.

Complications of laser photocoagulation were corneal oedema due to corneal decompensation, corneal ulcers, corneal opacity, and cataracts. Hyphaemas have been described as a common event during the lasering, in up to 40% of animals, but most of them resolve spontaneously within 48 hours.[141]

Similar models with application of laser to the limbal vessels have been successfully used in several mouse strains.[112, 142-144]

1.4.2.2. Sclerosing of the trabecular meshwork

In the laboratory rat, the most significant portion of drainage of aqueous humour occurs through the trabecular meshwork into Schlemm's canal. Numerous collector channels then drain the fluid into a venous plexus, which encircles the entire limbus and connects to multiple episcleral radial veins.[145] Morrison *et al*. developed a model based on injection of a mild sclerosant into this aqueous humour outflow pathway.[146] A glass micro needle with a diameter between 30 and 50 μm at the tip is inserted into one radial aqueous vein in the superior quadrant to inject 50 μl micro-filtered 1.75 M hypertonic saline. This causes sclerosis of the trabecular meshwork and the anterior chamber angle, which, after 7-10 days, produces persistent elevation of the IOP for a duration between 1 and 5 weeks. However, in some rats, this was only achieved by repeated injections. The drawbacks of this model are the considerable variability between individual rats, the difficult surgical injection technique that requires skills and training, and the need for a lateral canthotomy. In favour of this model is that IOP elevation tends to be longer than in the laser model. Optic nerve degeneration and cellular response have been shown to correlate with mean IOP, peak IOP elevation and cumulative pressure exposure.[147, 148] Gene expression patterns alterations have been documented in the optic nerve head and in the retina.[149, 150] To date, this model has almost exclusively been used in rats. One group recently reported successful application in mice.[151]

1.4.2.3. Cautery of episcleral vessels

While the previously described model increases outflow resistance at the level of the trabecular meshwork, cautery models are supposed to block drainage at the level of the episcleral veins.[152] However, the mechanism of pressure rise with this method is controversial and the treatment protocols in the literature vary considerable between different groups. Similarly variable are the pressure rises reported. While some groups report normalization of IOP after two weeks,[153] others claim pressure elevation for several months, even without retreatment.[154, 155] Some authors feel that the vessels that are cauterised are in fact vortex veins.[156]These vessels collect blood from the choroid, the anterior uvea and the base of the optic nerve in rats,[157, 158] and closure would result in complex alterations in the ocular perfusion, affecting several compartments of ocular tissues. The extent of optic nerve damage induced by this model ranges

from nothing[153, 156] to a maximum of 40%.[159, 160] This is in contrast to the laser models and the model of episcleral saline injection, where up to twice this much damage can be observed. This apparent neuroprotective effect can possibly be explained by the fact that choroidal veins are connected to the veins surrounding the optic nerve, and congestion of the choroidal vasculature might increase perfusion around the optic nerve head and protect the nerve fibres. The episcleral vein cautery model has also been used in mice.[161] Complications of cauterization of the episcleral veins were damage to the sclera, intraocular inflammation and ocular surface damage.

1.4.2.4. Microbeads

In search of a less acute experimental glaucoma model with sustained, moderate pressure elevation over several weeks, number of groups[136, 162-164] have recently reported the use of models based on injection of microparticles into the anterior chamber to occlude the trabecular meshwork in mice and rats. However, succesful application of this technique seems variable between different laboratories and the method is not yet considered very reliable for comparing results between various research groups.

Microbead models have the advantage that they can be used in pigmented animals and access to laser facilities is not necessary. Similar attempts have been made previously in rats[165] and primates[166] but in rodents the microbead approach has so far been neglected in favour of the laser models. Injection of microspheres into the anterior chamber of rats produces a moderate elevation of the IOP in the order of 30-40% above baseline for about 2 weeks. This time can be extended to approximately 8 weeks when a second injection is given between day 14 and 17.[164] Samsel *et al.* used paramagnetic microbeads and were able to direct the beads towards the trabecular meshwork to reduce the risk of visual axis occlusion.[163] The microbead approach is also applicable in mice to achieve sustained IOP elevation of about 30% for 3 weeks and up to 8 weeks with repeated injections.[164, 167] It has been shown that the susceptibility to experimental glaucoma is both strain and age dependent.[167]

1.4.2.5. S-antigen

Ocular hypertension is also observed after injection of S-antigen in rat eyes.[168] However, this model provokes an intense inflammatory reaction of the anterior and posterior segment. Hence, it has been postulated as suitable to study uveitic glaucoma and is not widely used.

1.4.2.6. Genetic rodent models of glaucoma

Although some rat strains with elevated IOPs have been described, their use in research is not common. Genetic mouse models, on the other hand, are very popular. Mouse systems offer the possibility to conduct complex genetic manipulations,[169] and are easy to breed. Such rodent lines are highly suitable to investigate molecular mechanisms and biochemical pathways. Some models involve mutations of glutamate receptors on RGC or other genes and are not associated with increased IOP.[170] Others present with anterior chamber abnormalities and are models of congenital glaucoma.[171] However, the most popular mouse models exhibit glaucomatous optic nerve atrophy that is associated with elevated IOP.

Several mouse strains (DBA/2J, DBA/2Nnia, AKXD-28/Ty) have been bred which spontaneously develop raised IOP secondary to pigment dispersion.[172-174] The DBA/2J mouse is the most frequently used model and has been well characterized.[175] Pigment dispersion causes iris atrophy, iris transillumination and anterior synechiae.[176] However, the mice develop elevation of IOP only after 8-9 months of age. Measurable RGC loss and a decrease of the inner plexiform

layer thickness is noticed at the age of 10-14 months.[177] Despite the absence of extracellular matrix plates[178], a typical pattern of sectoral RGC death has been described. A robust network of astrocytes is present in the region corresponding to the human lamina cribrosa and has been called glial lamina[179]. The sectoral nerve fibre damage supports the hypothesis that the primary site of injury in this model is the optic nerve head[180]. Moreover, axonal degeneration with compromised retrograde axonal transport precedes RGC soma degeneration in the retina.[181] and in BAX-deficient DBA/2J mice axon damage occurs without RGC cell death.[175]

Several mouse models have been generated by specific manipulation of distinct gene loci. One such example would be transgenic mice with a mutated myocilin gene.[182, 183] These animals express the mutated myocilin protein in the trabecular meshwork and have moderately elevated IOPs at older age. RGC death and optic nerve degeneration has been demonstrated. Collagen accumulation after mutation in the collagen type-1gene produces chronic open-angle glaucoma in another mouse line.[184] There exists also a mouse model for acute angle-closure glaucoma based on overexpression of a adrenomedullin-receptor in the pupillary sphincter muscle.[185]

1.4.3. Models for certain aspects of glaucomatous optic neuropathy

1.4.3.1. Retrograde RGC death

Retrograde RGC degeneration is likely to play a substantial part in glaucoma pathogenesis, since the primary insult is presumably situated at the optic nerve head. Optic nerve crush and axotomy models represent classical representatives of retrograde axonal degeneration and are applicable in mice and rats. Total axotomy of the optic nerve certainly leads to degeneration of the entire optic nerve and apoptosis of almost all RGCs.[186] Crush models produce only a partial lesion.[187] This causes primary damage in a proportion of RGC cell bodies and axons, but, as opposed to axotomy, also leads to secondary degeneration.[187] Secondary degeneration might be of relevance in glaucomatous optic neuropathy and would explain progression despite adequate treatment of IOP. The severity of the primary lesion in the crush model is very reproducible and intraocular excitatory amino acid levels have been shown to be increased subsequently.[188] This model has therefore been used widely to investigate the pathophysiology of RGC degeneration and neuroprotective substances interfering with apoptotic pathways.

1.4.3.2. Anterograde RGC death

In humans and experimental glaucoma models, increased glutamate concentrations have been measured in the vitreous.[189] However, it is still controversial to what extent excitotoxicity is involved in RGC death in glaucoma.[190] Nevertheless, animal models of excitotoxicity have been widely used in neuroprotection experiments. In these models, excitatory amino acids (e.g. glutamate, aspartate) or their analogues (N-Methyl-D aspartate (NMDA), kainate, 2-amino-3-(5-methyl-3-oxo-1,2- oxazol-4-yl)propanoic acid(AMPA)) are injected intravitreally in mouse or rat eyes. At low dose, only the inner retinal layers are affected. After injection of glutamate, degeneration of the ganglion cell and the inner nuclear layer occurs.[191] Massive cellular swelling is followed by necrosis. NMDA injection produces classic apoptotic RGC degeneration involving the caspase pathway.[192]

1.5. Epidemiological evidence and controversy

Epidemiologic research in glaucoma has a long tradition and several large population based surveys have analysed the risk factors associated with glaucomatous optic neuropathy. While diabetes mellitus is considered a risk factor for glaucoma in major textbooks of ophthalmology, it has to date not been possible to confirm this dogma with evidence-based studies and the issue remain controversial.[193]

The controversy started five decades ago when Armstrong *et al*. reported an increased incidence of glaucoma in diabetic patients.[194] Several clinic-based studies subsequently tried to confirm or reject this claim.[195-200] Since the issue remained controversial, a series of population-based studies in different populations were launched from 1980 onwards and published over the following quarter of a century.

1.5.1. Cross-sectional population surveys

Framingham study – Massachusetts, USA[201]

The data for the Framingham Eye Study was collected between 1973 and 1975 in a standardized ophthalmologic examination of the 2433 surviving members aged 52-85 from the Framingham Heart Study cohort, which had started in 1948. The screening examination included history of glaucoma, Goldmann applanation tonometry (IOP > 21) and disc examination by indirect ophthalmoscopy. The definitive examination consisted of disc evaluation, repeated Goldmann applanation tonometry, gonioscopy and Goldmann's perimetry. The diagnosis of open-angle glaucoma was confirmed if a field defect was documented in a suspect. The specific visual field defects were: blind spot enlargement, arcuate scotoma, paracentral scotoma, nasal step or advanced glaucomatous field loss. Diabetes mellitus was diagnosed if diabetic retinopathy was present. Diabetes was associated with higher IOP, but not with glaucoma. The prevalence of glaucoma in diabetics was 2.2% and did not differ from that in non-diabetics.

Beaver Dam Eye Study – Wisconsin, USA[202]

In The Beaver Dam Eye Study 4926 subjects aged 43-84 years were screened. Glaucoma was defined as enlarged cupping, corresponding visual field defect on Henson static perimetry and elevated IOP greater than 22 mmHg or a history of medical or surgical glaucoma treatment. Older-onset diabetes mellitus was defined as either a history of diabetes treatment or a glycosylated haemoglobin level greater than two standard deviations above the age-sex-matched mean and a blood glucose level over 11.1 mmol/l. A significant association between high-tension open-angle glaucoma and older-onset diabetes mellitus was found. The prevalence of glaucoma in diabetics was 4.2% versus 2.0% in non-diabetics (p=0.004).

Baltimore Eye Survey – Maryland, USA[203]

5308 participants 40 years of age or older underwent a detailed ophthalmologic screening examination. This included Goldmann applanation tonometry, stereo colour disc photography, and Hymphrey automated or Goldmann perimetry. 48% of participants were black. The criteria for glaucoma included an open angle and characteristic optic disc damage associated with a consistent visual field defect. Hence, normal-tension glaucoma was included. 161 subjects were diagnosed as having POAG. The definition of diabetes was based on a reported history of diabetes. Diabetes, which was highly prevalent in the population, was associated with higher IOP,

but not with POAG. However, subjects whose POAG had been diagnosed before the examination showed a positive association with diabetes and the investigators concluded that selection bias could explain the positive results of previous clinic-based investigations. However, the investigators admitted that their definition of diabetes was very open and potentially biased the odds ratio toward the null hypothesis. They further pointed out that the increased risk of mortality associated with diabetes might lead to underestimating the frequency of subjects having both diabetes and open-angle glaucoma. This is a potential limitation of the prevalence-based approach compared to the incidence-based approach.

Barbados Eye Study – Barbados[204, 205]

The Barbados Eye Study included 4709 Barbados-born residents, 40 to 84 years of age. Between 1987 to 1992, 4314 black participants were examined at the study site following a standardized protocol including Goldmann applanation tonometry, Humphrey perimetry, fundus photography and an interview. The prevalence of open-angel glaucoma, defined by the presence of both characteristic visual field changes and optic disc appearance, was 7%. Although diabetes was common in the study population, there was no association with open-angle glaucoma. A subsequent study in the same population analysed risk factors for incident open-angle glaucoma in 3222 persons at risk, who did not have definite open-angle glaucoma at baseline. After the standardized study visits at baseline the participants had a follow-up examination after 4 and 9 years. The incidence was estimated at 4.4% with age, family history, higher IOP and low mean perfusion pressure as significant risk factors. A history of diabetes mellitus, however, was not a significant risk factor for the development of glaucoma.

Rotterdam Study – Netherlands[206, 207]

This study investigated the association between newly diagnosed diabetes mellitus and POAG and IOP. Between 1990 and 1993, 4095 subjects aged over 55 years participating in the Rotterdam Study were examined according to a standard protocol including medical history interview, automated suprathreshold Humphrey visual field perimetry, Goldmann applanation tonometry, and nonfasting glucose tolerance test. This prospective population-based study investigated factors that determine the occurrence of cardiovascular, neurological, ophthalmological, endocrinological and psychiatric disease in the elderly. High-tension open-angle glaucoma was defined by the presence of a glaucomatous visual field defect in combination with an IOP greater than 21 mmHg. Newly diagnosed diabetes mellitus was defined by a random serum glucose level or a serum glucose level after a 75 gram glucose load above 11.0 mmol/l. Subjects on antidiabetes medication were excluded from the analysis. The study found that participants with newly diagnosed diabetes had higher mean IOP and a threefold increased presence of high-tension open-angle glaucoma.

A follow-up study investigating the risk factors for incident open-angle glaucoma. 3837 participants without open-angle glaucoma at baseline were re-examined between 1997 and 1999. 87 persons developed glaucoma after a mean follow-up time of 6.5 years. Of note, IOP was no longer included in the diagnosis of open-angel glaucoma. In this longitudinal study diabetes mellitus was not a risk factor for open-angle glaucoma.

The Blue Mountains Eye Study – New South Wales, Australia[208]

In the Blue Mountains eye study 3654 people 49-96 years of age underwent a detailed eye examination, which included automated Humphrey perimetry, stereo optic disc photographs, and

Goldmann applanation tonometry. Glaucoma was diagnosed if a visual field defect matching the optic disc cupping was present. IOP was not included in the diagnosis. Ocular hypertension was diagnosed as IOP higher than 21 mmHg without visual field changes. Fasting plasma glucose levels were measured. Diabetes was diagnosed from history or elevated fasting plasma glucose level over 7.8 mmol/l. The prevalence of glaucoma was 5.5% in diabetics versus 2.8% in subjects without diabetes. However, in the participants with known glaucoma and diabetes mellitus, the diagnosis of glaucoma had been made 15.7 years before the diagnosis of diabetes, on average. Ocular hypertension was almost twice as common in diabetic participants. The IOP of the persons with glaucoma did not differ between diabetics and non-diabetics and the authors concluded that the association between diabetes and open-angle glaucoma was independent of the effect of diabetes on IOP.

Proyecto VER – Arizona, USA[209]

4774 persons from the Pima and Santa Cruz counties of southern Arizona older than 40 years completed an extensive interview and the ocular examination, which consisted of automated Humphrey perimetry, Goldmann applanation tonometry, slit lamp dilated fundus examination, stereophotography of the optic disc and nerve fibre layer imaging. Diabetes mellitus was diagnosed when the HbA1c was at least 7% or when the participant had been told by a physician that he was suffering from diabetes mellitus. The prevalence of open-angle glaucoma among diabetic persons was 2.9% compared with 1.7% among nondiabetic persons. This difference was not significant when adjusted for age. However, diabetic persons did have a significantly higher IOP than nondiabetic persons.

Nurses' Health Study – USA[210]

The Nurses' Health Study started in 1976 in the US. 121700 female registered nurses aged between 30 and 55 participated in this study looking at the links between lifestyle habits and chronic disease. Data collection in regards to type 2 diabetes mellitus and open-angle glaucoma occurred between 1980 and the year 2000. Participants were required to be 40 years or older at baseline without any history of glaucoma and returned questionnaires on dietary and lifestyle patterns every 2 years. Also, they were required to receive eye examinations to contribute person time until a report of glaucoma, diagnosis of cancer, death, loss to follow-up or the end of the study in May 2000. 76318 women contributed person time. Reported cases of incident open-angle glaucoma were confirmed based on the medical records from the community ophthalmologist, which needed to comprise slit-lamp biomicroscopy and consistent visual field defects on subsequent examinations. Diabetes mellitus was confirmed using a questionnaire asking about diagnosis and treatment. 429 cases of incident POAG were indentified in 998292 person-years. The age-adjusted relative risk of POAG of diabetic participants was 1.53 (CI 1.06-2.22). The association was stronger for duration of diabetes less than 5 years than for longer duration of diabetes. The authors concluded that type 2 diabetes mellitus was associated with an increased risk of POAG.

Los Angeles Latino Eye Study – California, USA[211]

From 2000 to 2003, 5894 Latinos 40 years and older, living in the city of La Puente, answered an interviewer-administered questionnaire and had a comprehensive ocular examination, which included Humphrey automated visual field testing and stereo fundus photography. Glaucoma was defined if there was evidence of a glaucomatous visual field defect and/or glaucomatous optic

disc damage in at least one eye. The IOP was not considered in establishing the diagnosis of open-angle glaucoma. HbA1c and random blood glucose were measured. Participant were considered diabetic if they had a history of being treated for diabetes mellitus, glycosylated haemoglobin was measured at 7.0% or higher, or random blood glucose was 200 mg/100ml or greater. The type was defined as type 2 if the participant was 30 years or older at the time of first diagnosis. The prevalence of open-angle glaucoma was found to be higher in diabetic patients (odds ratio 1.4; CI 1.03-1.8), and longer duration of type 2 diabetes mellitus was associated with higher prevalence of open-angle glaucoma.

1.5.2. Longitudinal population surveys

DARTS/MEMO Collaboration - Scotland[212]

An incidence study conducted in Scotland evaluated the 2-year incidence of open-angle glaucoma or ocular hypertension. The investigators followed 6631 subjects with diabetes and 166144 subjects without diabetes for 2 years using a registration database for diabetes, a prescription database for anti-glaucoma medication, and a glaucoma surgical statutory record database in the Tayside region of Scotland. The diagnosis of glaucoma or ocular hypertension was confirmed in all diabetic patients and in a random sample of 10% of the nondiabetic cohort. Open-angle glaucoma was defined by disc cupping with corresponding visual field defect regardless of IOP. Ocular hypertension was defined as IOP greater 21 mmHg without field defect or asymmetric cupping. The 2-year incidence of open-angle glaucoma glaucoma was 1.1‰ in diabetics vs. 0.7‰ in nondiabetics. For ocular hypertension, the numbers were 1.8‰ and 1.3‰ respectively. These associations were not statistically significant. Furthermore, the investigators attributed 22% of newly diagnosed glaucoma in the diabetic cohort to detection bias due to increased healthcare contact.

The Visual Impairment Project – Melbourne, Australia[213]

In a cohort of 2415 subjects, which was followed between 1997 and 1999, several risk factors for the incidence of open-angle glaucoma were studied. The study subjects underwent an ophthalmic examination and a comprehensive standardized interview at baseline and at 5-year follow-up. Sociodemographic, anthropometric, dietary, familial, medical and ocular characteristics were analysed. The ophthalmic exam consisted of Humphrey automated perimetry, handheld tonometry (which was confirmed by Goldmann applanation tonometry if measured greater than 21 mmHg), biomicroscopic slit lamp examination and stereo disc photographs. Although the investigators did not describe their definition of diabetes and the incidence rate observed, the report mentioned that diabetes was not associated with open-angle glaucoma.

In summary, the findings of the population-based studies regarding an association between diabetes mellitus and open-angle glaucoma are controversial and not conclusive. In part, this might be due to different inclusion criteria and different criteria for the diagnosis of diabetes and open-angle glaucoma in the multiple studies. Furthermore, the populations studied were all different and had heterogeneous genetic backgrounds and environmental influences. It is possible that there are fundamental differences in regards to the association of diabetes and open-angle glaucoma in different populations. Longitudinal studies might be of particular interest, although time-consuming and costly; none of these so far did show an association.

1.6. Hyperglycaemia in brain and retinal ischemia

Diabetes mellitus is clearly a risk factor for the occurrence of stroke and is associated with a poor prognosis.[214, 215] Of note, even hyperglycaemia without pre-existing diabetes mellitus significantly increases mortality and morbidity in stroke patients.[216] While longstanding diabetes clearly affects both micro- and macrocirculation,[217] it is not entirely clear how acute hyperglycaemia, which is commonly seen in acute stroke,[218] leads to worse stroke outcomes, and whether hyperglycaemia is genuinely linked to brain infarction or just an epiphenomenon of other pathophysiological changes associated with ischemic stroke, such as stress-related catecholamine and corticosteroid production.[219, 220] However, insulin therapy resulting in lower blood glucose levels has been shown to reduce ischemic brain damage in animal models[221] and seems to improve outcomes in stroke patients.[222, 223] The neuroprotective effect could be mediated by the lower glucose levels and reversal of the damaging effects of glucose, or result from the beneficial action of insulin itself.[224]

In animal experiments, several mechanisms have been proposed for hyperglycaemia-mediated exacerbation of brain damage after ischemic stroke: Decreased blood flow to the ischemic penumbra,[225] increase in NMDA receptor-mediated calcium influx into neurons secondary to glutamate accumulation,[226] increase in local oedema,[227] exacerbation of oxidative stress and inflammation,[228] and, finally, changes in metabolism[229] characterized by lactic acid accumulation, acidosis, hypometabolism and mitochondrial dysfunction.[230]

The retina is derived from an outpouching of the diencephalon and, as such, is considered to be a specialized part of the central nervous system. Several of the above mentioned mechanisms can be found in the retina.

The retinal circulation is autoregulated and characterised by a low level of flow and high oxygen extraction. Since there is no autonomic innervation, local endothelium-dependent vasoactive modulation, mediated by nitric oxide (NO),[231] plays a major role.[232] In ocular tissues, NO has also a multitude of other functions and is involved in the pathogenesis of glaucoma, retinal ischemia and diabetic retinopathy.[233] In diabetics, carbon dioxide-induced cerebral vasodilatation, mediated through NO, is decreased.[234] Furthermore, glucose-induced reactive oxidative species (ROS) can neutralize NO[235] and impair microcirculation. Owing to autoregulation, the oxygenation of the inner retina seems to be little affected by increased IOP. However, choroidal perfusion and outer retina oxygen partial pressure (pO_2) decreases.[236] Similarly, the oxygenation of the prelaminar optic nerve head does not seem to be impaired by increased IOP.[237]

The role of excitotoxicity, NMDA receptor-mediated neuronal apoptosis through excitatory amino acids, is controversial in glaucoma,[190] but has been claimed to be relevant in RGC death[238] and axonal degeneration in glaucomatous optic neuropathy[239] by some authors. In the retina, diabetes has been associated with glutamate transporter dysfunction in Müller cells.[240] After experimental forebrain ischemia, the extracellular glutamate concentrations were pronouncedly more elevated in hyperglycaemic rats and correlated with the amount of cell damage.[226] Thus, hyperglycaemia seems to increase glutamate availability and calcium-mediated cell death.

ROS are involved in the pathogenesis of a wide variety of ocular diseases ranging from retinopathy of prematurity[241] to age-related-macular degeneration.[242] In particular, ROS have been attributed a significant role in the pathogenesis of both diabetic retinopathy[243] and glaucoma.[244] ROS trigger the release of proinflammatory cytokines, impair blood flow, worsen breakdown of the blood-brain barrier and oedema, and are procoagulant by inhibition of fibrinolysis.[217] After an ischemic stroke, hyperglycaemia increases ROS production and is thought to exacerbate the ROS-mediated injury.[216]

In the aspects mentioned so far, brain and the neurosensory tissues of the eye exhibit similar cellular processes and share common regulatory mechanisms. However, with regard to metabolism, there are fundamental differences. The retinal metabolism of mammals is characterised by its high glycolytic capacity and high glycolytic activity even during aerobic conditions.[245] Glycolysis increases further during anoxia[246] and can compensate almost completely for lack of oxygen under normoglycaemic conditions.[247, 248] The normal glucose concentration in retinas from control animals is about 5 mM. The vitreous glucose level is about half the serum concentration.[249, 250] Glycolytic production of adenosine triphosphate (ATP) is sufficient to maintain retinal function in the presence of 20 mM glucose.[251] However, this capacity is diminished during hypoglycaemia[252] and acute hypoglycaemia causes retinal apoptosis.[253]

Glycolysis as a pathway for generation of ATP is thought to be particularly relevant for the outer retina. The metabolic rate in the retina is highest in the photoreceptor cells. Oxygenation of the outer retina occurs by diffusion from the choroid and is first diminished in hypoxic conditions. Even under normoxic conditions, 80% of glucose supplied to the avascular outer retina by the choroid is converted to lactate.[254, 255] In the inner retina only 20% of glucose is metabolised through glycolysis.[256]

It is controversial whether the Crabtree effect, that is inhibition of respiration by glycolysis in the presence of elevated glucose levels, occurs in the retina. In the cat retina, acute hyperglycaemia in the order of 6 hours did not affect oxygen consumption of the outer retina and the average inner retinal pO_2 did not change.[257] Oxygen profiles were similar to normoglycaemic control animals, despite lowered choroidal pO_2; hence a larger fraction of oxygen was delivered to the photoreceptors by the retinal circulation and retinal blood flow was increased.[258] However, long-term hyperglycaemia may change retinal metabolism.[259]

The high glycolytic capacity, together with the regulation of blood flow in the retinal circulation, explains the resistance of the retina to hypoxia. The inner retina is particularly resistant to hypoxia.[260] However, in diabetic retinopathy, where tissue hypoxia plays a significant role and particularly affects the inner retina,[261] this resistance is impaired. At least in part because of altered oxygen flux from retinal arteries.[262] Even in the absence of capillary closure, a decrease in retinal blood flow has been noted in type 1 diabetes.[263, 264] Hyperglycaemia also decreases choroidal blood flow and pO_2 in diabetic cats.[265] However, in streptozotocin(STZ)-diabetic rats hypoxic changes seem to be relevant only in the long term, because the preretinal pO_2 is still normal after 6 weeks of diabetes.[262]

Neural tissue is completely reliant on glucose for normal metabolic activity. Glucose transport is facilitated by membrane proteins from the glucose transport protein (GLUT) family. Glucose supply to the retina occurs by saturable, facilitated diffusion through GLUT1, which is found on the endothelium of the retinal blood vessels and the retinal pigment epitelium.[266, 267] GLUT1 is saturated at normal blood glucose levels, but upregulation on retinal vascular endothelium has been observed in STZ-treated rats[268] and diabetic humans[269] which is thought to be relevant in diabetic retnopathy.[270] Within the retina, GLUT1 is found on photoreceptors, Müller cells and retinal ganglion cells.[271, 272] GLUT2 and GLUT3 are also found in retinal tissue. GLUT2 is found on the apical ends of Müller cells that form the external limiting membrane and potentially has a role in intra-retinal glucose regulation.[273] GLUT3 is found exclusively in the inner synaptic layer and thought to be the major neuronal glucose transporter.[274, 275] The factors regulating glucose transport in the retina are not well understood.[270] In cell cultures, endothelial GLUT1 is influenced by hypoxia, growth factors and glucose.[276, 277] In retinal pigment epithelium cultures GLUT1 transcription is upregulated by serum, insulin-like growth factor-1, basic fibroblast growth factor, platelet-derived growth factor and epidermal growth factor.[278]

1.7. Neuroprotection

Neuroprotection is a general term given to interventions aimed at halting disease progression. Despite the fact that several neuroprotective agents have been very successful in animal studies, the outcomes of clinical studies have been frustrating so far.[279] Memantine is an uncompetitive NMDA receptor antagonist. This compound has been shown to protect RGCs in several animal models of glaucoma.[280] However, two randomized phase III clinical trials of memantine in glaucoma failed to show a significant effect.[281] Glatiramer acetate is a synthetic oligopeptide of four naturally occurring amino acids, currently approved as treatment for multiple sclerosis. It has been proposed as a T cell-based neuroprotective vaccination in glaucoma. In the rat model of chronic ocular hypertension, vaccination with glatiramer acetate significantly reduced loss of RGCs.[282] Progression was limited by rendering the local extracellular environment less hostile to neuronal survival and allowed the RGC to better withstand the stress induced by IOP.[283] Clinical trials have not yet been conducted. Current strategies under investigation involve neurotrophins, antiapoptotic substances, stem cell therapies and bioenergetic strategies.[281]

2. Aims of study

Currently, lowering the IOP is the only evidence-based treatment approach for glaucomatous optic neuropathy. However, this does not stop progression in all patients.[25, 31, 34, 284] Factors other than IOP and direct mechanic stress must therefore contribute significantly to optic nerve damage and ganglion cell loss in these individuals and provide potential targets for alternative treatment approaches.

The retina, although considered to be a part of the central nervous system due to its derivation from the diencephalon, exhibits some fundamentally different metabolic characteristics in comparison with the CNS. In particular, hyperglycaemia seems to be neuroprotective in the context of acute or subacute retinal ischemia.[249, 285]

Although not yet understood in full detail, the primary insult in glaucomatous optic neuropathy seems to involve mitochondrial dysfunction, resulting in shortage of ATP and oxidative stress, at least in some forms of glaucoma.[286] This aspect of the disease might be amenable to bioenergetic neuroprotection and open new avenues of therapeutic approaches.[287, 288] Furthermore, hyperglycaemia might influence pathophysiological processes in other ways and hereby mitigate axonal loss and RGC death. The aim of this study was therefore to investigate the influence of hyperglycaemia on experimental glaucomatous optic neuropathy. Prior to the final experiment, a suitable model of glaucomatous optic neuropathy needed to be identified and characterised. Furthermore, efficacious and reliable methods for optic nerve damage quantification needed to be defined.

3. Choice and validation of the appropriate animal model of experimental glaucoma

Hyperglycaemia induces many deleterious ocular changes in the long-term, including microvascular pathology but, independently, also triggers neurodegeneration of RGC with dendrite remodelling and ensuing receptive fields changes.[289, 290] I was interested in the effects of hyperglycaemia before establishment of these chronic changes, which is around 1-3 months after induction of STZ-diabetes. Therefore, I relied on a glaucoma model, which produces significant damage in a shorter time frame, which eliminated genetic models as a working tool. Furthermore, a fairly acute model with a concisely defined onset of optic nerve pathology seemed favourable over chronic mouse models relying on spontaneous elevation of IOP and unpredictable gradual onset of pathology in the individual nerve fibres. For these reasons, the laser glaucoma model appeared to be the most appropriate choice.

In humans, functional deficits occur early in the progression of glaucoma. There is increasing evidence that the axons and dendrites are involved prior to loss of the perikarya (see Crish[291]). First evidence for an axonal transport deficit in glaucoma has been found 4 decades ago. Since then, the optic nerve head as the site of transport disruption has been a primary research focus. It has been hypothesized that the blockade of axoplasmic flow was primarily mechanical in nature and also impaired the retrograde transport of pro-survival factors, triggering apoptosis of RGCs.

The main structural support to the optic nerve bundles in humans is provided by the lamina cribrosa, which consists of several sheets of connective tissue with pores. This structure seems to play the key role in the pathogenesis of human glaucoma. But precisely this crucial structure is far more rudimentary and less solid in rodents,[292] and the absence of a collagenous component might compromise the validity of rodent models in experimental glaucoma research. Nevertheless, the cellular constituents and the composition of the extracellular matrix are similar to that of the human or primate lamina cribrosa and it has been documented that the cellular response to increased IOP in rats is very similar.[67]

The trabecular meshwork translimbal laser model has been used by several groups for almost 10 years. There clearly is a dose-effect relationship between IOP exposure and axonal damage. It has been demonstrated that retrograde transport is compromised in the pathology, predominantly and early at the optic nerve head.[293] Moreover, retinal ganglion cell loss occurs in a sectorial pattern suggestive of an optic nerve head insult.[294] As a novelty, the present study characterises changes of anterograde fast axonal transport relying on endogenous proteins of different size and confirms the optic nerve head as the likely site of generalized anterograde transport failure, verified by demonstrating accumulation of the neural tracer cholera toxin β-subunit at the optic nerve head. Furthermore, the paper shows that SMI-32 is a useful stain for immunohistochemical analysis of optic nerve damage.

The optic nerve head is the site of axonal transport disruption, axonal cytoskeleton damage and putative axonal regeneration failure in a rat model of glaucoma

Contribution of each author

Andreas Ebneter:

Animal experiments and immunohistochemistry
Acquisition of data
Analysis and interpretation of data
Critical revision of the manuscript for important intellectual content

Glyn Chidlow:

Conception and design
RT-PCR
Analysis and interpretation of data
Drafting, revision and finalization of the manuscript
Administrative, technical, or material support
Supervision

John Wood:

Western Blotting
Analysis and interpretation of data
Critical revision of the manuscript for important intellectual content
Supervision

Robert Casson:

Conception and design
Analysis and interpretation of data
Critical revision of the manuscript for important intellectual content
Statistical expertise
Obtaining funding
Supervision

Acta Neuropathol
DOI 10.1007/s00401-011-0807-1

ORIGINAL PAPER

The optic nerve head is the site of axonal transport disruption, axonal cytoskeleton damage and putative axonal regeneration failure in a rat model of glaucoma

Glyn Chidlow · Andreas Ebneter · John P. M. Wood · Robert J. Casson

Received: 17 November 2010 / Revised: 27 January 2011 / Accepted: 29 January 2011

Abstract The neurodegenerative disease glaucoma is characterised by the progressive death of retinal ganglion cells (RGCs) and structural damage to the optic nerve (ON). New insights have been gained into the pathogenesis of glaucoma through the use of rodent models; however, a coherent picture of the early pathology remains elusive. Here, we use a validated, experimentally induced rat glaucoma model to address fundamental issues relating to the spatio-temporal pattern of RGC injury. The earliest indication of RGC damage was accumulation of proteins, transported by orthograde fast axonal transport within axons in the optic nerve head (ONH), which occurred as soon as 8 h after induction of glaucoma and was maximal by 24 h. Axonal cytoskeletal abnormalities were first observed in the ONH at 24 h. In contrast to the ONH, no axonal cytoskeletal damage was detected in the entire myelinated ON and tract until 3 days, with progressively greater damage at later time points. Likewise, down-regulation of RGC-specific mRNAs, which are sensitive indicators of RGC viability, occurred subsequent to axonal changes at the ONH and later than in retinas subjected to NMDA-induced somatic excitotoxicity. After 1 week, surviving, but injured, RGCs had initiated a regenerative-like response, as delineated by Gap43 immunolabelling, in a response similar to that seen after ON crush. The data presented here provide robust support for the hypothesis that the ONH is the pivotal site of RGC injury following moderate elevation of IOP, with the resulting anterograde degeneration of axons and retrograde injury and death of somas.

Keywords Glaucoma · Retinal ganglion cell · Optic nerve head · Axonal transport · Axon degeneration · Amyloid precursor protein

Introduction

Glaucoma refers to a family of ocular diseases with multifactorial aetiology united by a clinically characteristic optic neuropathy. Pathologically, glaucoma is characterised by a loss of all retinal ganglion cell (RGC) compartments: somata, axons and dendrites; clinically, loss of axons at the optic nerve head (ONH) heralds the diagnosis of glaucoma. This observation, together with other converging clinical evidence, has given rise to a long-standing belief that the foremost site of injury is at the ONH [39]. Yet, the pathogenesis of glaucoma remains poorly understood. Evidence supporting the ONH as the primary locus of injury is circumstantial, whilst not much is known about the molecular pathways involved in the loss of RGCs and their axons. To date, treatment options for glaucoma remain limited to lowering intraocular pressure (IOP), the highest profile risk factor for the disease [23].

To facilitate a greater understanding of glaucoma, a number of rodent paradigms have been developed. These can broadly be divided into rat models, in which elevated IOP is induced experimentally [33], and mouse models,

Electronic supplementary material The online version of this article (doi:10.1007/s00401-011-0807-1) contains supplementary material, which is available to authorized users.

G. Chidlow (✉) · A. Ebneter · J. P. M. Wood · R. J. Casson
Ophthalmic Research Laboratories, South Australian Institute of Ophthalmology, Hanson Institute Centre for Neurological Diseases, Frome Rd, Adelaide, SA 5000, Australia
e-mail: glyn.chidlow@health.sa.gov.au

G. Chidlow · A. Ebneter · J. P. M. Wood · R. J. Casson
Department of Ophthalmology and Visual Sciences, University of Adelaide, Frome Rd, Adelaide, SA 5000, Australia

Published online: 11 February 2011

where IOP elevation occurs spontaneously [18]. Of particular importance has been the discovery and characterisation of the DBA/2J inbred mouse strain [19]. DBA/2J mice exhibit a form of pigmentary glaucoma featuring an age-related elevation of IOP and progressive optic neuropathy. In recent years, a substantive body of work has been conducted on DBA/2J mice, providing new insights into the spatio-temporal pattern of RGC dysfunction and degeneration. A consistent view on the chronology of pathological events in this disease model is, however, still to be reached. For example, Howell et al. [16] provided robust evidence for an early insult at the lamina of the ONH with Wallerian-like degeneration of axons distal to the site of injury. In contrast, Crish et al. [12] ascertained that axonal transport dysfunction and axon degeneration appear first at the superior colliculus with a distal-proximal progression, findings in broad agreement with earlier work [44]. Furthermore, somatic alterations in RGCs, including downregulation of mRNA synthesis and abnormal neurofilament labelling, have been described as occurring more or less simultaneously [17], or subsequent to [5], retrograde axon transport dysfunction.

Certain strengths of the DBA/2J mouse as a relevant model for human glaucoma, including its gradual progression, unpredictable timing and inter-individual variability, make unequivocal identification of the sequence of events problematic. Here, we use a validated, experimentally induced rat glaucoma model [26] to address several fundamental issues. These include ascertaining the spatio-temporal pattern of orthograde axonal transport disruption and its correlation with IOP elevation, delineating the site of initial axonal cytoskeletal damage and determining any association with altered neurofilament phosphorylation, documenting the timing of RGC somal injury and whether RGCs attempt to regenerate their injured axons, and finally, comparing the pattern of injury observed in glaucoma with those seen after optic nerve crush or NMDA-induced excitotoxicity, the classical methods of eliciting axonal and somato-dendritic death of RGCs, respectively.

Materials and methods

Animals and procedures

This study was approved by the Animal Ethics Committees of the Institute of Medical and Veterinary Science and the University of Adelaide and conforms to the Australian Code of Practice for the Care and Use of Animals for Scientific Purposes, 2004. All experiments conformed to the ARVO Statement for the Use of Animals in Ophthalmic and Vision Research. Adult Sprague–Dawley rats (200–250 g) were housed in a temperature- and humidity-controlled environment with a 12-h light, 12-h dark cycle and were provided with food and water ad libitum.

For experimental glaucoma experiments, rats were anaesthetised with 100 mg/kg ketamine and 10 mg/kg xylazine. Ocular hypertension was then induced in the right eye of each animal by laser photocoagulation of the trabecular meshwork using a slightly modified protocol [14] of the method described by Levkovitch–Verbin et al. [26]. IOPs were measured in both eyes at baseline, 8 h, days 1, 3, 7 and 14 using a rebound tonometer factory calibrated for use in rats. No animals were excluded for reasons relating to inadequate IOP elevation. Two animals were excluded as a result of death under anaesthesia and two due to hyphema. Two cohorts of rats were used in the current study. The first cohort was used for immunohistochemistry/histology of the retina, ONH, optic nerve (ON) and optic tract (OT). The number of rats analysed at each time point was as follows: 8 h ($n = 4$), 1 day ($n = 8$), 3 days ($n = 10$), 7 day ($n = 9$), 14 days ($n = 10$). In addition, three rats were killed at 2 days and used for transverse sectioning of the ONH. For axonal tracing, 4 rats were injected intravitreally with 5 µl of 0.1% AlexaFluor 594-conjugated cholera toxin β-subunit (CTB) dissolved in sterile PBS. After 24 h, right eyes were lasered as above. Rats were killed at 2 days and taken for immunohistochemistry. The second cohort was used for RT-PCR/Western blotting of the retina and ON. The number of rats analysed at each time point was as follows: 1 day ($n = 4$), 3 days ($n = 7$), 7 days ($n = 7$), 14 days ($n = 4$). The chiasm from each rat was taken for immunohistochemistry to verify that the procedure had induced an injury response commensurate with the first cohort.

For excitotoxicity experiments, an intravitreal injection of 30 nmol of NMDA (5 µl in sterile saline) was performed in one eye. The control eye was injected with vehicle. The number of rats analysed at each time point for RT-PCR of the retina was as follows: 6 h ($n = 7$), 1 day ($n = 6$), 3 days ($n = 6$), 7 days ($n = 7$). In addition, four rats were taken at each time point for immunohistochemistry. For ON crush experiments, the superior muscle complex was divided and the ON exposed by blunt dissection. The ON was then crushed 3-mm posterior to the globe under direct visualisation using number 5 forceps for 20 s. ON crush produces complete disruption of the RGC axons, which can be seen as a separation of the proximal and distal optic nerve ends within the meningeal sheath. To avoid confusing retinal ischaemic changes with the effects of crush, the fundus was observed ophthalmologically immediately after nerve crush. A total of six rats were subjected to ON crush, all of which were killed at 14 days.

Tissue processing and histology

All rats were killed by trans-cardial perfusion with physiological saline under deep anaesthesia and, in those rats where tissue was not taken for RT-PCR/Western blotting, subsequently with 4% paraformaldehyde. Initially, the brain was removed. Next, each eye with ON, optic chiasm and the proximal part of the OT attached was carefully dissected. From the dissected tissue, a short piece of ON (2-mm long), 1.5-mm behind the globe, was removed for resin embedding. The brain, globe, remaining ON, chiasm and proximal segment of OT were fixed in 10% buffered formalin for at least 24 h. Following fixation, the brain was positioned in the Kopf rat brain blocker (Kopf Instruments PA001) and 2-mm coronal slices were taken in a dorsal-caudal direction. Brain slices, along with the globe and optic pathway, were processed for routine paraffin-embedded sections. Globes were embedded sagitally; ONs and chiasmata were embedded longitudinally. In all cases, 4-μm serial sections were cut. As detailed above, three rats killed at 2 days were used for transverse sectioning of the ONH. The short piece of proximal ON taken for resin sectioning and toluidine blue staining was treated as previously reported [14].

Immunohistochemistry

Colorimetric immunohistochemistry was performed as previously described [9]. In brief, tissue sections were deparaffinized before treatment with 0.5% H_2O_2 for 30 min to block endogenous peroxidase activity. Antigen retrieval was achieved by microwaving the sections in 10-mM citrate buffer (pH 6.0). Tissue sections were then blocked in PBS containing 3% normal horse serum, incubated overnight in primary antibody, followed by consecutive incubations with biotinylated secondary antibody and streptavidin-peroxidase conjugate. Colour development was achieved with 3′-,3′-diaminobenzidine. Sections were counterstained with haematoxylin, dehydrated and mounted. Specificity of antibody staining was confirmed by incubating adjacent sections with isotype controls (mouse IgG1 and IgG2a isotype controls) for monoclonal antibodies, or normal rabbit/goat serum for polyclonal antibodies.

Double labelling fluorescent immunohistochemistry was performed as previously described [9]. In brief, visualisation of one antigen was achieved using a three-step procedure (primary antibody, biotinylated secondary antibody, streptavidin-conjugated AlexaFluor 594), whilst the second antigen was labelled by a two-step procedure (primary antibody, secondary antibody conjugated to AlexaFluor 488). In summary, sections were prepared as above, except for the omission of the endogenous peroxidase block, then incubated overnight at room temperature in the appropriate combination of primary antibodies. On the following day, sections were incubated with the appropriate biotinylated secondary antibody (1:250) for the three-step procedure plus the correct secondary antibody conjugated to AlexaFluor 488 (1:250, Invitrogen) for the two-step procedure for 30 min, followed by streptavidin-conjugated AlexaFluor 594 (1:500) for 1 h. Sections were then mounted using anti-fade mounting medium and examined under a confocal fluorescence microscope. Primary antibody details are provided in Supplementary Table 1.

Evaluation of histology and immunohistochemistry

All assessments of ON injury were performed in a randomized, blinded manner. Loss of RGC axons in the ONs of glaucomatous eyes was assessed using a semi-quantitative ON grading scheme based on the toluidine blue-stained cross-sections [8, 14], where grade 0 corresponds to no damage, grade 5–50% axon loss, and grade 10–100% axonal loss. Of note, if the calculated damage grade was zero, but the nerve contained at least 20 damaged axons within the whole cross-section, the grade was recorded as 1 as a nominal indication that the nerve was damaged.

β-Amyloid precursor protein (APP) accumulation in the ONH as a result of disrupted axonal transport was assessed semi-quantitatively using a 4-point grading system, ranging from 0 = undetectable to 3 = numerous intensely stained APP-positive axons covering a substantial area of the prelaminar to post-laminar ONH. The APP score of each rat was then correlated with the peak IOP elevation of that rat and with the IOP at the time of death. Statistical analysis of correlations were performed by GraphPad Prism 5.0b (GraphPad Software Inc., La Jolla, CA) using non-parametric tests.

Quantification of SMI-32 immunolabelling in longitudinal sections of the medial ON and proximal OT was performed as previously described [14]. In brief, immunostained sections, each expressing a representative level of immunoreactivity, were photographed at 200×. They were then imported into NIH Image-J 1.42q software (http://www.rsb.info.nih.gov/ij/), where they underwent colour deconvolution to separate diaminobenzidine reaction product from haematoxylin counterstain [41]. Images were subsequently analysed with regard to the specifically stained area in pixels using the in-built functions of the Image-J software. Statistical analysis was carried out by ANOVA followed by post hoc Tukey's test.

Electrophoresis/Western blotting

The entire ON was taken for Western blotting except for 1.5 mm at the proximal and distal ends; thus, only the

myelinated segment of the nerve was analysed. Retinas and ONs from 3 to 7 days, and ONs from 14-day experimental glaucoma rats were processed for Western blotting as previously described [9]. In brief, after electrophoresis, samples were transferred onto PVDF membranes. Following a block of non-specific binding, blots were probed with primary antibodies (see Supplementary Table 1), appropriate secondary antibodies conjugated to biotin, and streptavidin-peroxidase conjugate. Blots were then developed and the images captured and analysed for densitometry. Densitometry values were normalised for actin. Statistical analysis was performed by Kruskall–Wallis followed by Mann–Whitney for comparison of SMI-32, SMI-37 and SMI-31 expression in 3, 7 and 14 days ON samples and by Student's paired *t* test for Gap43 expression in treated versus control retinas.

Real-time RT-PCR

Reverse-transcription polymerisation chain reaction (RT-PCR) studies were carried out as described previously [11]. In brief, retinas were dissected, total RNA was isolated and first-strand cDNA was synthesised from 2-µg DNase-treated RNA. Real-time PCR reactions were carried out in 96-well optical reaction plates using the cDNA equivalent of 20-ng total RNA for each sample in a total volume of 25 µl containing 1× SYBR Green PCR master mix (Bio-Rad), forward and reverse primers at a final concentration of 400 nM. The thermal cycling conditions were 95°C for 3 min and 40 cycles of amplification comprising 95°C for 12 s, 63°C for 30 s and 72°C for 30 s. Primer sets used were as follows (sense primer, antisense primer, product size, accession number): GAPDH (5′-TGCACCACCAACTGCTTAGC-3′, 5′-GGCATGGACTGTGGTCATGAG-3′, 87 bp, NM_017008), NFL (5′-ATGGCATTGGACATTGAGATT-3′, 5′-CTGAGAGTAGCCGCTGGTTAT-3′, 105 bp, AF031880), Thy1.1 (5′-CAAGCTCCAATAAAACTATCAATGTG-3′, 5′-GGAAGTGTTTTGAACCAGCAG-3′, 83 bp, X03150). After the final cycle of the PCR, primer specificity was checked by the dissociation (melting) curve method. In addition, specific amplification was confirmed by electrophoresis of PCR products on 3% agarose gels. PCR assays were performed using the IQ5 icycler (Bio-Rad) and all samples were run in duplicate. The results obtained from the real-time PCR experiments were quantified using the comparative threshold cycle (C_T) method ($\Delta\Delta C_T$) for relative quantitation of gene expression [27], corrected for amplification efficiency [36]. All values were normalised using the endogenous housekeeping gene GAPDH and expressed relative to controls. Statistical analysis was carried out by ANOVA followed by post hoc Tukey's test. The null hypothesis tested was that C_T differences between target and housekeeping genes would be the same in control and experimental retinas.

Results

Axonal transport disruption at the ONH is an early event during experimental glaucoma

The ONH has long been considered a site of early axonal transport failure in glaucoma [1, 29, 37, 39, 40], but recent data from rodents indicate that distal axons are affected first [12]. To address this important issue, we performed immunolabelling for APP, a protein synthesised by RGCs [30] and conveyed along the ON by fast axonal transport. We found accumulation of APP in axons in the pre- and post-laminar ONH as early as 8 h following induction of raised IOP (Fig. 1a, b). By 24 h, intense APP immunoreactivity was observed throughout the ONH, a result that was typical of the majority of rats analysed within the first 7 d. By 14 d, however, not much APP accumulation was detectable at the ONH in most animals (Fig. 1c–f). To ascertain whether axonal transport disruption correlated with the peak increase in IOP or the terminal IOP, representative sections from the central ONH of every rat were graded for APP accumulation and related to the peak IOP value recorded from that rat and to the IOP at the time of death. A Spearman's rank correlation was then performed. The maximal APP score was documented at 24 h after induction of experimental glaucoma, with similar, somewhat lower values obtained at 3 and 7 days, and a substantially lower grade at 14 days (Table 1). There was no correlation between peak IOP and APP grade ($r = 0.27$, $P = 0.11$). In contrast, the terminal IOP showed a

Table 1 Grading of APP accumulation at the ONH at various times after induction of experimental glaucoma

Time	Cont eyes	8 h ($n = 4$)	1 day ($n = 7$)	3 days ($n = 8$)	7 days ($n = 9$)	14 days ($n = 10$)
Integral exposure IOP[a]	–	–	16.5 ± 2.1	47.1 ± 11.1	97.7 ± 8.7	189.2 ± 13.2
Peak increase in IOP[a]	–	28.5 ± 2.7	24.2 ± 4.6	25.8 ± 5.4	26.3 ± 2.5	24.2 ± 2.2
IOP increase at time of death[a]	–	28.0 ± 3.0	21.5 ± 4.0	15.0 ± 7.0	13.3 ± 2.6	5.0 ± 1.3
APP grade	0.0 ± 0.0	1.5 ± 0.3	3.8 ± 0.2	2.9 ± 0.3	2.7 ± 0.2	1.5 ± 0.2

[a] Calculated as IOP of treated eye—IOP of untreated contralateral eye and expressed in mmHg

significant correlation with the APP grade ($r = 0.47$, $P = 0.004$). The results indicate, as expected, that elevated IOP at the time of death is a risk factor for axonal transport disruption. It is, however, noteworthy that the correlation between APP grade and terminal IOP ($r = 0.47$) was not high, indicating that considerable variation exists between rats with regard to how raised IOP affects axonal viability.

We next sought to identify the spatial distribution of axonal transport failure. To ascertain whether axonal transport disruption is restricted to the ONH, we performed double labelling immunohistochemistry of APP with myelin basic protein (MBP) in both longitudinal (Fig. 2a–c) and transverse sections of the ONH and proximal ON (Fig. 2d–i). The results clearly showed that APP immunoreactivity was not associated with the myelinated portion of the ON. In addition, it was apparent that APP accumulation in the lamina was not uniform, but regionalised and asymmetric (Fig. 2h), a result that corresponds with previous findings of regionalised RGC and axonal loss in the DBA/2J mouse [16, 44]. To identify whether any distal parts of the optic pathway feature axonal transport disruption, medial and distal sections of the ON and OT were immunostained for APP. Images of the ONH, medial ON and proximal OT from a typical 3-day rat are shown (Fig. 2j–l). No sites of APP accumulation were detected beyond the ONH at any time point, indicating the crucial significance of this structure in the pathology of experimental glaucoma.

To further characterise the nature of axonal transport disruption during experimental glaucoma, we performed immunostaining for two additional molecules, synaptophysin and brain-derived neurotrophic factor (BDNF), that are synthesised by RGCs and undergo anterograde, fast axonal transport [6, 31]. Synaptophysin displayed broadly similar patterns of accumulation at the ONH as APP, although differences were evident. APP was observed in highest amounts in the pre-laminar ONH and in axons at the margins of the ONH; synaptophysin extended further into the ONH and was distributed more evenly (Fig. 3b–i). BDNF also accumulated at the ONH, but was in lower abundance than APP and was largely pre-laminar. BDNF and synaptophysin both colocalized with APP (Fig. 3d–f, j). The results suggest that all molecules undergoing anterograde fast axonal transport are disrupted by chronic IOP elevation. To confirm that accumulations of APP and synaptophysin represent disrupted fast axonal transport, we performed double labelling in ocular hypertensive rats that had been labelled with the neural tracer cholera toxin β-subunit (CTB). After 2 days of experimental glaucoma, CTB was associated with RGC somata, dendrites and axons, and accumulated at the ONH in many of the same axons as APP and synaptophysin (Fig. 3g–i). Double labelling of APP with microglial and astocytic markers (Fig. 3k, l) failed to show any colocalisation indicating APP immunoreactivity resided solely within axons.

Characterisation of axonal cytoskeleton damage during experimental glaucoma

Our next goal was to define the temporal relationship between disrupted axonal transport and damage to the ON

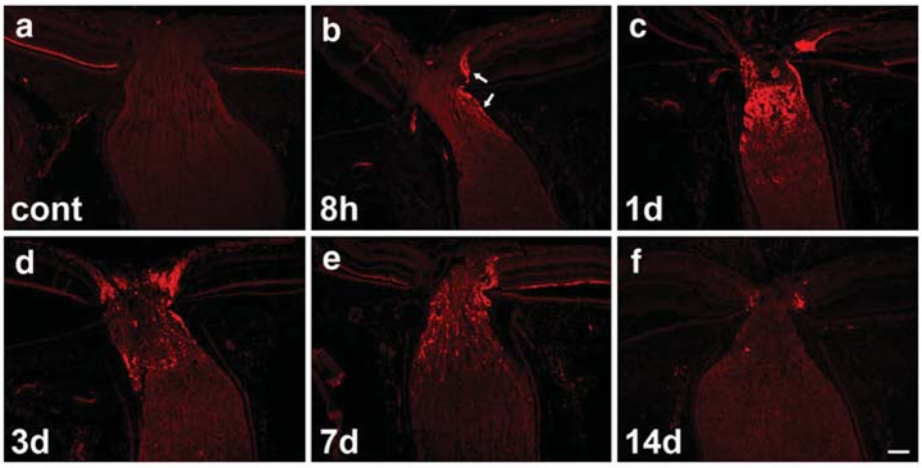

Fig. 1 Accumulation of APP at the ONH at various times following induction of experimental glaucoma. In normal rats, APP immunoreactivity is localised to RGC bodies, but only very low intensity labelling is associated with RGC axons in the ONH and ON (**a**). By 8 h after induction of chronic ocular hypertension, accumulation of APP is evident within some axons in the pre- and post-laminar ONH (**b** *arrows*). At 24 h, intense APP immunoreactivity is typically observed throughout the ONH (**c**). Analysis of rats at 3 d (**d**) and 7 d (**e**) shows APP immunolabelling in the ONH remains high, although not as widespread as 1 day. By 14 days after induction of experimental glaucoma (**f**), not much APP immunoreactivity is observed in the pre- or post-laminar ONH. *Scale bar* 100 μm

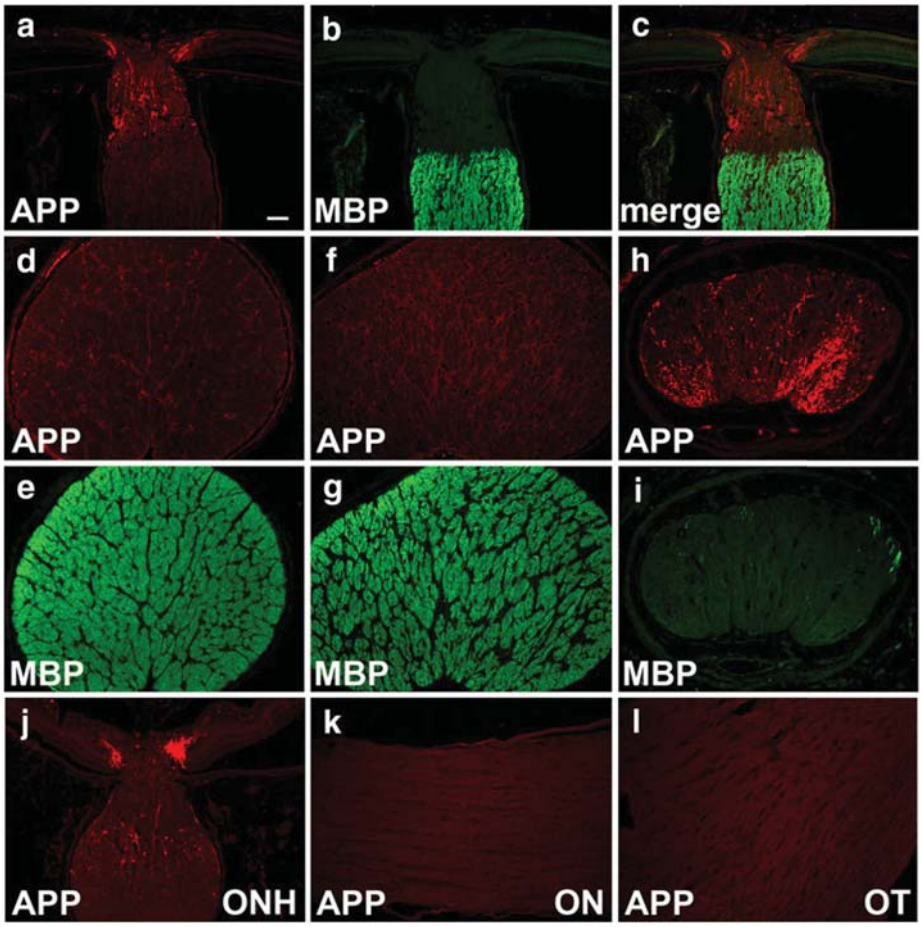

Fig. 2 APP accumulation is restricted to the ONH during experimental glaucoma. **a**–**i** Feature double labelling immunohistochemistry of APP (*red*) with MBP (*green*) showing that axonal transport disruption occurs only within the initial, non-myelinated portion of the nerve; **a**–**c** highlight the ONH and proximal ON of a rat killed 7 days after induction of experimental glaucoma in longitudinal orientation; **d**–**i** show three levels of the proximal ON of a typical 2 day rat in cross-sectional plane, where transverse sections were taken through the ON at 400 µm intervals in a distal to proximal direction showing the mature myelinated ON (**d**, **e**), the early portion of the myelinated ON (**f**, **g**) and the unmyelinated lower neck region (**h**, **i**), which features widespread APP immunolabelling. A rat killed after 3 days of ocular hypertension: APP accretion is clearly visible at the ONH (**j**), but not more distally in the ON (**k**) or OT (**l**). *Scale bar* **a** and **d**–**f** 100 µm, **b**, **c** and **g**–**l** 50 µm

axonal cytoskeleton. This provides information on whether axonal transport deficiencies are functional or mechanical. The standard methodology for evaluating ON injury is quantitative evaluation of transverse sections of the proximal nerve stained with toluidine blue [33]. Accordingly, we analysed ONs for damage at increasing times after induction of raised IOP (Fig. 4). At 1 day, when axonal transport disruption is maximal, there was no evidence of any axonal abnormalities. Between 3 and 14 days, axonal disruption increased dramatically, which was manifest initially as the enlargement of a few axons, then progressed to the appearance of hyperdense axons, myelin disruption and reduced axon density.

The toluidine blue methodology is well suited to identifying gross abnormalities and axonal loss; however, it may lack the sensitivity to detect early or subtle axonal injury. An alternative, complementary technique involves analysis of longitudinal sections immunostained for specific markers of the axonal cytoskeleton. This approach is routinely employed for delineation of axonal damage in other white matter tracts. Initially, we evaluated the sensitivity and efficacy of eight immunohistochemical markers for detection of early ON damage. SMI-32, an antibody that recognises the heavy chain of non-phosphorylated neurofilament (npNFH), was unequivocally the most sensitive indicator. This was the case both at 3 and 7 days, in rats with slight damage and in rats with numerous abnormalities. The pattern of SMI-32 immunolabelling changed from one consisting of light, uniform staining of axons to one featuring axonal beading, swellings and spheroids. Representative images of the eight markers in sections from the medial ON of a 3-day rat with only a small number of injured fibres are shown (Supplementary Fig. 1a).

Next, we utilised SMI-32 to quantify axonal damage. Sections from the medial ON and proximal OT of 1, 3 and 7 days rats were immunolabelled for SMI-32 (see Supplementary Fig. 1b for typical staining patterns), and the extent of abnormalities calculated. The results, revealed no evidence of axonal injury in either location at 1 day, but significant damage by 3 days, and fourfold greater damage by 7 days (Table 2). Comparison of the ON with the OT showed the mean damage level in the OT was somewhat higher than the ON at the 3-day time point, but there was

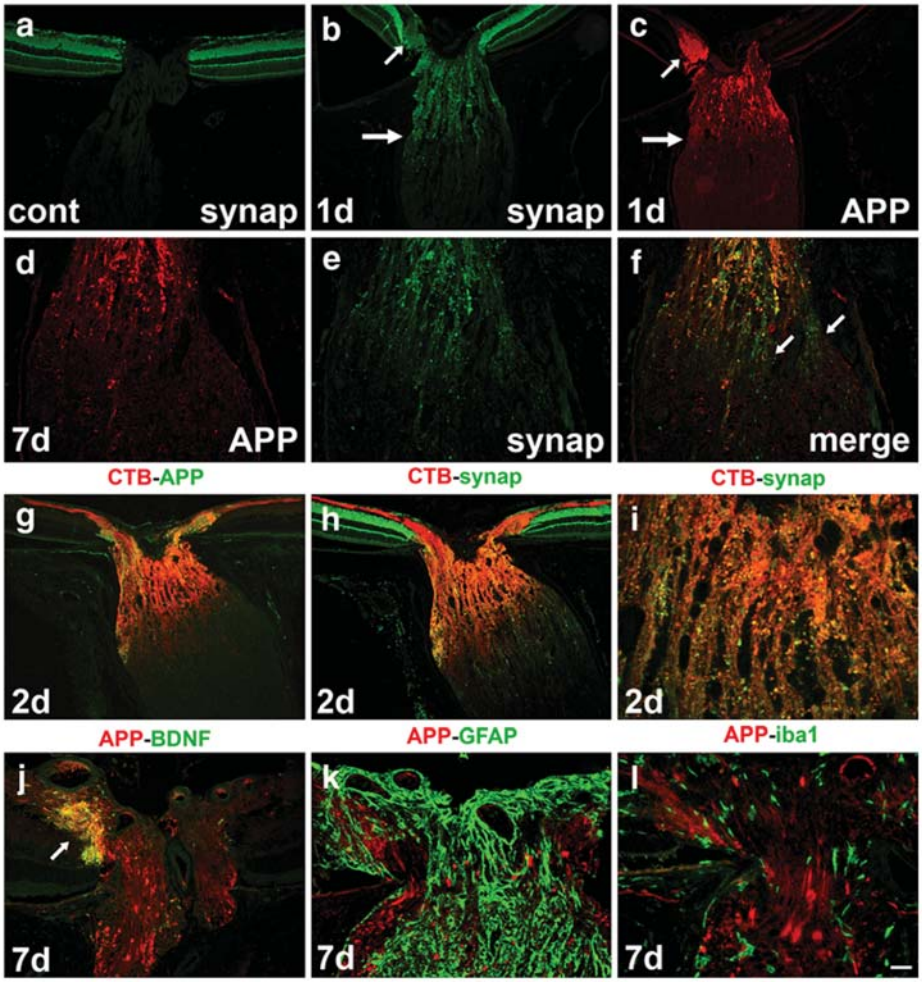

Fig. 3 Comparison of APP with other markers of axonal transport disruption after induction of experimental glaucoma. In normal rats, synaptophysin immunoreactivity is localised to post-synaptic terminals in the retina, but only very low intensity labelling is associated with RGC axons in the ONH and ON (**a**). At 24 h after induction of experimental glaucoma, accumulation of synaptophysin (**b**) is observed throughout the ONH in a similar pattern to APP (**c**). Synaptophysin colocalises with APP, as seen in this rat killed at 7 days (**d–f**). At 2 days after induction of experimental glaucoma, CTB (**g–i** *red*) is associated with RGC somata, dendrites and axons in the retina and accumulates throughout the ONH. CTB colocalises with APP (**g** *green*) and with synaptophysin (**h**, **i** *green*). In every rat, synaptophysin immunoreactivity extends further into the ONH than APP (**b**, **c**, **f**, **h** *arrows*). BDNF (**j** *green*) also colocalises with APP (**j** *red*), predominantly in the pre-laminar ONH (*arrow*). In contrast, the astrocytic marker GFAP (**k** *green*) and the microglial marker iba1 (**l** *green*) do not colocalise with APP (**k**, **l** *red*). *CTB* cholera toxin β-subunit. *Scale bar* **a–c**, **j**, **k** 100 μm, **d–f** 50 μm, **g–i** l, 25 μm

no difference at 7 days. A number of conclusions can be drawn: first, SMI-32 and toluidine blue provided complementary results; secondly, despite axonal transport disruption at the ONH commencing by 8 h, no axonal cytoskeletal abnormalities were evident in the myelinated nerve at 24 h; thirdly, degeneration may have commenced, or proceeded more rapidly, in the distal part of the axon.

The SMI-32 analyses described above relate to the central portion of the visual pathway. To better understand whether the primary locus of axonal degeneration is at the distal or the proximal end of pathway, it is necessary to analyse the entire tract, from the ONH to the lateral geniculate nucleus and superior colliculus. Accordingly, we performed a spatial assessment of SMI-32 immunostaining in rats subjected to experimental glaucoma. The results were as follows: (1) no alterations to SMI-32 immunostaining were noted in the visual pathway at 8 h; (2) at 1 d, SMI-32 abnormalities, visualised as beading and swellings, were evident in the pre-laminar and laminar ONH in some, but not all animals, however, no such abnormalities were manifest distal to this location in the entire myelinated ON and OT; (3) after 3 days, SMI-32 abnormalities were apparent throughout the length of the white matter tract from the ONH via the optic chiasm to the brachium of the superior colliculus. Figure 5 shows representative images from the ONH, optic chiasm and distal

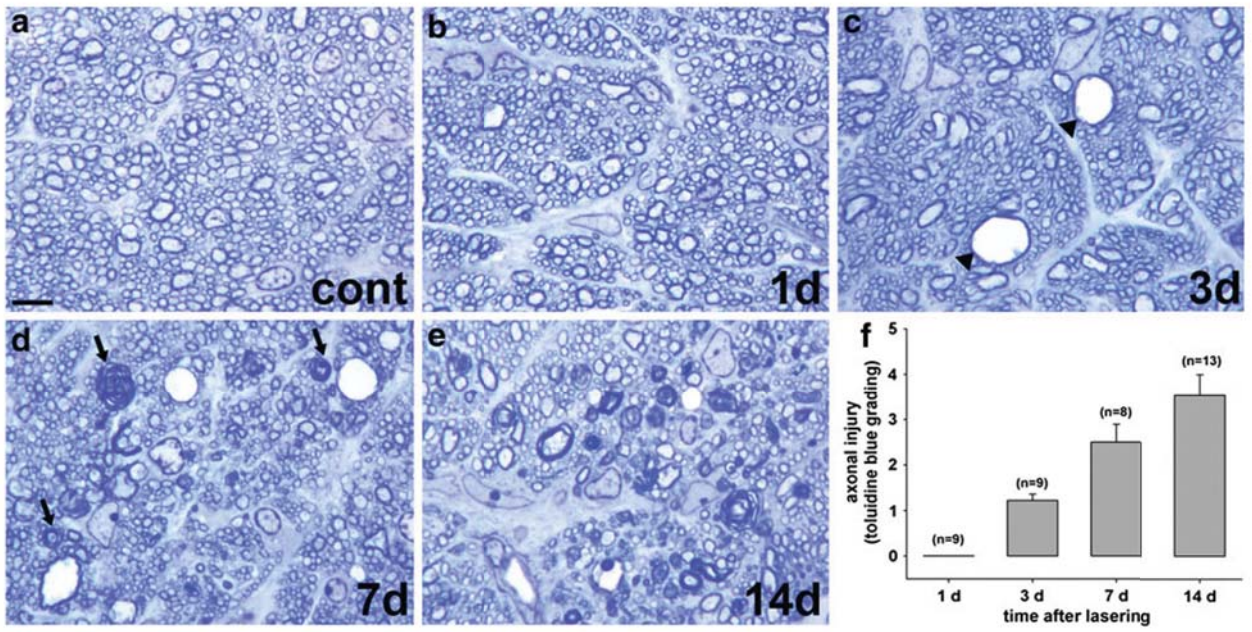

Fig. 4 Transverse sections of ONs stained with toluidine blue at various times subsequent to induction of experimental glaucoma. At 1 day after induction of chronic ocular hypertension (**b**), the axonal structure is unchanged relative to control ONs (**a**). By 3 days, a few enlarged axons (*black arrowheads*) are typically visible (**c**). After 7 days of experimental glaucoma, reduced axon density and myelin disruption (*black arrows*) are evident (**d**), features that are even more prevalent after 14 days of raised pressure (**e**). Mean axonal injury at increasing times after induction of experimental glaucoma is shown (**f**). *Scale bar* 25 μm

Table 2 Quantification of SMI-32 abnormalities at various times after induction of experimental glaucoma

Time	Control	1 day	3 days	7 days
Medial ON	0.39 ± 0.28	0.13 ± 0.13	24.7 ± 7.2	106.7 ± 31.0†
Proximal OT	0.40 ± 0.17	0.38 ± 0.30	37.0 ± 9.1*	110.5 ± 26.7†

Immunoreactivities were quantified (see "Materials and methods") and expressed as area in pixels ($\times 10^3$)

All values are presented as mean ± SEM, where $n = 9$ (control), $n = 8$ (1 day), $n = 10$ (3 days), $n = 9$ (7 days)

Statistical analysis of immunoreactivities was performed by ANOVA followed by a post-hoc Tukey's test for multiple comparisons

Significant differences versus controls are indicated by * $P < 0.05$ and † $P < 0.001$

OT. To confirm axonal cytoskeletal abnormalities at the ONH at 1 day, sections were also immunostained for neurofilament medium. The pattern of abnormalities produced was almost identical to SMI-32 (data not shown). The overall results indicate that axonal cytoskeleton changes occur first at the ONH.

There is debate as to whether increased or decreased neurofilament phosphorylation signifies injury in neurodegenerative diseases in general [35] and glaucoma in particular [22, 42, 45]. As described above, we observed numerous npNFH (SMI-32) abnormalities in ON sections; however, it is unclear whether this represents an overall dephosphorylation of NFH or merely breakdown of the more labile non-phosphorylated subunit. Thus, we undertook Western blotting in ON samples from control and treated eyes using two antibodies, SMI-32 and SMI-37, which exclusively recognise npNFH (Fig. 6). Each antibody detected a protein of 200 kDa signifying native npNFH, but in treated ONs, a continuum of lower molecular weight proteins reactive to SMI-32 and SMI-37 was also observed. Densitometry showed no significant (SMI-32, $P = 0.42$; SMI-37, $P = 0.24$) difference in the intensity of the 200 kDa species between the 3, 7 and 14-day time points. In contrast, there was a marked increase in intensity of the lower molecular weight products over the time period analysed (SMI-32, $P = 0.036$; SMI-37, $P = 0.011$). The data indicate that there is no increase in npNFH in the ON during ocular hypertension-induced axonal degeneration, rather there is a progressive degradation of npNFH. Western blots performed using the antibody SMI-31, which exclusively recognises pNFH, failed to reveal a continuum of lower molecular weight protein bands.

The ONH is the site of putative axonal regeneration failure during experimental glaucoma

In the ON, axonal injury is not followed by any beneficial regeneration. Severed or crushed RGC axons display only

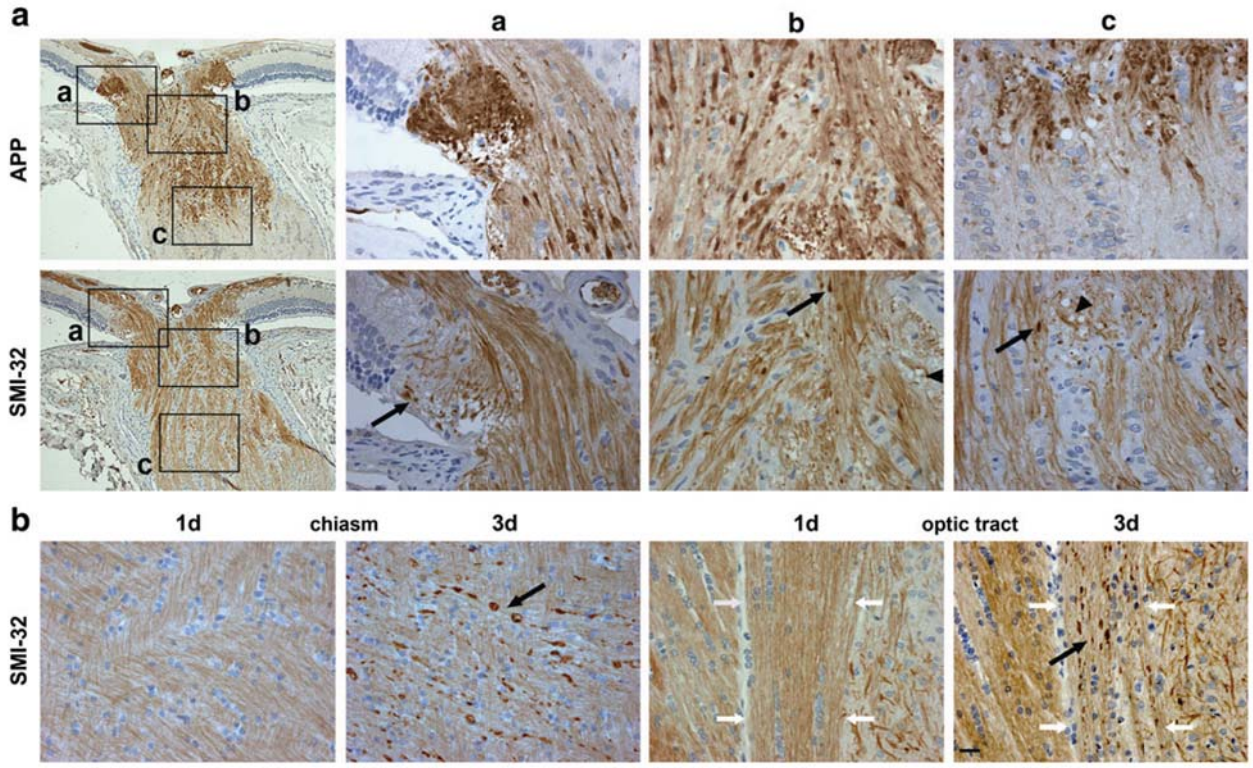

Fig. 5 Axonal degenerative changes in the visual pathway at early time points during experimental glaucoma. **a** Representative images of APP and SMI-32 staining in three regions of the ONH at 1 day after induction of chronic ocular hypertension. At 1 day, widespread APP accumulation is evident in axons throughout the ONH. SMI-32-labelled axon fibres show swellings and beading (*arrows*) and vacuolization (*arrowhead*) in areas of axonal transport disruption. **b** Representative images of SMI-32 staining at the level of the optic chiasm and optic tract 1 and 3 days after induction of chronic ocular hypertension. Unlike the ONH, the myelinated ON and optic tract appear normal at 1 day. By 3 days, SMI-32 abnormalities are evident throughout the length of the white matter tract (*black arrows*). The boundaries of the optic tract are demarcated by *white arrows*. *Scale bar* **a** ONH overview, 45 µm, magnified images, 16.7 µm, **b** 25 µm

transient, local sprouting proximal to the site of damage [3]. Unlike ON crush or transection, RGCs are lost gradually during experimental glaucoma; moreover, the locus of injury to RGCs is unclear. Thus, evaluation of the spatiotemporal pattern of any endogenous axonal regeneration that occurs during glaucoma will be greatly informative to our understanding of the pathology of the disease. To achieve this objective, we analysed expression of growth-associated protein 43 (Gap43), the classical marker of axonal regeneration in the ON [4, 13, 25].

In normal adult rats, negligible Gap43 immunoreactivity was associated with RGC bodies or their axons (Fig. 7a). The situation was unchanged at 24 h after induction of raised IOP, even in rats with widespread axonal transport disruption and neurofilament damage (Fig. 7b). By 3 days, limited Gap43 immunohistochemistry was detectable in RGC axons of some rats, particularly at the level of the prelaminar ONH (Fig. 7c), whilst Western blotting showed that all rats analysed had a markedly upregulated level of retinal Gap43 protein (Fig. 8a, b). The expression of Gap43 increased further at 7 and 14 days, as evidenced by immunohistochemistry (Fig. 7d–i) and Western blotting (Fig. 8a, b). The pattern of Gap43 immunoreactivity in ocular hypertensive rats was broadly equivalent to that of APP with accumulation throughout the ONH, but was significantly delayed in onset. Although APP immunostaining was maximal at 1 day and then gradually declined, the opposite occurred for Gap43. Unlike APP, a few Gap43-positive axons extended beyond the ONH into the initial myelinated portion of the ON (Fig. 6f). Nevertheless, Western blotting (Fig. 8b) showed no measureable increase in the Gap43 content of the myelinated ON at 7 days. The overall results suggest that injured RGCs attempt to regenerate their axons during experimental glaucoma, but the process fails at the ONH. A caveat to this conclusion is that Gap43 expression alone is not conclusive of axonal regeneration. To verify that injured RGCs, rather than healthy cells, are responsible for re-instigating Gap43 expression, we performed double labelling of Gap43 with heat shock protein 27 (Hsp27) in retinas subjected to 14 days of experimental glaucoma. Hsp27, a molecular chaperone induced by cellular stress, is not constitutively

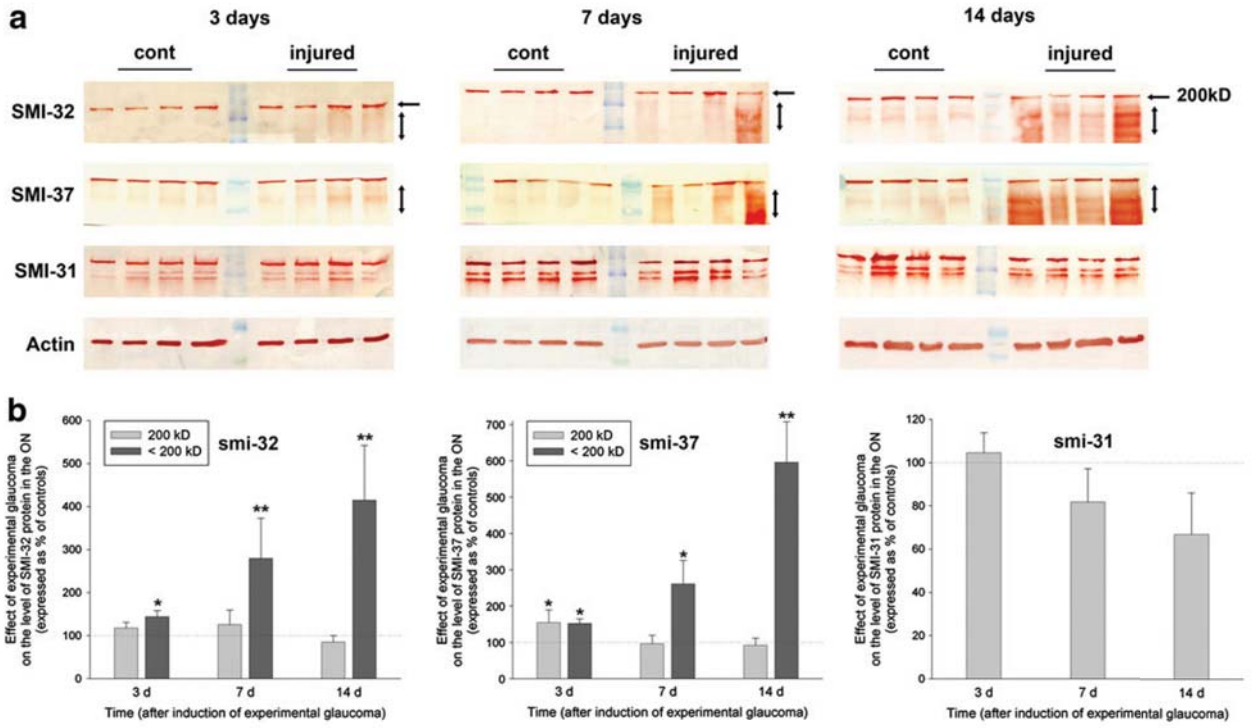

Fig. 6 Expression of npNFH and pNFH in the ON following induction of experimental glaucoma, as evaluated by Western blotting using two antibodies, SMI-32 and SMI-37, that recognise npNFH and one antibody, SMI-31, that recognises pNFH. **a** Representative blots from control and treated ONs from four animals killed at 3, 7 and 14 days are shown. Both antibodies recognise a 200 kDa band that represents native npNFH. A continuum of lower molecular weight bands reactive to SMI-32 and SMI-37, but not SMI-31, are visible in the treated ONs, as indicated by the *vertical arrows*. **b** Densitometry measurements (normalised for actin and expressed relative to the control ON) are provided in the *graphs* below, where $n = 7$ (3 days), $n = 7$ (7 days) and $n = 4$ (14 days). $^{*}P < 0.05$, $^{**}P < 0.01$ compared with controls by Mann–Whitney U test

expressed by RGCs; however, within an ongoing pathological setting, such as axotomy or glaucoma, is persistently upregulated in severely injured RGCs [21, 24]. The results showed that many RGCs were immunopositive for both Hsp27 and Gap43 (Fig. 8c) indicating their increased stress status.

The pattern of injury during experimental glaucoma displays pathological similarities to optic nerve crush, but not to NMDA-induced excitotoxicity.

Hitherto, it is unclear whether degeneration of RGC axons precedes degeneration of RGC somata during glaucoma. Whilst a body of evidence supports this hypothesis, other data endorse the view that atrophy of RGC perikarya occurs first [45]. To elucidate the timing of RGC somatic injury, we performed a temporal analysis of RGC gene expression during experimental glaucoma. The rationale for this approach is that down-regulations of RGC-specific mRNAs, including Thy1 and neurofilament light (NFL), are sensitive early indicators of RGC viability [10, 43]. Following induction of raised IOP, negligible down-regulation of Thy1 and NFL had occurred by 24 h (Fig. 9a). By 3 days, the levels of both mRNAs had decreased, but the changes failed to reach statistical significance. After 7 days, highly significant ($P < 0.001$) decreases of Thy1 and NFL were measured. The time courses of these changes are delayed compared with the axonal responses described above, indicating that altered gene transcription occurs subsequent to axonal disruption.

To impart perspective on the results, we assessed RGC gene expression, disruption of axonal transport and damage to the axonal cytoskeleton in rats that underwent NMDA-induced excitotoxicity. NMDA treatment is the classical method of eliciting somato-dendritic death of RGCs, since NMDA receptors are present on the soma but not the axon of the RGC. Moreover, excitotoxicity is implicated in the pathogenesis of glaucoma [7]. The results were in complete contrast to those of the glaucoma model. Down-regulation of Thy1 and NFL mRNAs was in evidence as early as 6 h after NMDA administration and by 24 h both mRNAs were maximally down-regulated, signalling death of the RGC soma (Fig. 9b). Despite the fatal injury to the RGC body, no disruption to the axonal cytoskeleton, either at the ONH or within the ON, was detectable at 24 h after NMDA administration (Fig. 9c). By 2 days, however, axonal

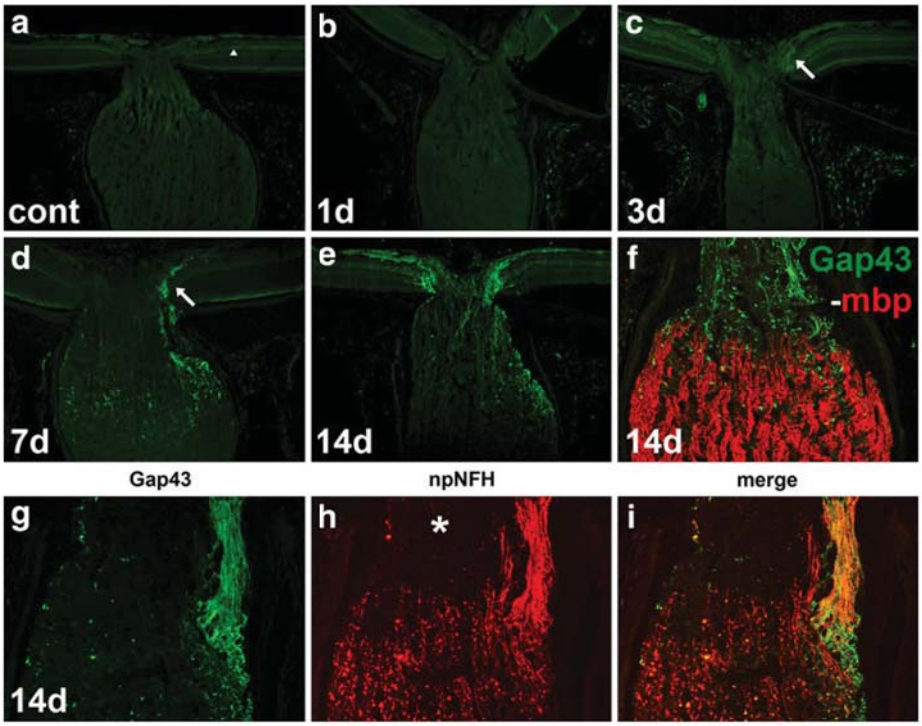

Fig. 7 Gap43 expression in RGC axons following induction of experimental glaucoma. In control rats (**a**), minimal Gap43 immunoreactivity is associated with RGC bodies or their axons, but a lamina of punctae is visible in the inner plexiform layer at the border with the INL (*arrowhead*). No discernible alteration to the pattern of Gap43 staining is evident at 1 day (**b**) after induction of chronic ocular hypertension. By 3 days (**c**), occasional Gap43-immunopositive fibres are apparent in the pre-laminar ONH of some rats (*arrow*). After 7 days (**d**), numerous axons in the pre- (arrow) and post-laminar ONH label for Gap43. Three representative rats are shown after 14 days of experimental glaucoma: the first rat (**e**) displays intense Gap43 immunoreactivity in the nerve fibre layer and within the ONH; the second rat (**f**) displays abundant Gap43-positive axons throughout the ONH with a few axons extending into the initial myelinated portion of the ON (Gap43, *green*, *mbp red*). The third rat (**g–i**) has substantial axonal loss in the ONH (*highlighted by asterisk*) and features robust Gap43 labelling of surviving axons in this region of the ON. *Scale bar* **a–e** 100 μm, **f–i** 50 μm

swelling and beading was visible throughout the entire ON and OT (Fig. 9d). Unlike experimental glaucoma, no accumulation of APP occurred at the ONH following NMDA treatment (Fig. 9e). The overall results show the two paradigms of RGC death have quite distinct pathologies.

Further evidence illustrating the different injury profiles of experimental glaucoma and excitotoxicity was provided by comparison of their Hsp27 and Gap43 responses (Supplementary Fig. 2a, b), which, as discussed above, can be viewed as indicative of ongoing somatic and axonal injury, respectively. After 14 days of chronic ocular hypertension, a proportion of surviving (β_3-tubulin-labelled) RGCs expressed Hsp27 and synthesized Gap43. In contrast, 7 days after NMDA administration, surviving RGCs were Hsp27- and Gap43-negative. Thus, excitotoxicity causes acute, fatal injury to a proportion of RGCs, but surviving RGCs are somatically and axonally healthy, whilst glaucoma damages the axon, but spares the soma of a proportion of RGCs, leading to ongoing perikaryal stress and delayed death. To ascertain whether the response seen during glaucoma is characteristic of ON crush, we also analysed rats subjected to intraorbital ON crush 14 days previously. Similar to glaucoma, RGCs from ON crush rats expressed Hsp27 and synthesized Gap43 (Supplementary Fig. 2a, b). When compared with glaucoma, substantially more Gap43 immunoreactivity was observed, which extended well beyond the ONH. This is to be expected; however, as the entire population of RGCs is affected by crush and the site of crush was 3 mm distal to the ONH.

Discussion

In the current study, we have employed a rat model of optic neuropathy induced by chronic elevation of the IOP together with a combination of histology, immunohistochemistry, Western blotting and real-time RT-PCR to address the spatial and temporal nature of RGC pathology. As identified by Morrison et al. [33], the advantage of such a model compared with spontaneous models of chronic ocular hypertension is that the timing of the IOP increase following

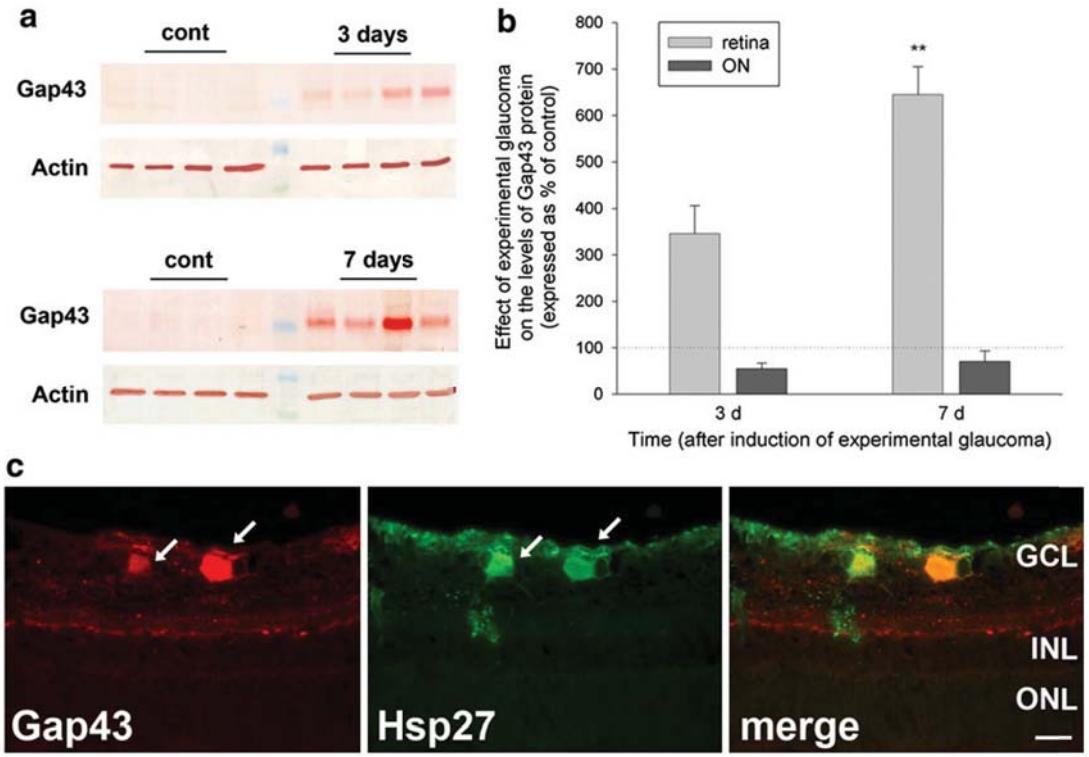

Fig. 8 Gap43 expression in the retina and ON following induction of experimental glaucoma. **a** Expression of Gap43 in the retina as evaluated by Western blotting. Representative blots from control and treated retinas from four animals killed at 3 and 7 days after induction of chronic ocular hypertension are shown. **b** Densitometry measurements (normalised for actin and expressed relative to the control eye) for retinas and ONs are shown in the accompanying *graph*, where $n = 7$. $^{**}P<0.01$ by paired Student's t test (control vs. treated). **c** Double labelling immunofluorescence of Gap43 with Hsp27 in a representative rat killed 14 days after induction of experimental glaucoma. Gap43-positive RGCs frequently express Hsp27. *GCL* ganglion cell layer, *INL* inner nuclear layer, *ONL* outer nuclear layer. *Scale bar* 25 μm

the surgical intervention is known. This engenders greater confidence in conclusions drawn about the chronology of pathological events. The data presented here provide robust support for the hypothesis that the ONH is the pivotal, and likely the primary, site of RGC injury following moderate elevation of IOP, with resulting anterograde degeneration of axons and retrograde injury and death of somas.

Anterograde fast axonal transport conveys newly synthesized molecules away from the cell body. Obstruction of this process rapidly compromises the integrity of the distal axon. In glaucoma, the lamina cribrosa of the ONH has long been considered a likely site of axonal transport failure. This hypothesis was formed after pioneering work performed in monkeys, which demonstrated that radioactive leucine accumulated within axons at the ONH after moderate elevation of IOP [1, 29, 37, 38, 40]. Similar results have been found in pigs [2]. However, current glaucoma research is mainly performed in rodents, and rodents lack a true lamina cribrosa. Rats possess a rudimentary structure, whilst mice have no connective tissue [15, 32]. As such, it is important to ascertain whether the ONH is an important site of axonal transport failure in rodents. We achieved this aim by immunolabelling for proteins (APP, synpatophysin and BDNF) that are routinely synthesised by RGCs and conveyed along the ON by fast axonal transport [6, 31]. Because the molecules analysed are of different molecular weights and have distinct physiological roles, this approach provides biologically meaningful information about transport viability during chronic ocular hypertension. Our results showed accumulation of all three proteins within axons at the ONH, but not distal to this location in the myelinated ON or OT, results confirmed by the use of the neural tracer CTB. The time course correlated well with the early monkey studies, with detectable accumulation by 8 h and widespread dysfunction from 24 h. By 14 days, however, the mean IOP had decreased markedly and disruption was measurably lower. The reduced accumulation of APP at this time point can be accounted for in two ways: (1) in axons that were not irreversibly damaged, the lower IOP allows normal transport of APP to resume; (2) axons that were irreversibly damaged by high IOP have now degenerated. Quigley and

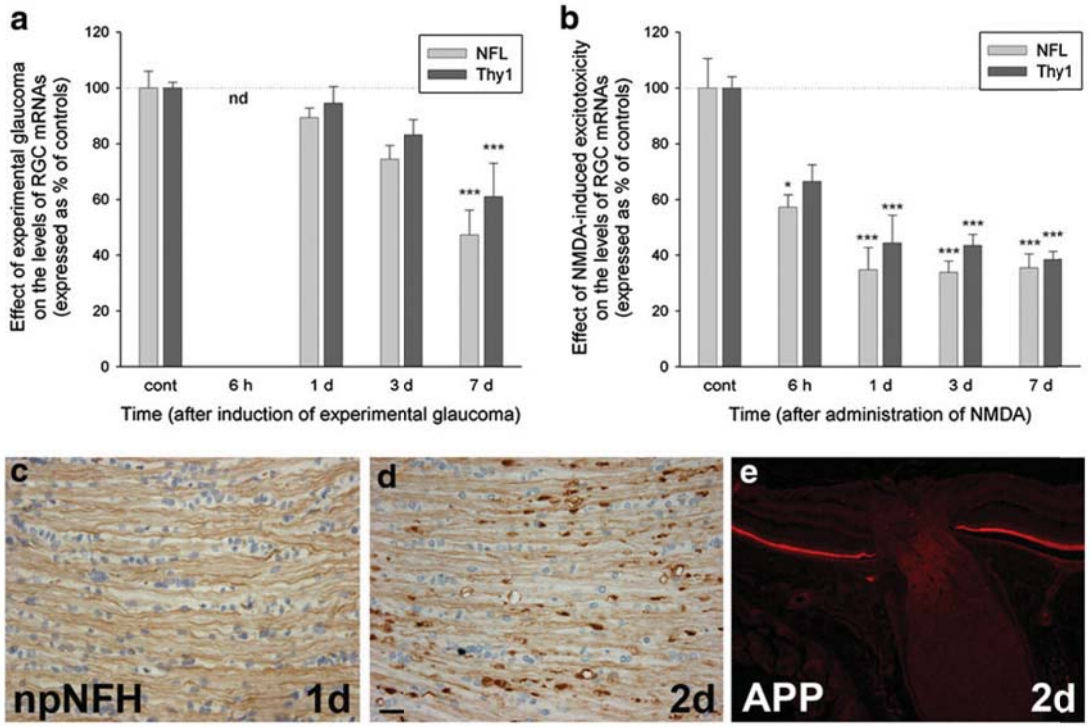

Fig. 9 Temporal characterisation of downregulation of the RGC-specific mRNAs Thy1 and NFL in the retina following induction of experimental glaucoma (**a**, $n = 4$–9) and NMDA-induced excitotoxicity (**b**, $n = 6$–7), as determined by quantitative real-time RT–PCR. $*P < 0.05$, $***P < 0.001$ by one-way ANOVA followed by post hoc Tukey's test. **c**–**e** Evaluation of axonal degeneration and axonal transport disruption in the ONH after NMDA-induced excitotoxicity. At 1 day after NMDA treatment, SMI-32 (npNFH) immunostaining throughout the ONH and ON appears normal (**c**). By 2 days, numerous axonal swellings and abnormalities are visible throughout the white matter tract (**d**). No accumulation of APP is evident at the ONH following administration of NMDA, as shown in this rat killed at 2 days (**e**). *Scale bar* **c**, **d** 25 μm, **e** 100 μm

Addicks [38] noted that a return to normal IOP within 1 week restored transport in some axons in monkeys.

Previous studies in rats have found results compatible with the hypothesis that chronically elevated IOP disrupts active retrograde axonal transport to the retina at the level of the ONH [28, 42], findings consistent with this study. In contrast, Crish et al. [12] showed that axonal transport dysfunction in both spontaneous and induced rodent models of IOP elevation appeared first at the superior colliculus and progressed distal proximal, with ONH deficits occurring much later. The disparity between these studies may relate to the models used. In the micro-bead model used by Crish et al., the IOP elevations were maximally 10 mmHg and maintained for long periods, whilst the laser model used here and by others produces typical IOP rises of 25 mmHg for shorter periods. It is possible that modest, prolonged increases in IOP gradually compromise axonal transport efficiency, which is first manifest at the distal synapses, whilst greater increases in IOP physically constrict axons at the ONH.

We found axonal cytoskeletal abnormalities, including neurofilament beading and swellings, in the ONH at 24 h after induction of raised IOP. This suggests that axonal transport disruption is mechanical, and not simply functional, in a subset of axons at very early time points. Nevertheless, in other axons, it is likely that active axonal transport dysfunction significantly preceded physical damage, an argument supported by the results of Salinas-Navarro et al. [42], who counted fewer RGCs in retinas back-labelled by a tracer that undergoes active transport than in retinas back-labelled by a passively diffusing tracer. In contrast to the ONH, no axonal cytoskeletal abnormalities were present in the entire myelinated ON and OT until 3 days, with progressively greater damage at 7 and 14 days. The results support the findings of others that IOP elevations of the magnitude recorded in this study elicit an early insult at the lamina of the ONH with Wallerian-like degeneration of axons distal to the site of injury [16, 20, 38]. Regarding axonal cytoskeletal degeneration, a previous study in monkeys showed accumulation of npNFH in the ON following raised IOP [22]. Using immunohistochemistry, we found a similar, robust increase in npNFH labelling in degenerating axons; however, Western blotting of ON samples revealed no increase in the npNFH 200-kDa

band, rather the appearance of a continuum of low-molecular weight bands. These bands almost certainly represent breakdown products and may account for the increased immunoreactivity in tissue sections. npNFH is more labile and sixfold more susceptible than pNFH to degradation by calpain [34] and our data indicate that it degenerates more rapidly than pNFH.

The strikingly early nature of pathological changes at the ONH prompted the question as to whether RGC somas are irreversibly injured at this same time. Our data indicate not. Down-regulation of RGC-specific mRNAs, which are sensitive early indicators of RGC viability [10, 16, 43], occurred subsequent to axonal changes at the ONH and markedly later than in retinas subjected to NMDA-induced somatic excitotoxicity. It can be argued that the elevated IOP placed a considerable physiological stress on a proportion of RGC somas as evidenced by their upregulation of the molecular chaperone Hsp27; yet, this response also occurred in rats with normal IOPs that underwent ON crush and may simply have been caused by damage to the axonal compartment.

The long-term objective of glaucomatous pharmacotherapy is not merely neuroprotection of surviving RGCs, but regeneration of injured/disconnected axons. Within the CNS, endogenous regenerative attempts are always unsuccessful. In the visual system, RGC axons display only transient, local sprouting, proximal to the lesion site after ON crush [3], and interestingly, even this limited response occurs only when the injury is within 3 mm of the eye, not if it is administered to the distal ON [13]. Unlike the catastrophic injury caused by traumatic axonopathies, such as ON crush, RGCs are lost gradually during chronic ocular hypertension and only a proportion of the population will die. It follows that the inhibitory environment for regeneration may be less pronounced and regeneration strategies more effective. Surprisingly, no data are available on the endogenous regenerative response of RGCs during experimental glaucoma. Delineating such information is of utmost importance. We have shown in the current study that RGC axonal injury is first evident at the ONH and that the somas remain viable for a number of days; thus, we hypothesised that endogenous RGC regeneration should proceed at least to the ONH. To examine putative axonal regeneration, we employed Gap43, the quintessential marker of axon growth, but one which can be expressed in non-regenerative situations [25], hence the caveat "putative". Upregulation of Gap43 protein in the retina was first detectable by 3d after IOP elevation. By 14 days, numerous Gap43-positive axons were observed in the pre-laminar ONH, some extending to the transition region of the ONH. For comparative purposes, we analysed Gap43 in rats subjected to NMDA-induced excitotoxicity and ON crush. After NMDA treatment, no Gap43 expression was detected, a result consistent with early RGC somal death. After ON crush, substantial Gap43 immunoreactivity was observed, which extended to the crush site. The overall results provide further evidence that the ONH is the principal site of axonal injury in this rat glaucoma model and that chronically raised IOP induces a crush-like insult at this location.

Acknowledgments The authors are grateful to the NHMRC (508123, 565202, 626964) and the Ophthalmic Research Institute of Australia for providing financial support and to Mark Daymon for expert technical assistance.

References

1. Anderson DR, Hendrickson A (1974) Effect of intraocular pressure on rapid axoplasmic transport in monkey optic nerve. Invest Ophthalmol 13:771–783
2. Balaratnasingam C, Morgan WH, Bass L, Matich G, Cringle SJ, Yu DY (2007) Axonal transport and cytoskeletal changes in the laminar regions after elevated intraocular pressure. Invest Ophthalmol Vis Sci 48:3632–3644
3. Benowitz L, Yin Y (2008) Rewiring the injured CNS: lessons from the optic nerve. Exp Neurol 209:389–398
4. Blaugrund E, Lavie V, Cohen I, Solomon A, Schreyer DJ, Schwartz M (1993) Axonal regeneration is associated with glial migration: comparison between the injured optic nerves of fish and rats. J Comp Neurol 330:105–112
5. Buckingham BP, Inman DM, Lambert W et al (2008) Progressive ganglion cell degeneration precedes neuronal loss in a mouse model of glaucoma. J Neurosci 28:2735–2744
6. Caleo M, Menna E, Chierzi S, Cenni MC, Maffei L (2000) Brain-derived neurotrophic factor is an anterograde survival factor in the rat visual system. Curr Biol 10:1155–1161
7. Casson RJ (2006) Possible role of excitotoxicity in the pathogenesis of glaucoma. Clin Exp Ophthalmol 34:54–63
8. Chauhan BC, Levatte TL, Garnier KL et al (2006) Semiquantitative optic nerve grading scheme for determining axonal loss in experimental optic neuropathy. Invest Ophthalmol Vis Sci 47:634–640
9. Chidlow G, Holman MC, Wood JP, Casson RJ (2010) Spatiotemporal characterization of optic nerve degeneration after chronic hypoperfusion in the rat. Invest Ophthalmol Vis Sci 51:1483–1497
10. Chidlow G, Osborne NN (2003) Rat retinal ganglion cell loss caused by kainate, NMDA and ischemia correlates with a reduction in mRNA and protein of Thy-1 and neurofilament light. Brain Res 963:298–306
11. Chidlow G, Wood JP, Manavis J, Osborne NN, Casson RJ (2008) Expression of osteopontin in the rat retina: effects of excitotoxic and ischemic injuries. Invest Ophthalmol Vis Sci 49:762–771
12. Crish SD, Sappington RM, Inman DM, Horner PJ, Calkins DJ (2010) Distal axonopathy with structural persistence in glaucomatous neurodegeneration. Proc Natl Acad Sci USA 107:5196–5201

13. Doster SK, Lozano AM, Aguayo AJ, Willard MB (1991) Expression of the growth-associated protein GAP-43 in adult rat retinal ganglion cells following axon injury. Neuron 6:635–647
14. Ebneter A, Casson RJ, Wood JP, Chidlow G (2010) Microglial activation in the visual pathway in experimental glaucoma: spatio-temporal characterisation and correlation with axonal injury. Invest Ophthalmol Vis Sci
15. Fujita Y, Imagawa T, Uehara M (2000) Comparative study of the lamina cribrosa and the pial septa in the vertebrate optic nerve and their relationship to the myelinated axons. Tissue Cell 32:293–301
16. Howell GR, Libby RT, Jakobs TC et al (2007) Axons of retinal ganglion cells are insulted in the optic nerve early in DBA/2J glaucoma. J Cell Biol 179:1523–1537
17. Jakobs TC, Libby RT, Ben Y, John SW, Masland RH (2005) Retinal ganglion cell degeneration is topological, but not cell type specific in DBA/2J mice. J Cell Biol 171:313–325
18. John SW (2005) Mechanistic insights into glaucoma provided by experimental genetics the Cogan lecture. Invest Ophthalmol Vis Sci 46:2649–2661
19. John SW, Smith RS, Savinova OV et al (1998) Essential iris atrophy, pigment dispersion, and glaucoma in DBA/2J mice. Invest Ophthalmol Vis Sci 39:951–962
20. Johnson EC, Deppmeier LM, Wentzien SK, Hsu I, Morrison JC (2000) Chronology of optic nerve head and retinal responses to elevated intraocular pressure. Invest Ophthalmol Vis Sci 41:431–442
21. Kalesnykas G, Niittykoski M, Rantala J et al (2007) The expression of heat shock protein 27 in retinal ganglion and glial cells in a rat glaucoma model. Neuroscience 150:692–704
22. Kashiwagi K, Ou B, Nakamura S, Tanaka Y, Suzuki M, Tsukahara S (2003) Increase in dephosphorylation of the heavy neurofilament subunit in the monkey chronic glaucoma model. Invest Ophthalmol Vis Sci 44:154–159
23. Kass MA, Heuer DK, Higginbotham EJ et al (2002) The Ocular Hypertension Treatment Study: a randomized trial determines that topical ocular hypotensive medication delays or prevents the onset of primary open-angle glaucoma. Arch Ophthalmol 120:701–713
24. Krueger Naug AM, Emsley JG, Myers TL, Currie RW, Clarke DB (2002) Injury to retinal ganglion cells induces expression of the small heat shock protein Hsp27 in the rat visual system. Neuroscience 110:653–665
25. Leon S, Yin Y, Nguyen J, Irwin N, Benowitz LI (2000) Lens injury stimulates axon regeneration in the mature rat optic nerve. J Neurosci 20:4615–4626
26. Levkovitch-Verbin H, Quigley HA, Martin KR, Valenta D, Baumrind LA, Pease ME (2002) Translimbal laser photocoagulation to the trabecular meshwork as a model of glaucoma in rats. Invest Ophthalmol Vis Sci 43:402–410
27. Livak KJ, Schmittgen TD (2001) Analysis of relative gene expression data using real-time quantitative PCR and the 2(-Delta Delta C(T)) Method. Methods 25:402–408
28. Martin KR, Quigley HA, Valenta D, Kielczewski J, Pease ME (2006) Optic nerve dynein motor protein distribution changes with intraocular pressure elevation in a rat model of glaucoma. Exp Eye Res 83:255–262
29. Minckler DS, Bunt AH, Johanson GW (1977) Orthograde and retrograde axoplasmic transport during acute ocular hypertension in the monkey. Invest Ophthalmol Vis Sci 16:426–441
30. Morin PJ, Abraham CR, Amaratunga A et al (1993) Amyloid precursor protein is synthesized by retinal ganglion cells, rapidly transported to the optic nerve plasma membrane and nerve terminals, and metabolized. J Neurochem 61:464–473
31. Morin PJ, Liu NG, Johnson RJ, Leeman SE, Fine RE (1991) Isolation and characterization of rapid transport vesicle subtypes from rabbit optic nerve. J Neurochem 56:415–427
32. Morrison J, Farrell S, Johnson E, Deppmeier L, Moore CG, Grossmann E (1995) Structure and composition of the rodent lamina cribrosa. Exp Eye Res 60:127–135
33. Morrison JC, Johnson EC, Cepurna W, Jia L (2005) Understanding mechanisms of pressure-induced optic nerve damage. Prog Retin Eye Res 24:217–240
34. Pant HC (1988) Dephosphorylation of neurofilament proteins enhances their susceptibility to degradation by calpain. Biochem J 256:665–668
35. Petzold A (2005) Neurofilament phosphoforms: surrogate markers for axonal injury, degeneration and loss. J Neurol Sci 233:183–198
36. Pfaffl MW (2001) A new mathematical model for relative quantification in real-time RT-PCR. Nucleic Acids Res 29:e45
37. Quigley H, Anderson DR (1976) The dynamics and location of axonal transport blockade by acute intraocular pressure elevation in primate optic nerve. Invest Ophthalmol 15:606–616
38. Quigley HA, Addicks EM (1980) Chronic experimental glaucoma in primates. II. Effect of extended intraocular pressure elevation on optic nerve head and axonal transport. Invest Ophthalmol Vis Sci 19:137–152
39. Quigley HA, Addicks EM, Green WR, Maumenee AE (1981) Optic nerve damage in human glaucoma. II. The site of injury and susceptibility to damage. Arch Ophthalmol 99:635–649
40. Quigley HA, Anderson DR (1977) Distribution of axonal transport blockade by acute intraocular pressure elevation in the primate optic nerve head. Invest Ophthalmol Vis Sci 16:640–644
41. Ruifrok AC, Johnston DA (2001) Quantification of histochemical staining by color deconvolution. Anal Quant Cytol Histol 23:291–299
42. Salinas-Navarro M, Alarcon-Martinez L, Valiente-Soriano FJ et al (2010) Ocular hypertension impairs optic nerve axonal transport leading to progressive retinal ganglion cell degeneration. Exp Eye Res 90:168–183
43. Schlamp CL, Johnson EC, Li Y, Morrison JC, Nickells RW (2001) Changes in Thy1 gene expression associated with damaged retinal ganglion cells. Mol Vis 7:192–201
44. Schlamp CL, Li Y, Dietz JA, Janssen KT, Nickells RW (2006) Progressive ganglion cell loss and optic nerve degeneration in DBA/2J mice is variable and asymmetric. BMC Neurosci 7:66
45. Soto I, Oglesby E, Buckingham BP et al (2008) Retinal ganglion cells downregulate gene expression and lose their axons within the optic nerve head in a mouse glaucoma model. J Neurosci 28:548–561

4. Influence of sampling patterns on estimated axon counts in experimental glaucoma

The primary outcome measure for experimental optic neuropathies are axon counts, and manual counting on transmission electron microscopy is considered to be the gold standard.[295] However, processing and analysing tissue on electron microscopy is extremely time consuming and labour-intensive, and hence not practical for the large number of samples that would need to be analysed in this study. Counting axons on semi-thin resin embedded sections is an excellent alternative and widely used in optic nerve de- and re-generation research. Estimates generated by automated axon counting are generally preferred over manual counting of individual axons because of the massive timesaving effect. The sampling methods used vary between different research groups and various approaches have been validated against the gold standard. While some researchers analyse entire cross-sections[296] or a randomly selected percentage thereof,[297] others extrapolate the number of axons based on estimated damage[298-300] or approximate counts[301] in subjectively demarcated zones of equal damage. However, a direct comparison between sampling approaches has not yet been conducted. This issue is addressed in the following paper. It illustrates that random sampling is not significantly inferior to targeted sampling.

Comparison of fixed-pattern sampling with targeted sampling for estimation of axon counts in a rat model of glaucoma

Contribution of each author

Andreas Ebneter:

Conception and design
Animal experiments and histology work
Acquisition of data
Analysis and interpretation of data
Drafting and finalization of the manuscript

Glyn Chidlow:

Conception and design
Critical revision of the manuscript for important intellectual content
Supervision

John Wood:

Critical revision of the manuscript for important intellectual content
Supervision

Robert Casson:

Critical revision of the manuscript for important intellectual content
Obtaining funding
Supervision

Ebneter, A., Casson, R.J., Wood, J.P. & Chidlow, G. (2012) Estimation of axon counts in a rat model of glaucoma: comparison of fixed-pattern sampling with targeted sampling
Clinical & Experimental Ophthalmology, Early View Online Version

NOTE
Published article is titled:
'Estimation of axon counts in a rat model of glaucoma:
comparison of fixed-pattern sampling with targeted sampling'.

NOTE:
This publication is included on pages 43-65 in the print copy of the thesis held in the University of Adelaide Library.

It is also available online to authorised users at:

http://dx.doi.org/10.1111/j.1442-9071.2011.02741.x

5. Glial markers as alternative parameters for quantification of optic nerve damage

The previous papers have shown that the laser glaucoma model is a valid choice, with the optic nerve head likely as the site of the primary insult, and that estimated axon counts are a valuable parameter to measure optic nerve damage. However, one single outcome generally does not provide enough evidence to reliably substantiate experimental data and several convergent lines of results would be preferable to confer more credibility to investigational findings.

Glial cells are clearly involved in a number of optic nerve pathologies, reflecting stress and alterations in the environment of the RGC axons. In glaucoma, the most dramatic and earliest change is observed in the astrocyte population.[294] Activation coincides or even heralds axonal loss. The astrocyte cell number significantly increases; this phenomenon is called 'gliosis'.[302] In contrast, the density of oligodendrocytes decreases. However, oligodendrocyte loss is only observed when substantial numbers of axons have been lost and lags behind axon degeneration.[294] Although, its magnitude is probably underestimated since replacement occurs by increased proliferation and differentiation of oligodendrocyte precursor cells.[303] Microglial activation, characterised by phagocytosis and proliferation, has been observed in retina in glaucoma animal models.[304] The following paper explores microglia activation in the visual pathway in greater detail and illustrates ways of exploiting microglial changes to quantify axonal damage in the optic nerve.

Microglial Activation in the Visual Pathway in Experimental Glaucoma: Spatiotemporal Characterization and Correlation with Axonal Injury

Contribution of each author

Andreas Ebneter:

Conception and design
Animal experiments and immunohistochemistry
Acquisition of data
Analysis and interpretation of data
Drafting and finalization of the manuscript
Obtaining funding

Glyn Chidlow:

Conception and design
Analysis and interpretation of data
Critical revision of the manuscript for important intellectual content
Administrative, technical, or material support
Supervision

John Wood:

Analysis and interpretation of data
Critical revision of the manuscript for important intellectual content
Supervision

Robert Casson:

Conception and design
Analysis and interpretation of data
Critical revision of the manuscript for important intellectual content
Statistical expertise
Obtaining funding
Supervision

Microglial Activation in the Visual Pathway in Experimental Glaucoma: Spatiotemporal Characterization and Correlation with Axonal Injury

Andreas Ebneter,[1,2] *Robert J. Casson,*[1,2] *John P. M. Wood,*[1,2] *and Glyn Chidlow*[1,2]

Purpose. Glia are the main cellular CNS elements initiating defense mechanisms against destructive influences and promoting regenerative processes. The aim of the current work was to characterize the microglial response within the visual pathway in a rat model of experimental glaucoma and to correlate the microglial response with the severity of axonal degeneration.

Methods. Experimental glaucoma was induced in each right eye of adult Sprague-Dawley rats by translimbal laser photocoagulation of the trabecular meshwork. Rats were subsequently killed at various times from 3 days to 6 weeks. Tissue sections were obtained from globes, optic nerves, chiasmata, and optic tracts for immunohistochemistry and toluidine blue staining.

Results. This model of experimental glaucoma led to a marked activation of microglia in the retina, optic nerve, and tract. Indeed, microglial activity remained elevated, even after intraocular pressure returned to basal levels. It is postulated that this process accompanies ongoing axonal degeneration. The degree of activation in the optic nerve correlated with axonal damage. Activation was characterized by increased density and morphologic changes. Both major histocompatibility complex (MHC) class I and MHC class II surface proteins were persistently upregulated in optic nerves and localized to microglial cells; however, this did not correlate with any significant T-cell infiltration. Interestingly, MHC class II expression was not detected in the retina.

Conclusions. The present data may have implications for the study of the pathology associated with the visual pathway in diseases such as glaucoma. (*Invest Ophthalmol Vis Sci.* 2010; 51:6448–6460) DOI:10.1167/iovs.10-5284

Glaucomatous optic neuropathy (glaucoma), the second leading cause of blindness in the world,[1] is a neurodegenerative disease characterized by structural damage to the optic nerve and the slow, progressive death of retinal ganglion cells (RGCs). RGCs represent the third-order neurons in the visual pathway. In the retina, their unmyelinated axons converge at the optic nerve head (ONH), where they exit the globe and become the myelinated optic nerve (ON). In the rat, most fibers decussate at the optic chiasm, forming the contralateral optic tract (OT) and synapsing in the lateral geniculate nucleus. In recent years, several rodent models of experimental glaucoma have been developed[2] that exhibit many of the characteristics of the human condition. Shared pathophysiological events between such models include axon transport disruption, selective loss of RGCs and their axons, oxidative stress, and reactive gliosis.

One cell type whose involvement in the pathogenesis of neurodegenerative diseases is increasingly being recognized is the microglial cell. Microglia are the resident immunocompetent cells of the CNS parenchyma and can be viewed as bridging elements between the neuronal and immune systems. They are part of the mononuclear phagocyte system but, under normal physiological conditions, assume a quiescent, ramified form with highly motile processes that monitor the environment.[3] Microglia respond rapidly to the disruption of tissue homeostasis: they proliferate, assume an ameboid morphology, migrate to the site of injury, express a multitude of receptors,[4] produce numerous types of cytokines,[5–7] participate in the complement cascade,[8] phagocytose cellular debris, and can function as antigen-presenting cells.[9] Recent debate has focused on whether microglial activation is harmful or beneficial in CNS injury.[10] One theory proposed is that in the early stages of disease, moderate activation of microglia may be beneficial and may contribute to the regeneration of damaged tissue,[11] but in an overactivated and chronically dysregulated state, microglia probably exacerbate preexisting damage and contribute to secondary disease progression[12,13]; however, the role of microglia may depend on the type and severity of injury.

Microglia have been implicated in the pathogenesis of various experimental retinal and ON neuropathies. In the retina, these include autoimmune uveoretinitis,[14,15] diabetic retinopathy,[16] ischemia,[17,18] excitotoxicity,[19] photoreceptor degeneration,[20–23] AMD,[24] and trauma,[25–27] whereas in the ON, a robust microglial response has been demonstrated in ischemia,[28–29] and experimental allergic encephalomyelitis (EAE).[30] With regard to glaucoma, there is some limited information regarding microglial activation in the retina/ONH region[31–33] in both experimental models and human specimens[34]; however, to date, no data are available concerning this process in the optic pathway distal to the ONH. The ONH region is considered by some to be the primary site of injury in glaucoma.[35] Some evidence, however, suggests that the distal portion of the ON may be more severely affected by glaucoma.[36] It is of interest, therefore, to discover where the microglial response occurs earliest and with greatest magnitude. Delineating the spatiotemporal microglial response in the optic pathway would assist in addressing this matter. Further subjects of interest relate to the expression of immunologic cell surface markers by microglia during glaucoma; the infiltration, if any, of macrophages or T lymphocytes, such as occurs in ischemic,

From the [1]Ophthalmic Research Laboratories, South Australian Institute of Ophthalmology, Hanson Institute Centre for Neurological Diseases, Adelaide, Australia; and the [2]Department of Ophthalmology, University of Adelaide, Adelaide, Australia.

Supported by National Health and Medical Research Council Grant 508123 and by the OPOS Stiftung zugunsten von Wahrnehmungsbehinderten, St. Gallen, Switzerland (AE).

Submitted for publication January 28, 2010; revised May 28, 2010; accepted July 15, 2010.

Disclosure: **A. Ebneter**, None; **R.J. Casson**, None; **J.P.M. Wood**, None; **G. Chidlow**, None

Corresponding author: Glyn Chidlow, Hanson Centre for Neurological Diseases, Frome Road, Adelaide, SA 5000, Australia; glyn.chidlow@health.sa.gov.au.

Investigative Ophthalmology & Visual Science, December 2010, Vol. 51, No. 12

traumatic, and autoimmune models of ON injury; and whether microglial activation correlates closely with the degree of ON damage. Such a finding would provide the opportunity for using the detection of microglial activation as a surrogate or adjunct marker for ON injury in studies relating to neuroprotection. The aim of the present study, therefore, was to address these issues using a well-characterized rat model of glaucoma.

Materials and Methods

Animals and Procedures

This study was approved by the Animal Ethics Committees of the Institute of Medical and Veterinary Science and the University of Adelaide and conformed to the Australian Code of Practice for the Care and Use of Animals for Scientific Purposes, 2004, and the ARVO Statement for the Use of Animals in Ophthalmic and Vision Research. Adult Sprague-Dawley rats (weight range, 200–250 g) were housed in a temperature- and humidity-controlled room with a 12-hour light/12-hour dark cycle and were provided food and water ad libitum. Rats were anesthetized with intraperitoneal injection of 100 mg/kg ketamine and 10 mg/kg xylazine, and local anesthetic drops were applied to the eye. Ocular hypertension was then induced in the right eye of each animal by laser photocoagulation of the trabecular meshwork using a slightly modified protocol of the method described by Levkovitch-Verbin et al.[37] In brief, 80 to 100 spots of 50-μm diameter, 550 to 600 mW power, and 0.5-second duration were applied to the trabecular meshwork. An additional 10 to 20 spots, 100-μm diameter, 450 mW, and 0.5-second duration were delivered to three of the four episcleral veins. A second laser treatment was often given on day 4 or 7, depending on the IOP. If the difference in IOP between the two eyes was less than 8 mm Hg on day 3, these rats were given a second laser treatment on day 4. In the remaining rats, if the IOP difference was less than 8 mm Hg on day 7, they, too, received a second laser treatment. Some animals had persistently raised IOP and consequently received only one laser treatment. IOPs were measured in both eyes at baseline, day 1, day 3, day 7, and at least weekly thereafter using a rebound tonometer (TonoLab; Icare, Espoo, Finland) factory calibrated for use in rats. Rats were killed at various time points after treatment by cardiac perfusion with physiological saline under terminal anesthesia. The number of rats analyzed at each time point was as follows: 3 days (n = 6), 7 days (n = 13), 2 weeks (n = 24), 6 weeks (n = 7). No animals were excluded from the present study for reasons relating to inadequate IOP elevation. Five animals were excluded as a result of death caused by anesthesia and four from death caused by hyphema.

Tissue Processing and Histology

Initially, the brain was removed. Next, each eye with ON, optic chiasm, and the proximal part of the OT attached was carefully dissected. From the dissected tissue, a short piece of ON, 1.5 mm behind the globe, was removed for toluidine blue staining. The brain, globe, and attached short proximal segment of ON, distal ON, chiasm, and proximal segment of OT were fixed in 10% buffered formalin for at least 24 hours. After fixation, the brain was positioned in a rat brain blocker (PA001; Kopf Instruments, Tujunga, CA), and 2-mm coronal slices were taken starting from the rostral and proceeding to the caudal portion of the brain. Brain slices, along with the globe and optic pathway, were then processed for routine paraffin-embedded sections. Globes were embedded sagittally, and ONs and chiasmata were embedded longitudinally. In all cases, 5-μm serial sections were cut. In some animals, the retina and ON were removed for cryosectioning rather than for paraffin sections. These tissues were fixed in 10% formalin for 1 hour and cryopreserved in 30% sucrose overnight, and 7-μm sections were taken using a cryostat.

The short piece of proximal ON taken for histology was fixed by immersion in 2.5% glutaraldehyde with 4% paraformaldehyde in 0.1 M phosphate buffer, pH 7.4, for 24 hours at 4°C. It was then placed in 1% osmium tetroxide in saline overnight and was washed with cacodylate buffer at room temperature. Subsequently, the tissue was dehydrated in graded alcohols and embedded in epoxy resin (TAAB Laboratories, Aldermaston Berks, UK) for transverse sectioning. Sections (0.75 μm) were cut on an ultramicrotome, mounted on glass slides, and enhanced with osmium tetroxide-induced myelin staining using 1% toluidine blue.

Immunohistochemistry

Paraffin-Embedded Sections. Tissue sections were deparaffinized in xylene and rinsed in 100% ethanol before treatment with 0.5% H_2O_2 for 30 minutes to block endogenous peroxidase activity. Antigen retrieval was achieved by microwaving the sections in 10 mM citrate buffer (pH 6.0). Tissue sections were then blocked in phosphate buffered saline (PBS) containing 3% normal horse serum and incubated overnight at room temperature in primary antibody (containing 3% normal horse serum) followed by consecutive incubations with biotinylated secondary antibody (Vector, Burlingame, CA) and streptavidin-peroxidase conjugate (Pierce, Rockford, IL). Color development was achieved with 3′-,3′diaminobenzidine. Sections were counterstained with hematoxylin, dehydrated, and mounted.

For immunohistochemical double labeling of iba1 and OX-6, visualization of OX-6 was achieved using a three-step procedure (primary antibody, biotinylated secondary antibody, streptavidin-conjugated AlexaFluor 488), whereas iba1 was labeled by a two-step procedure (primary antibody, secondary antibody conjugated to AlexaFluor 594). In summary, sections were treated as described except for the omission of the endogenous peroxidase block and then were incubated overnight at room temperature with anti-iba1 and anti-OX-6. On the following day, sections were incubated with AlexaFluor donkey anti–rabbit IgG 488 (1:250) together with biotinylated

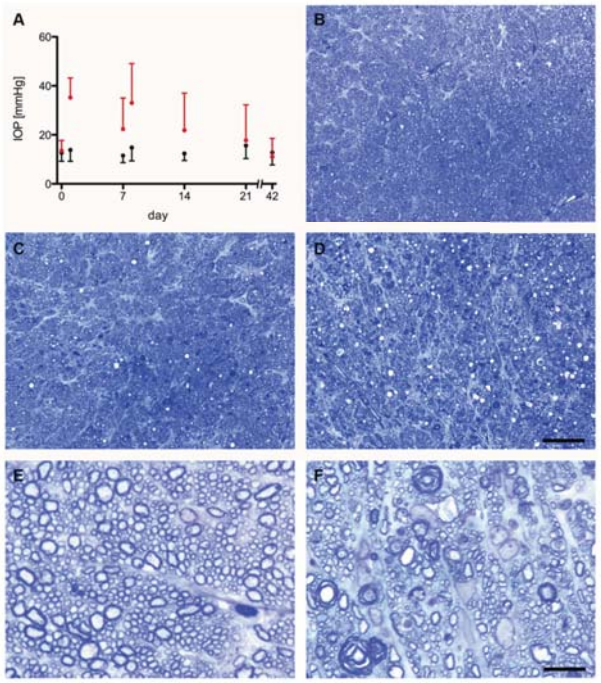

Figure 1. (**A**) IOP profiles of treated (*red*) and control (*gray*) eyes after the induction of experimental glaucoma by unilateral laser treatment. Data are expressed as mean area ± SD, where n = 44 (days 0, 1 and 7), n = 31 (days 8 and 14), and n = 7 (days 21, 35, and 42). (**B–F**) Transverse sections of representative ONs stained with toluidine blue showing different severities of ON injury. Control ON (**B**), treated ON showing moderate damage (grade 2; **C**), treated ON showing severe damage (grade 6; **D**). High-magnification images of control (**E**) and damaged ONs (**F**). Scale bars: 25 μm (**A–D**); 10 μm (**E**, **F**).

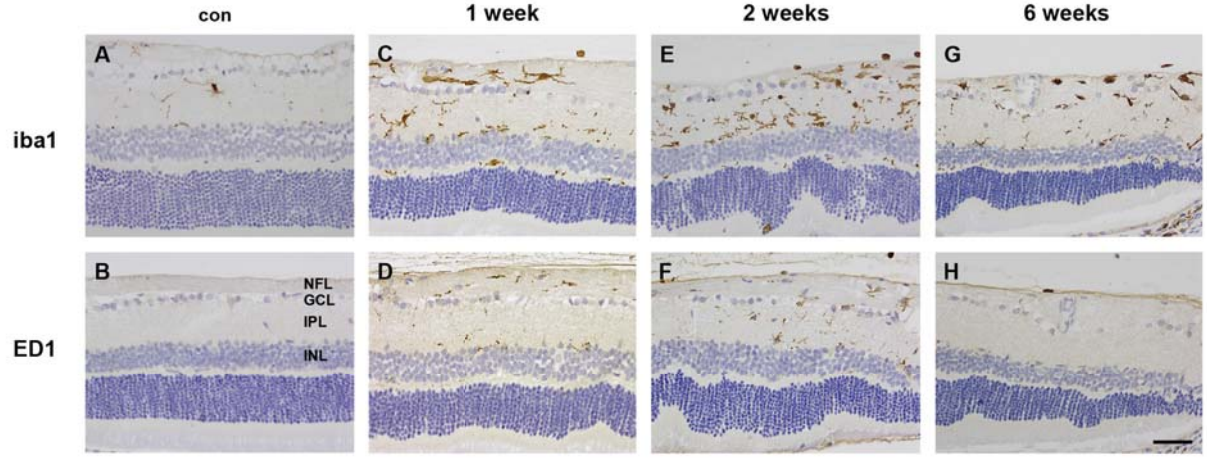

FIGURE 2. Microglial activation within the retina after the induction of experimental glaucoma. In the retinas of control rats, a relatively sparse population of ramified iba1-positive microglia was present within the inner retina (**A**). No ED1-positive cells were found (**B**). In treated retinas, an increased number of iba1-labeled cells was evident that was notable in the nerve fiber layer (**C**, **E**, **G**). Peak activity was noted at 2 weeks after lasering (**E**). Subtle signs of activation were still present at 6 weeks (**G**). Microglia were also immunopositive for ED1 (**D**, **F**, **H**). Maximum activation was noted at 2 weeks (**F**). ED1 was no longer present 6 weeks after the insult (**H**). NFL, nerve fiber layer; GCL, ganglion cell layer; IPL, inner plexiform layer; INL, inner nuclear layer. Scale bar, 50 μm (**A**–**H**).

anti–mouse IgG antibody (1:250; Vector) for 30 minutes, followed by streptavidin-conjugated AlexaFluor 594 (1:500; Invitrogen, Carlsbad, CA) for 1 hour before mounting (Fluorescence Mounting Medium; Dako, Carpinteria, CA).

Cryosections. Tissue sections were initially rinsed in PBS. For OX18, they were then postfixed for 5 minutes in acetone, which improved the signal-to-noise ratio of staining. Sections were washed in PBS before treatment with 0.5% H_2O_2 for 30 minutes to block endogenous peroxidase activity. Antigen retrieval was not required. Subsequently, sections were treated as for paraffin sections. For immunohistochemical double labeling of cryosections, sections were incubated overnight at room temperature with anti-iba1 and either anti-OX18 or anti-OX42. On the following day, sections were treated as for double labeling in paraffin sections.

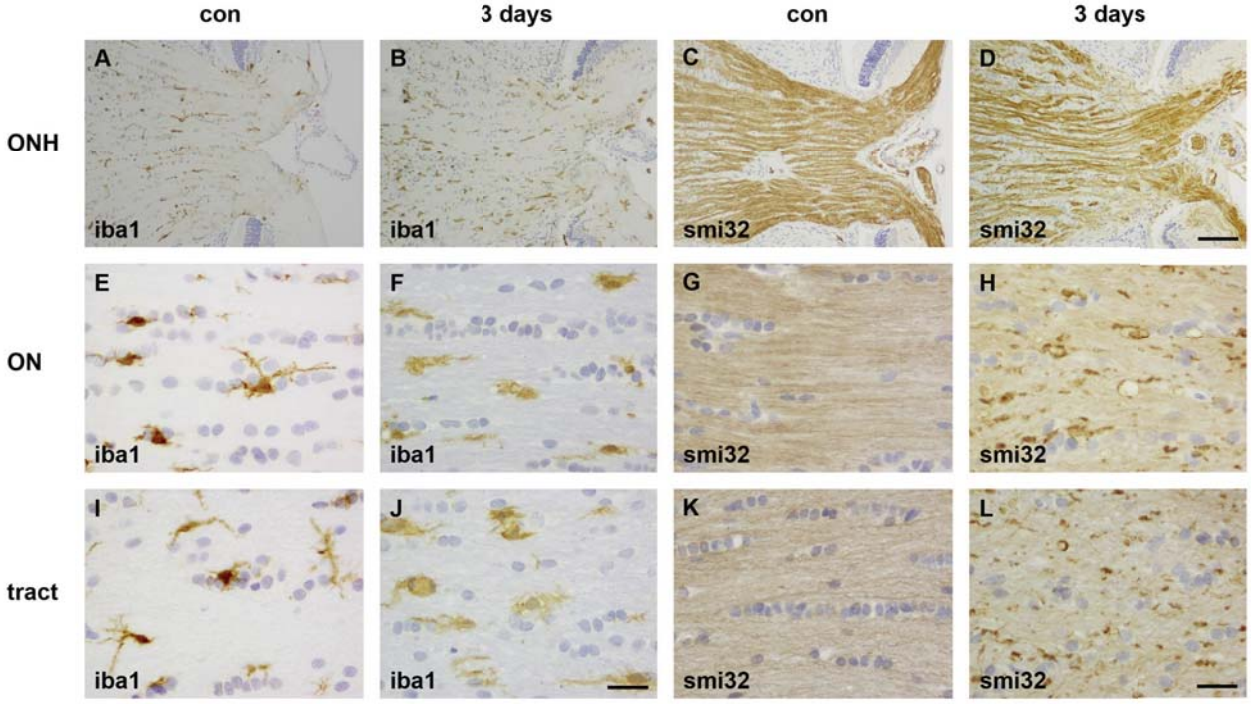

FIGURE 3. Microglial activation and axonal damage 3 days after the induction of experimental glaucoma. After 3 days of experimental glaucoma, iba1-positive microglia in the ONH (**B**), ON (**F**) and OT (**J**) showed cell body hypertrophy and retraction of processes and were more numerous than in the ONH (**A**), ON (**E**), and OT (**I**) of control rats. In addition, SMI-32 abnormalities were clearly visible in the ONH region (**D**, showing loss of background staining and subtle neurofilament abnormalities), ON (**H**), and OT (**L**), compared with control rats (**C**, **G**, **K**). Scale bars: 100 μm (**A**–**D**); 25 μm (**E**–**L**).

Antibodies. The following primary antibodies were used in the study: anti-mouse cd11b (1:2000, OX-42; Serotec, Raleigh, NC), anti-rabbit CD3 (1:3000, AO452; Dako), anti-rabbit ionized calcium-binding adapter molecule-1 (iba1, 1:50,000, 019-19741; Wako), anti-mouse ED1 (1:500, MCA341; Serotec), anti-mouse major histocompatibility complex (MHC) class II (1:500, OX-6; Serotec), anti-mouse MHC class I (1: 10,000, OX-18; Serotec), anti-mouse SMI-32 (1:10,000; Sternberger, Baltimore, MD). For double labeling, the antibodies were used at the concentrations listed with the exception that iba1, when used in the two-step procedure, was diluted to 1:5000.

Evaluation of Histology and Immunohistochemistry

All assessments of ON injury were performed in a randomized, blinded manner. Loss of RGC axons in the ONs of glaucomatous eyes was assessed using a previously developed semiquantitative ON grading scheme based on toluidine blue-stained cross-sections.[38] In summary, zones of equal damage were defined on pictures showing the entire cross-section taken with the 10× microscope objective. The percentage of the nerve cross-section occupied by each zone was determined using ImageJ software (developed by Wayne Rasband, National Institutes of Health, Bethesda, MD; available at http://rsb.info.nih.gov/ij/index.html). Representative photographs of each zone were then taken using a 40× objective. The severity of damage (0%, 15%, 30%, 45%, 60%) was then estimated for each zone by two independent graders using the templates shown by Chauhan et al.[38] The overall axonal damage was calculated by summing the products of the mean percentage of damage within each zone and the area of the nerve occupied by the zone. This number was then multiplied by 10 and rounded to obtain an entire number between 0 and 10. Hence, grade 0 corresponds to no damage, grade 5 to 50% axon loss, and grade 10

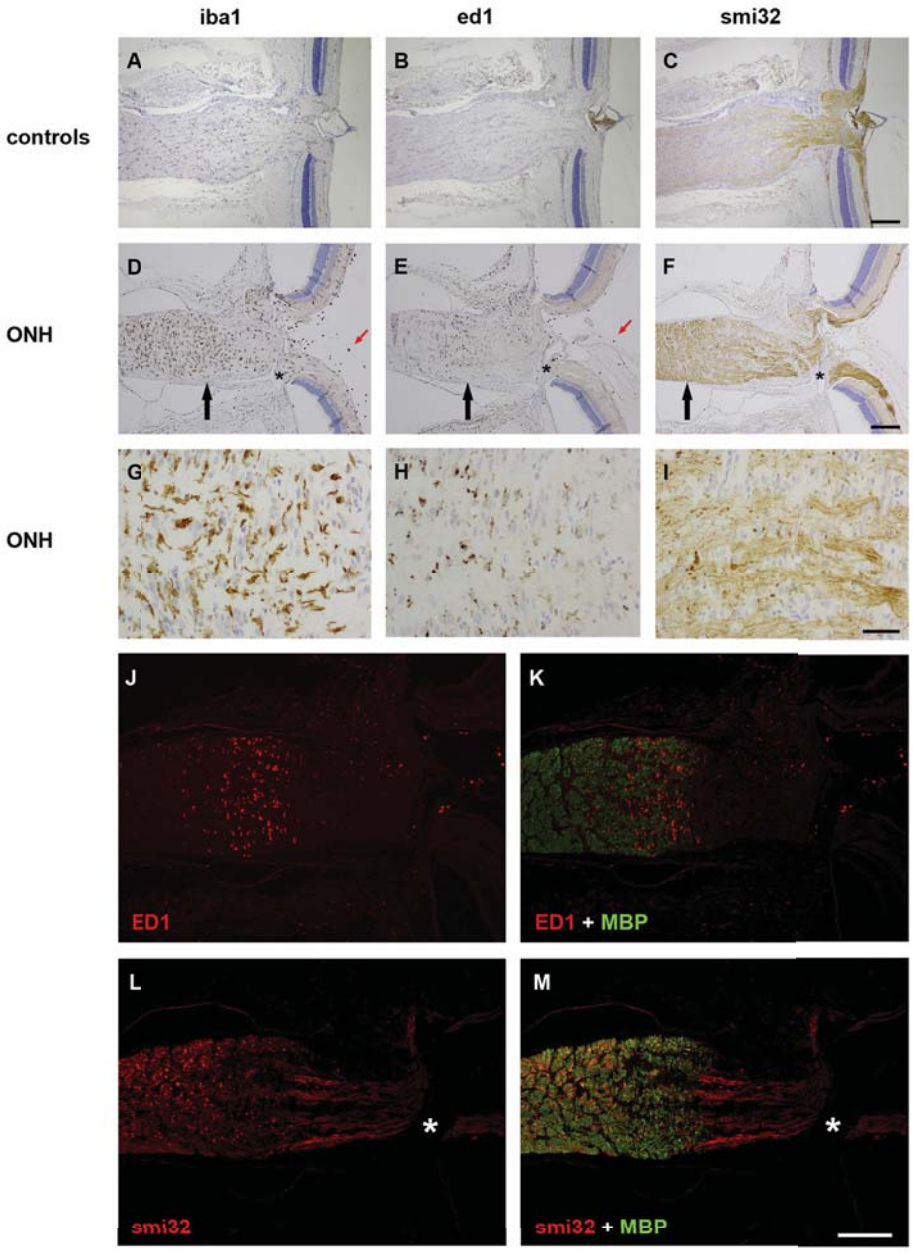

FIGURE 4. Microglial activation and axonal damage within the ONH and proximal ON 7 days after the induction of experimental glaucoma. Sections taken from a control (**A–C**) and an injured (**D–M**) animal are shown. Microglial activation and increased microglial density were apparent throughout the ONH and proximal ON, as evidenced by robust labeling for iba1 (**D**) and ED1 (**E**). In addition, macrophages were present in the vitreous humor (**D**, **E**, *red arrows*). Higher microglial activity and increased axonal cytoskeletal abnormalities (**F**, *black arrows*) occurred at the transitional zone between unmyelinated and myelinated axons. This region is shown at higher magnification in (**G–I**): iba1 (**G**), ED1 (**H**), SMI32 (**I**). Double-labeling immunofluorescence of ED1 (**J**, **K**, *red*) and myelin basic protein (MBP; **K**, *green*) and of SMI-32 (**L**, **M**, *red*) with MBP (**M**, *green*) was performed to reveal the precise site of myelination. This confirmed that greater microglial activity and increased axonal cytoskeletal abnormalities were present in the myelinated portion of the ON. *Asterisk*: note the gap in axonal fibers, caused by a penetrating blood vessel also visible in (**D–F**). Scale bars: 200 μm (**A–F**, **J–M**); 50 μm (**G–I**).

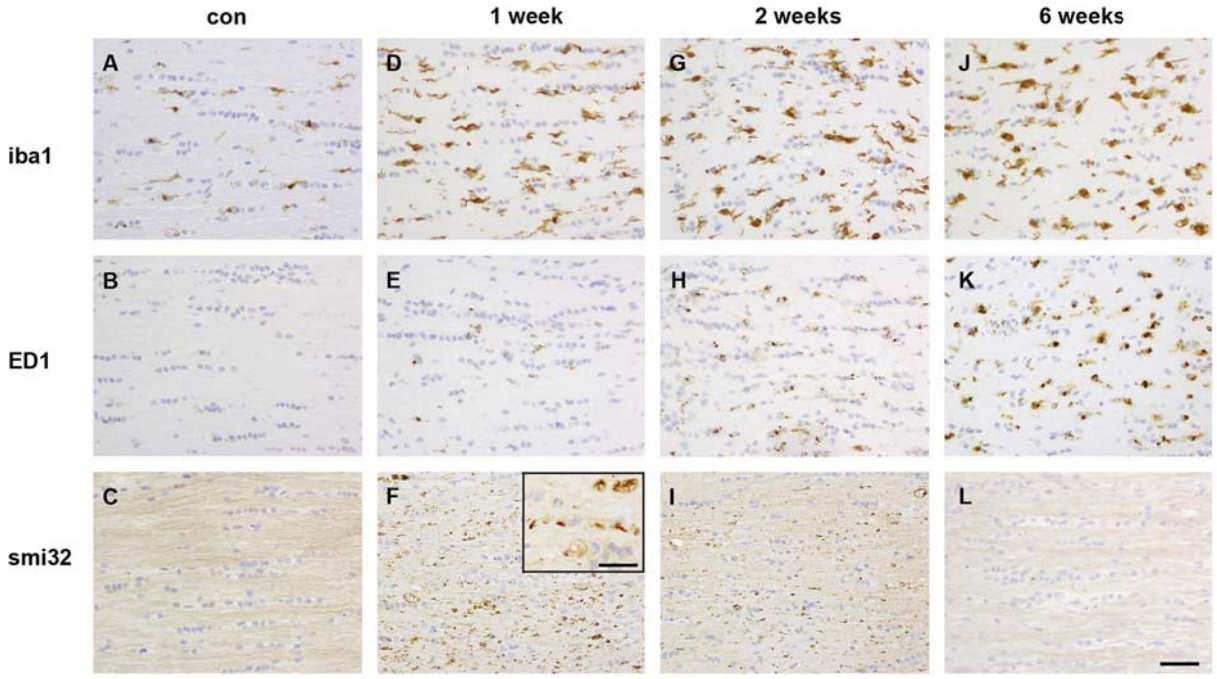

FIGURE 5. Temporal characterization of microglial activation and axonal cytoskeletal damage in the ON during experimental glaucoma. Sections taken from the distal ON in representative animals are shown. Control (**A–C**), 7 days (**D–F**), 2 weeks (**G–I**), and 6 weeks (**J–L**) after the induction of elevated IOP. In control rats, iba1-labeled microglia showed a classical ramified morphology (**A**) and were ED1-negative (**B**). Axonal fibers are homogenously labeled by SMI-32 (**C**). At 7 days, a greater number of iba1-positive microglia was noted (**D**), together with expression of ED1 (**E**), whereas numerous axons showed SMI-32 abnormalities (**F**). There was an increased number of iba1- and ED1-positive microglia at 2 weeks (**G**, **H**) and again at 6 weeks (**J**, **K**). Note the change in morphology of ED1-positive microglia at 6 weeks; they have a foamy appearance indicative of phagocytic activity (**K**). In contrast, abnormal SMI-32 immunolabeling gradually decreased at later time points (**I**, **L**), leaving a reduced number of lightly stained, surviving axons. Scale bar: 50 μm (**A–L**); 25 μm (*inset*).

to 100% axonal loss. Of note, if the calculated damage grade was zero but the nerve contained at least 20 damaged axons within the whole cross-section, the grade was recorded as 1 as a nominal indication that the nerve was damaged. An example of optic nerve grading is shown in Supplementary Figure S1, http://www.iovs.org/content/51/12/6448/suppl/DC1.

To ascertain whether ON injury correlated with the microglial response, for each animal, transverse sections of the proximal ON were graded for severity of damage by conventional examination of toluidine blue–stained transverse sections (as described), whereas longitudinal sections of the adjacent medial ON were immunolabeled for nonphosphorylated neurofilament heavy (SMI-32) and for the microglial markers iba1 and ED1. Immunostained sections, each expressing a representative level of immunoreactivity, were photographed at 200× magnification. They were then imported into NIH Image J 1.42q software, where they underwent color deconvolution to separate the diaminobenzidine reaction product from hematoxylin counterstain.[39] SMI-32 and ED1 images were subsequently analyzed with regard to the specifically stained area in pixels using the in-built functions of the ImageJ software. For iba1, the number of nuclei with immunoreactive perikarya and processes was counted. Statistical analysis of correlations was performed (Prism 5.0b; GraphPad Software Inc., La Jolla, CA) using nonparametric tests (see Fig. 9 for the results).

RESULTS

Validation of the Experimental Model of Glaucoma

The present model gave rise to a consistent elevation of IOP (Fig. 1A), with the peak pressure most commonly occurring at day 1 after lasering (35.2 ± 8.0 mm Hg [mean ± SD]). Most eyes needed a second treatment at day 4 or 7 to maintain elevated IOP levels for longer than 2 weeks. By 3 weeks, IOP values had returned to basal levels (Fig. 1A). The amount of ON damage, as assessed by semiquantitative grading of toluidine blue–stained transverse sections,[38] ranged from nominal damage to an axonal injury grade of 6, equating to a loss of axons of approximately 60% (see Figs. 1B–D for representative images). The mean axonal injury grade at 1 week was 1.6 ± 1.3, whereas at 2 weeks, the mean axonal injury grade was 1.8 ± 1.4. These figures equate to a loss of axons of approximately 16% and 18%, respectively, and are consistent with those recorded in other studies[40–42] with similar elevations of IOP.

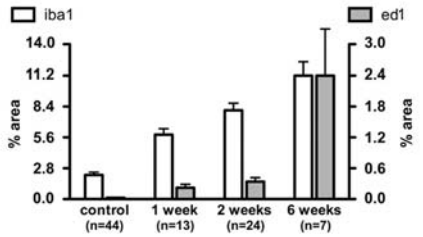

FIGURE 6. Quantification of iba1 and ED1 immunoreactivities in the distal ON in control rats at 1, 2, and 6 weeks after the induction of experimental glaucoma. There was a gradual increase in iba1 immunoreactivity over time compared with controls. ED1 immunoreactivity was minimal in control ONs, increased steadily during the first 2 weeks, and was dramatically higher by 6 weeks. Data are expressed as mean area ± SEM.

Spatiotemporal Characterization of Microglial Activation

When considering the microglial response during experimental glaucoma, some general points are worth making regarding the disease model. First, the induction of elevated IOP results in a chronic, relatively mild axonal injury. It is not thought to cause a focal lesion as occurs in other well-characterized paradigms of ON damage, including ON crush or transection, models of ON ischemia, or EAE. Second, unambiguous identification of the site of injury in human and rodent models of glaucoma has proved difficult, but some evidence suggests the ONH region is the primary site.[43] Third, considerable variability exists among animals with regard to the extent of axonal loss and the microglial response. The photomicrographs shown are from representative animals, but other rats killed at the same time points displayed lesser or greater damage.

Retina. Previous studies have shown microglial activation in the rat retina after elevation of the IOP induced by cauterization of the episcleral veins.[32,33,44] Similar results were obtained in the present study after the induction of raised IOP caused by laser photocoagulation of the trabecular meshwork. In control retinas, a relatively sparse population of ramified iba1-positive microglia was present, predominantly within the inner plexiform layer (Fig. 2A). ED1 immunoreactivity was not observed (Fig. 2B). At 3 days after lasering, iba1-positive microglia were marginally more numerous and were labeled more robustly (data not shown). By 7 days, iba1-labeled microglia were abundant within the inner retina and were observed in close proximity to RGC bodies and their axons located in the nerve fiber layer (Fig. 2C). A proportion of these microglia were now ED1 positive (Fig. 2D). This coincided with a decrease in the number of RGCs immunopositive for Brn-3, a transcription factor downregulated before cell death (data not shown). The pattern of iba1 immunoreactivity was similar at 2 weeks after lasering, whereas ED1 immunoreactivity was more prevalent (Figs. 2E, 2F). By 6 weeks, ED1-positive cells were no longer evident, and the density of iba1-labeled cells had decreased markedly (Figs. 2G, 2H). Indeed, in some

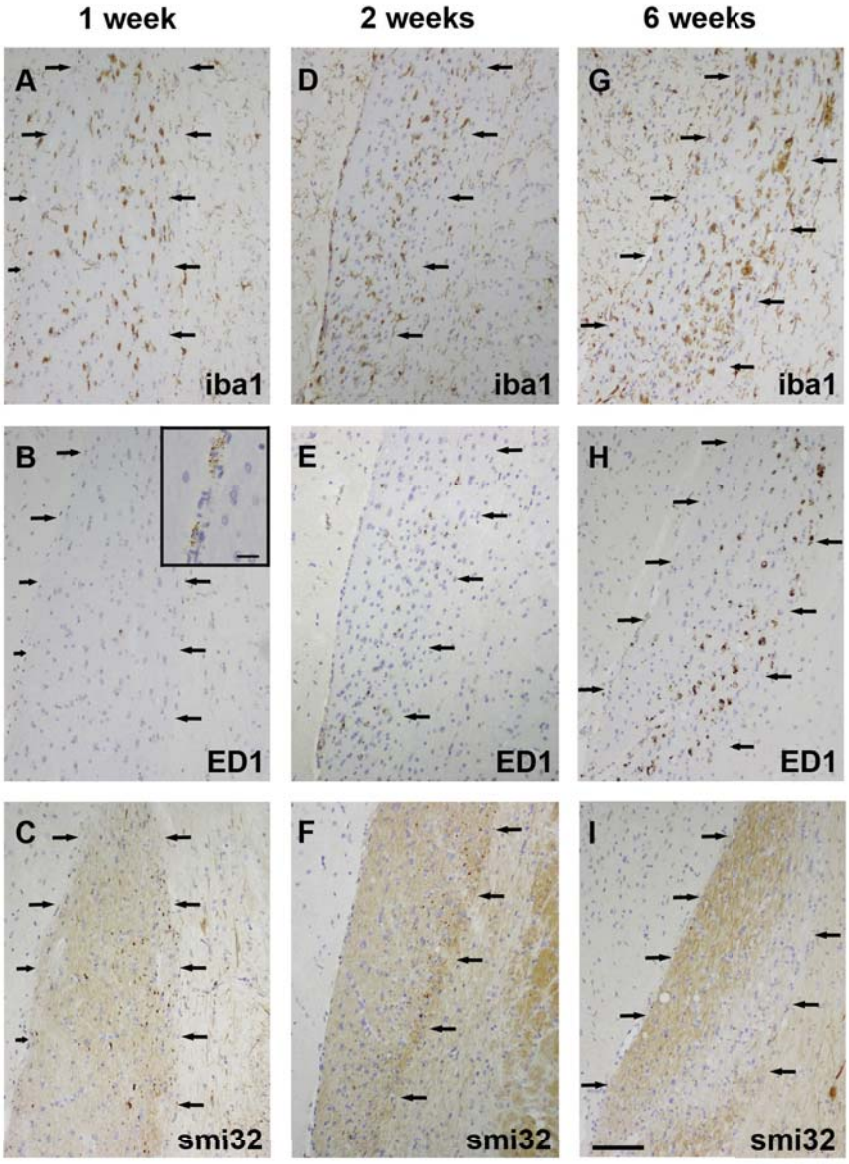

Figure 7. Temporal characterization of microglial activation and axonal cytoskeletal damage in the OT during experimental glaucoma. Sections taken from representative animals killed 1 week (**A–C**), 2 weeks (**D–F**), and 6 weeks (**G–I**) after the induction of elevated IOP are shown. *Arrows*: boundaries of the OT. In the 7 day animal (grade 1), iba1-labeled microglia displayed retraction in processes indicative of activation (**A**). There was no evidence of ED1-positive microglia within axonal tissue (**B**); however, perivascular staining was observed (*inset*). Axonal damage, denoted by intensely stained SMI-32 abnormalities, was clearly evident (**C**). In the 2-week rat (grade 2), an increased number of iba1-positive microglia was noted (**D**), together with the expression of ED1 (**E**) and numerous SMI-32 abnormalities (**F**). In the 6-week rat (grade 5), robust labeling for iba1 (**G**) and ED1 (**H**) was observed throughout the OT. There were few SMI-32 abnormalities, but the entire right side of the OT showed axonal loss. Note that in the region of heavy axonal loss, there was greater microglial activity. Scale bar: 100 μm (**A–I**); 10 μm (*inset*).

animals, iba1 immunolabeling was indistinguishable from control rats, although in other animals with severe degeneration an enhanced microglial presence was retained. Unlike in the white matter (see below), most iba1- and ED1-positive microglia in the retina retained a ramified morphology at all time points after the elevation of IOP.

Optic Nerve and Tract. Throughout the ON and OT of control rats, numerous iba1-positive microglia with small cell bodies and delicate processes were noted (Figs. 3–8). These cells were commonly aligned parallel to the axon bundles in the ON and OT, although in the laminar region of the ONH they were sometimes aligned perpendicularly to axons. As in the retina, minimal ED1 immunolabeling was detectable (Figs. 4–8).

By 3 days after the induction of experimental glaucoma, iba1-positive microglia in the ONH (Figs. 3A, 3B), ON (Figs. 3E, 3F), and OT (Figs. 3I, 3J) typically showed some retraction of processes and hypertrophy of the cell body and were marginally greater in number than in controls. There was no evidence of a spatial gradient in microglial activity along the optic pathway. The increased microglial activity was concurrent with early indications of axonal cytoskeleton damage, as evidenced by abnormalities in nonphosphorylated neurofilament heavy (SMI-32), at the ONH (Figs. 3C, 3D), and along the extent of the ON (Figs. 3G, 3H) and the OT (Figs. 3K, 3L).

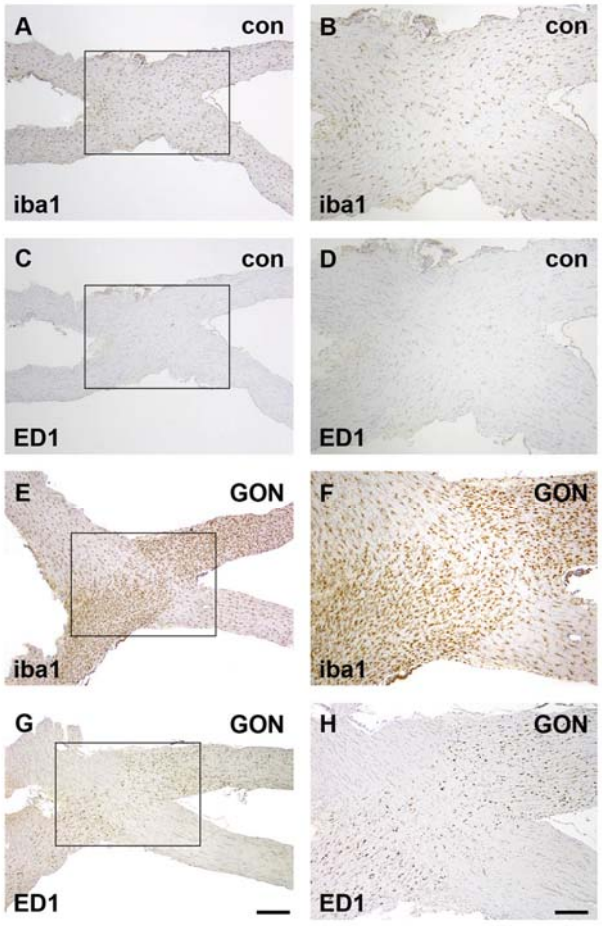

FIGURE 8. Microglial response at the level of the optic chiasm 2 weeks after the induction of experimental glaucoma. In control rats, iba1 labeled ramified, quiescent microglia throughout the distal ON and OT (**A**), whereas no ED1 immunoreactivity was detectable (**C**). In treated rats, increased microglial density, morphologic changes, and expression of ED1 were observed within the injured ON and the contralaterally projecting OT (**E**, iba; **G**, ED1). Areas within the boxed regions in (**A**), (**C**), (**E**), and (**G**) are shown at higher magnification in the accompanying images to the right (**B**, **D**, **F**, **H**). Of interest, there was minimal evidence of any injured, noncrossing fibers in the ipsilaterally projecting OT. Scale bars: 400 μm (**A–D**); 200 μm (**E–H**).

At 7 days after lasering, iba1-positive microglia throughout the proximal (Fig. 4) and distal (Fig. 5) ON and OT (Fig. 7) were more numerous than at 3 days and displayed a partially activated morphology, with a proportion of microglia expressing ED1-positive granules. In the proximal segment of the ON, there was a regional disparity in the microglial response. More iba1 (Figs. 4D, 4G) and ED1 (Figs. 4E, 4H) activities were typically observed in the retrobulbar ON than in the ONH. This was also the case for SMI-32 immunolabeling, which featured more abnormalities in the retrobulbar ON (Figs. 4F, 4I). Double-labeling immunofluorescence of myelin basic protein with ED1 and SMI-32 demonstrated that the increases in microglial activity and axonal cytoskeletal abnormalities occurred at the transition zone, where the axons become myelinated (Figs. 4J–M).

From 7 days to 6 weeks, throughout the myelinated ON and OT, there was a gradual increase both in the number of microglia and in their activation state. This is illustrated in Figures 5 and 6. Figure 5 shows sections from the distal ON of representative animals killed at 1, 2, and 6 weeks each with moderate ON damage (grade 2) according to toluidine blue grading, whereas Figure 6 is a quantitative representation of the overall results. At 1 week after injury, ongoing neurofilament dephosphorylation was prevalent (Fig. 5F), accompanied by a rise in the number of iba1-microglia (Figs. 5D, 6) but relatively modest ED1 accumulation (Fig. 5E, 6) compared with controls (Figs. 5A–C). At 2 weeks after lasering, neurofilament dephosphorylation was similar to that seen at 1 week (Fig. 5I), and there was a moderate increase in the number of iba1- and ED1-positive microglia (Figs. 5G, 5H, 6). By 6 weeks after lasering, ongoing neurofilament dephosphorylation had decreased markedly in most animals (Fig. 5L); however, the number of iba1-positive cells was higher than at 2 weeks (Figs. 5J, 6), and the abundance of ED1 was dramatically greater (Figs. 5K, 6). ED1-positive microglia displayed an activated morphology, with some cells adopting a macrophage-like, foamy appearance (Fig. 5K).

Findings similar to those found in the ON were noted in the OT. Figure 7 shows sections through the OT (at bregma −3.10) in representative rats killed at 1, 2, and 6 weeks. The number of iba1-labeled microglia increased with time after lasering and severity of injury (Figs. 7A, 7D, 7G). Very few ED1-positive cells were noted in the 1-week-old rat (Fig. 7B), but increased perivascular ED1 staining (Fig. 7B, inset) was seen. ED1 abundance was greater in the 2-week-old animal (Fig. 7E) and was markedly higher in the 6-week-old rat (Fig. 7H), which, like many animals, featured asymmetric damage (Figs. 7G–I).

At the optic chiasm, most ON axons from each eye meet, cross the midline, and project to the contralateral OT. In the adult rat, 5% to 10% of RGC axons do not cross the midline of the optic chiasm, projecting instead to the ipsilateral half of the brain. Figure 8 shows iba1 and ED1 immunoreactivities at the level of the optic chiasm in a control rat (Figs. 8A–D) and in a rat that underwent induction of experimental glaucoma 2 weeks previously (Figs. 8E–H). A robust microglial response was seen in the ipsilateral ON and contralateral OT in the treated animal; however, there was negligible evidence for any microglial activation in noncrossing fibers in the ipsilaterally projecting OT or indeed of any axonal cytoskeleton breakdown in the ipsilateral OT (data not shown). This was the case at all time points.

Correlation between Microglial Activation and Optic Nerve Injury

We were interested in whether ON injury correlated with the microglial response, particularly at early time points featuring mild or moderate pathologic changes. To achieve this aim, rats were killed at 1 and 2 weeks after the induction of experimental glaucoma. Transverse sections of the proximal ON were graded for severity of damage by conventional examination of toluidine blue–stained transverse sections, whereas longitudinal sections of the adjacent medial ON were immunolabeled for SMI-32 and for the microglial markers iba1 and ED1. Iba1 labels both quiescent and activated microglia, thus providing an index of microglial density, whereas abundance of the lysosomal antigen ED1 offers a measure of microglial phagocytic activity. Subsequently, both measures of axonal injury were correlated with each microglial marker. The overall results showed a highly statistically significant correlation between axonal injury and the microglial response (Fig. 9; Supplementary Table S1, http://www.iovs.org/content/51/12/6448/suppl/DC1). In summary, the greater the degree of ON injury (whether assessed by grading of toluidine blue–stained sections or by immunostaining for SMI-32), the greater the number of microglia and the greater the abundance of ED1 granules expressed by microglia. A number of specific observations can also be made: first, ON damage as assessed by grading of toluidine blue–stained transverse sections showed a greater correlation with both microglial markers at the 2-week than at the 1-week time point; second, the correlation was stronger for ED1 than for iba1; third, ON damage as assessed by extent of abnormal SMI-32 immunostaining correlated better with iba1 than with ED1.

Expression of Immunologic Cell Surface Markers

The morphology and distribution of complement receptor type 3 (cd11b, OX42) immunoreactive microglia in control and injured tissues closely matched those of iba1. In control animals, OX42 was expressed in ramified microglia with small cell bodies and delicate processes, which, in the ON, were typically aligned parallel to the nerve bundles (Fig. 10A). At 1 week (data not shown) and 2 weeks (Fig. 10B) after the induction of experimental glaucoma, OX42-positive microglia throughout the optic pathway were more numerous and tended to have larger cell bodies and shorter, thicker processes. Double-labeling studies showed that OX42 was exclusively localized to iba1-positive microglia; however, a small percentage of iba1-positive microglia were not immunolabeled by OX42 (Figs. 10C, 10D).

In control animals, MHC class I (OX18) lightly stained a population of cells that had the morphology of OX42- and iba1-positive microglia, featuring small cell bodies and fine processes (Fig. 10E). OX18 also faintly labeled a few cells with lateral processes that bore greater resemblance to astrocytes. After 1 week (data not shown) and 2 weeks (Fig. 10F) of experimental glaucoma, there was a marked upregulation in the number of OX18-labeled cells that showed an altered morphology analogous to that observed for OX42. Double-labeling studies revealed that most OX18-positive cells colocalized with iba1-positive microglia (Figs. 10G, 10H).

MHC class II (OX6) was absent from the optic pathway in control animals (Fig. 10I) except for the presence of occasional perivascular microglia, which constitutively express MHC class II. After the induction of experimental glaucoma, numerous OX6-positive cells with the morphology of OX42- and iba1-

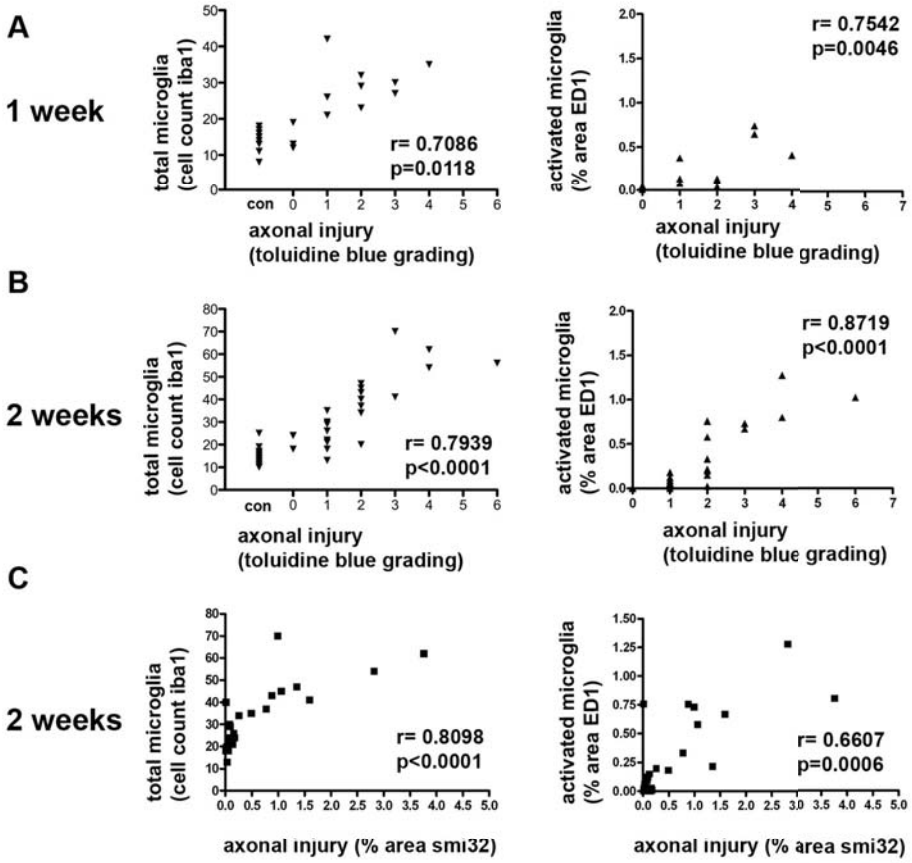

FIGURE 9. Correlations between axonal injury and iba1 and ED1 immunoreactivities in the ON after the induction of experimental glaucoma. (**A**, **B**) Correlations between semiquantitative grading of toluidine blue–stained transverse sections of the proximal ON and number of iba1 microglia or abundance of ED1 immunoreactivity in longitudinal sections of the distal ON at (**A**) 1 week and (**B**) 2 weeks. (**C**) Correlations between the amount of abnormal SMI-32 staining and the number of iba1 microglia or abundance of ED1 immunoreactivity in longitudinal sections of the distal ON at 2 weeks. Each data point represents one animal.

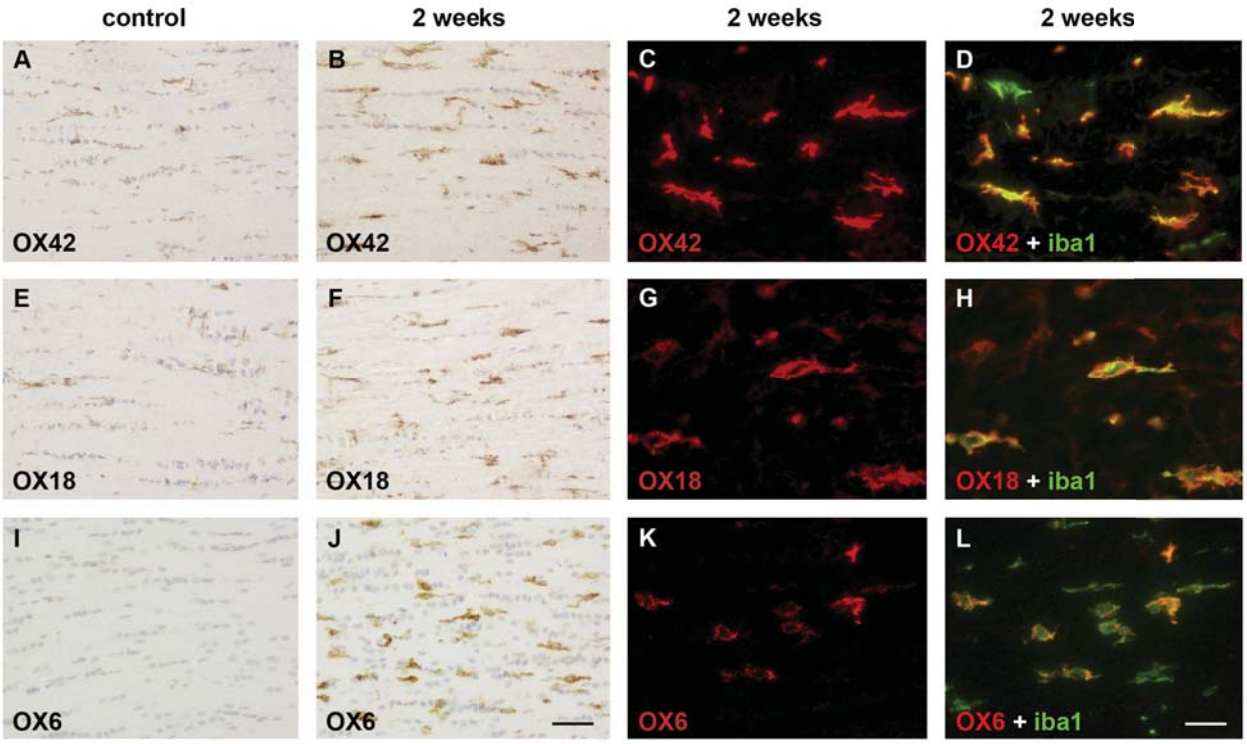

FIGURE 10. Microglial expression of complement type 3 receptor (OX-42, **A–D**), MHC class I (OX18, **E–H**), and MHC class II (OX-6, **I–L**) during experimental glaucoma. (**A**, **E**, **I**) Control ONs. The remaining images are of sections from moderately damaged ONs 2 weeks after the induction of elevated IOP. OX-42 is constitutively expressed by quiescent microglia in the normal ON (**A**) and is persistently upregulated on activation (**B–D**). Interestingly, a few iba1-positive microglia did not express cd11b (**D**). OX-18 is not exclusively, although it is predominantly, expressed by microglia in control ONs (**E**). Marked upregulation occurs in activated microglial cells (**F–H**). OX-6 is absent from control ONs (**I**) but is robustly and exclusively expressed by activated microglia (**J–L**). Scale bars: colorimetric images, 50 μm; immunofluorescence images, 25 μm.

positive cells were found throughout the ON. Cells were typically lightly stained at 1 week but were strongly labeled by 2 weeks (Fig. 10J). Double labeling demonstrated that the induction of OX6 expression occurred exclusively in iba1-positive microglia (Figs. 10K, 10L). Interestingly, and unlike OX42 or OX18, there was a spatial difference in the expression of OX6 within the optic pathway. No expression of OX6 was found in the retina at any time point after the induction of experimental glaucoma, even in animals that featured numerous ED1-positive retinal microglia, indicating ongoing neuronal damage and phagocytic activity. This finding is illustrated in Figure 11, which shows adjacent sections from the retina (Figs. 11A, 11B), ONH (Figs. 11C, 11D), and proximal ON (Figs. 11E, 11F) from one representative animal killed after 2 weeks and stained for ED1 and OX6. ED1 immunoreactivity was seen in all three locations. In contrast, robust labeling of OX6 was apparent in the ON, but only very limited expression of OX6 was evident in the ONH, and no staining was detectable in the retina. Of note, OX6 labeling in the neck of the ONH varied markedly between animals, with most rats showing few OX6-positive cells while others featured several OX6-labeled microglia. The presence or absence of OX6 immunoreactivity seemed unrelated to the severity of ON injury or grade of microglial activation within the ON.

Infiltration of Leukocytes

Very limited T-cell infiltration was found in the damaged ON (Figs. 12A, 12B) or retinas (data not shown) using an antibody that recognizes the pan T-cell marker CD3. The number of infiltrating cells tended to increase both with the severity of injury and with the passage of time after insult (Fig. 12C). The increased density of T cells observed in perivascular areas (Fig. 12D) was consistent with invasion from blood vessels. No infiltration of neutrophils, as defined by immunoreactivity to myeloperoxidase, was found in injured ONs during experimental glaucoma (data not shown).

Rat models of traumatic, ischemic, and autoimmune optic neuropathies all share a common pathologic feature: the presence of a focal lesion in the proximal ON with accompanying infiltration of hematogenous macrophages. We addressed the question of whether laser-induced experimental glaucoma also results in the presence of a focal lesion within the ON with accompanying infiltration of macrophages. After 1 and 2 weeks, there was an absence of ED1- and iba1-positive cells with the physical characteristics of macrophages in any part of the optic pathway, suggesting that the blood brain barrier remains intact in this disease paradigm. At 6 weeks, there was evidence of some cells with a macrophage-like morphology within the degenerating ON (Figs. 12E–H), particularly in rats with more severe damage, which corresponded with the disappearance of myelin basic protein. These cells could be resident microglia that had fully transformed into phagocytic macrophages or infiltrating macrophages.

DISCUSSION

There is increasing evidence that microglia play a central role in chronic degenerative conditions of the CNS, including Alzheimer's and Parkinson's diseases, multiple sclerosis, amyotrophic lateral sclerosis, and many others.[12] In the present study

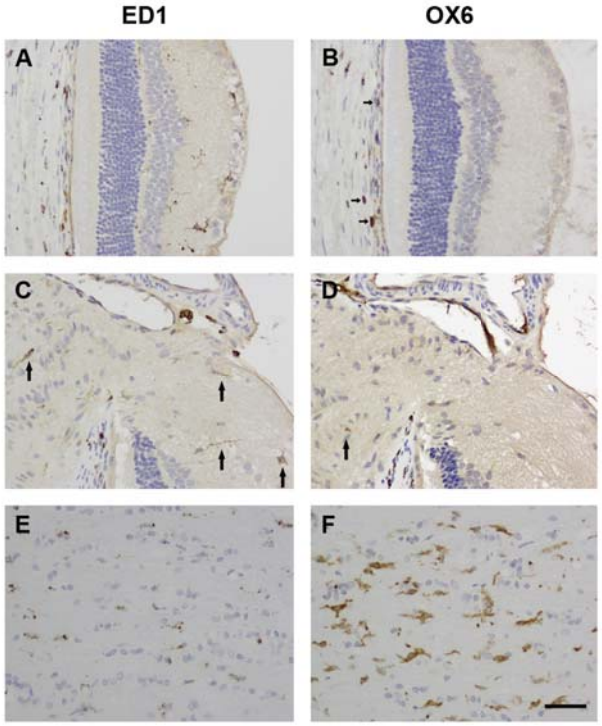

FIGURE 11. Spatial pattern of OX6 expression during experimental glaucoma. Adjacent sections from one representative animal killed 1 week after the induction of elevated IOP and stained for ED1 (**A**, **C**, **E**) and OX6 (**B**, **D**, **F**) are shown. Three locations are shown: midperipheral retina (**A**, **B**), ONH (**C**, **D**), and proximal ON (**E**, **F**). Numerous ED1-positive ramified microglia were present within the retina (**A**). ED1-labeled cells were somewhat reduced in density in the prelaminar and laminar portions of the ONH (**C**, *arrows*) but were numerous within the myelinated portion of the proximal ON (**E**). Interestingly, the pattern for OX6 was strikingly different from that for ED1. OX6 was absent from the retina (**B**). Note, however, the presence of many OX6-positive cells in the choroid (**B**, *arrows*). Expression of OX6-positive microglia in the ONH varied between animals, but typically only sparse labeling was observed, as in this rat (**D**, *arrow*). In the proximal ON, OX6 was robustly expressed on cells with the distinct features of activated microglia (**F**). Scale bar, 50 μm (**A**–**F**).

we have, for the first time, described the microglial response in the optic pathway of rats with experimental glaucoma. Microglial activation occurred along the entire optic pathway and correlated closely with axonal damage. It was, however, not accompanied by any overt infiltration of neutrophils. Microglia upregulated the expression of immunologic cell surface markers, including complement receptor type 3, MHC class I, and MHC class II, but the expression of MHC class II was limited to cells within the white matter. Despite the increased expression of molecules associated with antigen presentation, only nominal T lymphocyte infiltration was observed. Further studies are warranted to elucidate the role of microglial activation in glaucoma.

The primary site of injury in glaucoma is yet to be unequivocally identified, but some research points toward the ONH, the site at which RGC axons pass through the connective tissue of the lamina cribrosa.[43,45,46] Previous studies in rats[31] and humans[47] have described increased microglial activation in the ONH during glaucoma, but neither study examined other regions of the optic pathway. In the present study, we observed marked axon transport failure at the ONH as early as 3 days after the induction of raised pressure. This was accompanied in the ONH by an alteration in the morphology of iba1-positive microglia from a quiescent to an activated phenotype; yet, there was no indication of a specific or preferential microglial activation at this location at this time point. Throughout the retina, ON, and OT, iba1-positive microglia also showed some retraction of processes and cell body hypertrophy. Similarly, at 7 and 14 days, microglia in the ONH were more numerous and upregulated expression of the lysosomal antigen ED1. Again, these events were ostensibly concurrent in the other regions of the optic pathway. Indeed, somewhat contrary to expectation, there was a clear trend of greater microglial activity beyond the point of myelination in the retrobulbar ON that occurs immediately distal to the ONH. This corresponded with the finding of more numerous SMI-32 abnormalities in the myelinated region of the ON. The combined results are consistent with the results of a study by Schlamp et al.,[36] who analyzed axonal degeneration in the DBA/2J mouse model of glaucoma and documented greater structural preservation in the ONH compared with more distal segments of the pathway.

Five percent to 10% of RGC axons in the adult rat do not cross the midline of the optic chiasm, projecting instead to the ipsilateral half of the brain. These fibers originate from the inferior-temporal crescent of the retina.[48,49] In the present study, analysis of the optic chiasm revealed minimal evidence of any microglial activation in noncrossing fibers in the ipsilaterally projecting OT at any of the time points analyzed. The obvious conclusion to draw is that there is negligible death of RGCs in the region of the inferior-temporal retina from which these fibers originate. The results confirm and extend earlier observations of preferential damage in the superior segment of the retina and ON in the hypertonic saline and laser models of glaucoma.[50,51]

One important goal of the present study was to shed light on the temporal relationship between microglial activation and axonal loss in the ON. Two related aspects were of interest: first, to ascertain whether alterations in microglial markers preceded, were concomitant with, developed soon after, or were significantly delayed after axonal cytoskeletal damage; second, to evaluate whether microglial activation can be used in neuroprotection studies as a surrogate or an adjunct marker for ON injury, particularly at early time points featuring mild or moderate pathologic changes (1 and 2 weeks) when axon counting is less reliable. Microglia are known to be very sensitive to disturbances in milieu homeostasis, neuronal function, and disruption,[3] which would seem to put them in an ideal position to quantify the severity of early axonal damage.

With regard to the onset of microglial activation in the ON, at 3 days after the induction of glaucoma, the earliest time point analyzed, axonal loss as determined by conventional analysis of toluidine blue–stained ONs was marginal, but SMI-32 immunolabeling revealed subtle abnormalities in some axons. Expression of ED1, the rodent equivalent of CD68 whose presence is considered indicative of phagocytosis, was negligible. Conversely, iba1 immunostaining showed clear evidence of microglial activation, as discussed. Iba1 is increasingly used as a marker of microglial activation. It has been shown to be upregulated in a time-dependent manner after injuries such as axotomy[52] and focal cerebral ischemia[53] and is thought to contribute to microglial cell migration.[54] The present results show iba1 to be a highly sensitive marker of damage in the ON, which allows identification of early pathologic axonal changes soon after injury, before any overt axonal loss and phagocytosis have occurred.

To ascertain whether iba1 or ED1 might prove useful in neuroprotection studies as quantitative markers for ON injury, we correlated each antigen with two complementary measures of axonal injury, grading of toluidine blue–stained transverse sections, which is the most frequently used method for estimating axonal loss[2] and abundance of SMI-32 abnormalities in

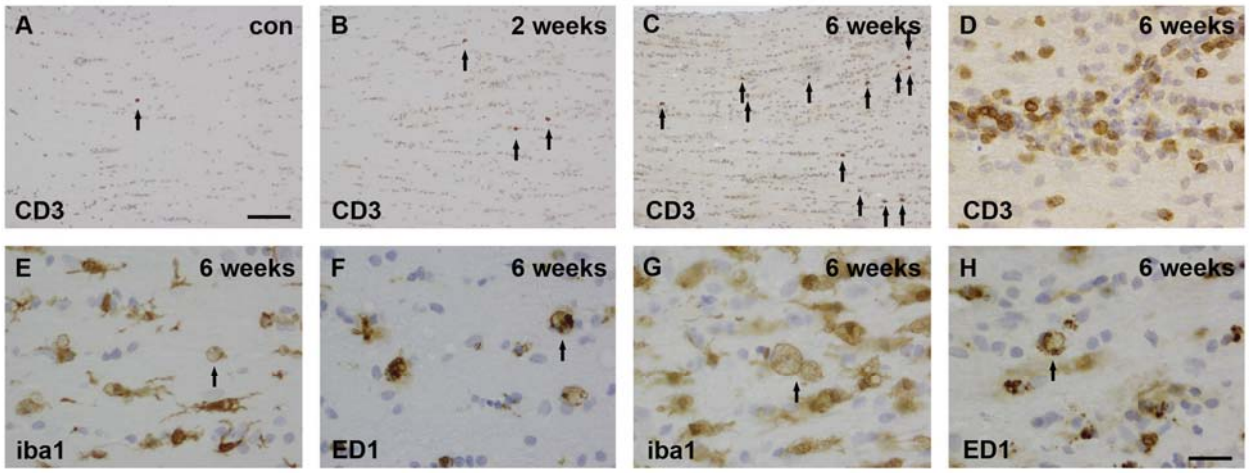

FIGURE 12. (A–D) Infiltration of T cells in the distal ON during experimental glaucoma. Occasional T cells, as identified by the pan T-cell marker CD3, are present in control ONs (A). Very limited infiltration occurred in moderately damaged ONs after 2 weeks (B). Severely damaged (grade 5) nerves at 6 weeks show greater T-cell infiltration (C). This is particularly evident around large blood vessels (D). (E–H) Presence of macrophages during experimental glaucoma. Immunolabeling for iba1 (E, G) and ED1 (F, H) in a moderately (grade 2; E, F) and a severely (grade 5; G, H) injured ON 6 weeks after the induction of elevated IOP showed occasional cells with the morphologic features of macrophages (large, round cells with foamy cytoplasm but no processes; E–H, *arrows*). However, most cells resembled phagocytic resident microglia, even in the severely damage ON. Of note: clear distinction between the two populations is not possible based on iba1 and ED1 immunolabeling. Scale bars: 100 μm (A–C); 25 μm (D–H).

longitudinal sections of the ON. SMI-32, which labels nonphosphorylated NF-H, has been shown by others to be an excellent marker of axonal injury[55,56] and, in our hands, was more sensitive than other axonal cytoskeletal proteins for early detection of pathologic changes in the ON (unpublished observations). The overall results showed a highly statistically significant correlation among all four combinations; nevertheless, minor differences were evident. The first disparity was that ON damage as assessed by toluidine blue staining correlated better with both microglial markers at the 2-week than at the 1-week time point. This may simply be due to the higher number (*n*) at the later time point. Alternatively, it may relate to the greater reliability of both the grading system and the microglial response in situations of increased injury. Two further observations were that the correlation with ON grading was stronger for ED1 than for iba1, whereas injury as assessed by SMI-32 immunostaining correlated better with iba1 than with ED1. These findings are understandable when viewed from a physiological perspective. Early axonal injury, comprising axonal transport disruption and dephosphorylation of neurofilaments but little measurable axonal loss, would result in increases in SMI-32 abnormalities and iba1 expression, but negligible ED1 expression since the phagocytosis of axonal debris is yet to commence. Later time points would comprise morphologically visible axonal breakdown, myelin disruption, and activation of the phagocytic system. Thus, it makes sense that ED1 and ON grading are closely matched.

The overall results advocate microglial activation as a useful adjunct quantitative tool for assessment of the status of ON damage in neuroprotection studies, although a cautionary note must be added that we do not yet have enough information to discern the precise relationship between microglial activation and neurodegeneration. Nevertheless, previous studies, both in the ON and the brain, have reached a similar conclusion that the extent of microglial activation reflects the severity of injury; for example, Zhang et al.[57] showed that the time course of microglial morphologic change after transient middle cerebral artery occlusion paralleled neuronal damage, whereas Kato et al.[58] highlighted that microglia were activated in a graded fashion in response to the severity of neuronal injury after temporal forebrain ischemia. The usefulness of microglia as a means of quantifying damage and neuroprotection has also been exploited in chronic models of injury, such as chronic cerebral hypoperfusion, which features slow, progressive damage to CNS white matter tracts.[59–61]

Rat models of traumatic (ON transection,[62] ON crush[63]), ischemic (anterior ischemic optic neuropathy, permanent occlusion of the common carotid arteries),[29] and autoimmune (EAE)[30] optic neuropathies all share a common pathologic feature: the presence of a focal lesion in the retrobulbar ON with accompanying infiltration of hematogenous macrophages.

It is known that blood vessels in the retrobulbar ON are permeable to intravascular tracers such as horseradish peroxidase, prompting the question whether there is a true blood-brain barrier at the optic nerve head.[64] This inherent weakness of the blood-brain barrier has been suggested to be responsible for the susceptibility of this region to lesion formation in both EAE and multiple sclerosis.[30] We examined whether there is a similar focal lesion with an accompanying presence of macrophages during experimental glaucomatous optic neuropathy. We found no evidence of a focal lesion or macrophage presence in the ON after the elevation of IOP, suggesting that the blood-brain barrier remains intact in this disease paradigm.

During glaucoma, the appearance of ED1-positive microglia with an ameboid, foamy, phagocytic appearance in the ON and OT was delayed, occurring between 2 and 6 weeks. This paralleled an increase in myelin basic protein disorganization. It is well known that the clearance of myelin debris after axonal cytoskeletal degeneration is a lengthy process in CNS neurodegenerative conditions because of the failure of microglia to develop into fully functional phagocytic cells,[65] coupled with the minimal role played by oligodendrocytes.[66] Phagocytic removal of tissue debris helps create a pro-regenerative environment. The inefficiency of white matter phagocytosis in the CNS compared with peripheral nerves is thought to account for the lack of neuronal regeneration under physiological conditions. This is clearly the case in glaucoma.

Microglia are the major cell population in the CNS with the potential to act as antigen-presenting cells. Under normal physiological conditions, the expression of MHC molecules, which are critical for T-cell interactions, is at low or undetectable

levels. After injury, microglia increase the expression of MHC class II. In some, but not all, models of acute and chronic injury, this is associated with a limited T-cell response. After the induction of experimental glaucoma, there was an upregulation in MHC class I and II in the ON and OT, which was most clearly evident at 1 week and which slowly declined thereafter. This did not correlate with any significant T-cell infiltration, suggesting either an insufficient presence of costimulatory molecules or that MHC antigens perform functions unrelated to the induction of an immune response. However, in more severely injured animals, we could observe limited infiltration, which is in accordance with the infiltration of only small numbers in nearly all neurodegenerative diseases.[10] Interestingly, there was a fundamental difference between the gray matter of the retina and the white matter of the ON and the OT: MHC class II was markedly upregulated on white matter microglia, but no expression was observed in retinal microglia. The same observation was made by Rao et al.[67] and Zhang and Tso[68] using intracranial and intraorbital models of ON transection, namely that MHC class II-positive cells were localized to degenerating myelinated fibers but not to the retina. The explanation for the regional difference is not simply attributed to the presence of injured myelin in the white, but not gray, matter, because ischemia-reperfusion[18] and kainic acid-induced excitotoxicity[19] both induced OX6 expression by resident retinal microglia. The explanation may be related to the fact that these latter models cause injury to more than one neuronal class in the retina, which is not the case with ON transection and glaucoma, or that they cause a more pronounced glial reactivity in general. The degree of retinal stress caused by the present model may simply not be sufficient to provoke the expression of MHC class II molecules on resident microglia or to cause invasion by bone marrow-derived macrophages, which in mice have been shown to be more prone to express MHC class II molecules.[69]

Acknowledgments

The authors thank Mark Daymon, Zhao Cai, and Kathy Cash for expert technical assistance.

References

1. Quigley HA. Number of people with glaucoma worldwide. *Br J Ophthalmol.* 1996;80:389–393.
2. Morrison JC. Elevated intraocular pressure and optic nerve injury models in the rat. *J Glaucoma.* 2005;14:315–317.
3. Nimmerjahn A, Kirchhoff F, Helmchen F. Resting microglial cells are highly dynamic surveillants of brain parenchyma in vivo. *Science.* 2005;308:1314–1318.
4. Pocock JM, Kettenmann H. Neurotransmitter receptors on microglia. *Trends Neurosci.* 2007;30:527–535.
5. Ambrosini E, Aloisi F. Chemokines and glial cells: a complex network in the central nervous system. *Neurochem Res.* 2004;29:1017–1038.
6. van Rossum D, Hilbert S, Strassenburg S, Hanisch UK, Bruck W. Myelin-phagocytosing macrophages in isolated sciatic and optic nerves reveal a unique reactive phenotype. *Glia.* 2008;56:271–283.
7. Hanisch UK. Microglia as a source and target of cytokines. *Glia.* 2002;40:140–155.
8. Ohlsson M, Bellander BM, Langmoen IA, Svensson M. Complement activation following optic nerve crush in the adult rat. *J Neurotrauma.* 2003;20:895–904.
9. Gehrmann J, Matsumoto Y, Kreutzberg GW. Microglia: intrinsic immuneffector cell of the brain. *Brain Res Brain Res Rev.* 1995;20:269–287.
10. Lucin KM, Wyss-Coray T. Immune activation in brain aging and neurodegeneration: too much or too little? *Neuron.* 2009;64:110–122.
11. Streit WJ. Microglia as neuroprotective, immunocompetent cells of the CNS. *Glia.* 2002;40:133–139.
12. Block ML, Zecca L, Hong JS. Microglia-mediated neurotoxicity: uncovering the molecular mechanisms. *Nat Rev.* 2007;8:57–69.
13. Cardona AE, Pioro EP, Sasse ME, et al. Control of microglial neurotoxicity by the fractalkine receptor. *Nature Neurosci.* 2006;9:917–924.
14. Rao NA, Kimoto T, Zamir E, et al. Pathogenic role of retinal microglia in experimental uveoretinitis. *Invest Ophthalmol Vis Sci.* 2003;44:22–31.
15. Robertson MJ, Erwig LP, Liversidge J, Forrester JV, Rees AJ, Dick AD. Retinal microenvironment controls resident and infiltrating macrophage function during uveoretinitis. *Invest Ophthalmol Vis Sci.* 2002;43:2250–2257.
16. Zeng XX, Ng YK, Ling EA. Neuronal and microglial response in the retina of streptozotocin-induced diabetic rats. *Vis Neurosci.* 2000;17:463–471.
17. Davies MH, Eubanks JP, Powers MR. Microglia and macrophages are increased in response to ischemia-induced retinopathy in the mouse retina. *Mol Vis.* 2006;12:467–477.
18. Zhang C, Lam TT, Tso MO. Heterogeneous populations of microglia/macrophages in the retina and their activation after retinal ischemia and reperfusion injury. *Exp Eye Res.* 2005;81:700–709.
19. Chang ML, Wu CH, Chien HF, Jiang-Shieh YF, Shieh JY, Wen CY. Microglia/macrophages responses to kainate-induced injury in the rat retina. *Neurosci Res.* 2006;54:202–212.
20. Harada T, Harada C, Kohsaka S, et al. Microglia-Muller glia cell interactions control neurotrophic factor production during light-induced retinal degeneration. *J Neurosci.* 2002;22:9228–9236.
21. Sasahara M, Otani A, Oishi A, et al. Activation of bone marrow-derived microglia promotes photoreceptor survival in inherited retinal degeneration. *Am J Pathol.* 2008;172:1693–1703.
22. Thanos S. Sick photoreceptors attract activated microglia from the ganglion cell layer: a model to study the inflammatory cascades in rats with inherited retinal dystrophy. *Brain Res.* 1992;588:21–28.
23. Thanos S, Richter W. The migratory potential of vitally labelled microglial cells within the retina of rats with hereditary photoreceptor dystrophy. *Int J Dev Neurosci.* 1993;11:671–680.
24. Penfold PL, Liew SC, Madigan MC, Provis JM. Modulation of major histocompatibility complex class II expression in retinas with age-related macular degeneration. *Invest Ophthalmol Vis Sci.* 1997;38:2125–2133.
25. Baptiste DC, Powell KJ, Jollimore CA, et al. Effects of minocycline and tetracycline on retinal ganglion cell survival after axotomy. *Neuroscience.* 2005;134:575–582.
26. Garcia-Valenzuela E, Sharma SC, Pina AL. Multilayered retinal microglial response to optic nerve transection in rats. *Mol Vis.* 2005;11:225–231.
27. Thanos S. The relationship of microglial cells to dying neurons during natural neuronal cell death and axotomy-induced degeneration of the rat retina. *Eur J Neurosci.* 1991;3:1189–1207.
28. Chidlow G, Holman MC, Wood JP, Casson RJ. Spatiotemporal characterisation of optic nerve degeneration after chronic hypoperfusion in the rat. *Invest Ophthalmol Vis Sci.* 2010;51:1483–1497.
29. Zhang C, Guo Y, Miller NR, Bernstein SL. Optic nerve infarction and post-ischemic inflammation in the rodent model of anterior ischemic optic neuropathy (rAION). *Brain Res.* 2009;1264:67–75.
30. Hu P, Pollard J, Hunt N, Taylor J, Chan-Ling T. Microvascular and cellular responses in the optic nerve of rats with acute experimental allergic encephalomyelitis (EAE). *Brain Pathol.* 1998;8:475–486.
31. Johnson EC, Jia L, Cepurna WO, Doser TA, Morrison JC. Global changes in optic nerve head gene expression after exposure to elevated intraocular pressure in a rat glaucoma model. *Invest Ophthalmol Vis Sci.* 2007;48:3161–3177.
32. Naskar R, Wissing M, Thanos S. Detection of early neuron degeneration and accompanying microglial responses in the retina of a rat model of glaucoma. *Invest Ophthalmol Vis Sci.* 2002;43:2962–2968.
33. Wang X, Tay SS, Ng YK. An immunohistochemical study of neuronal and glial cell reactions in retinae of rats with experimental glaucoma. *Exp Brain Res.* 2000;132:476–484.

34. Yuan L, Neufeld AH. Activated microglia in the human glaucomatous optic nerve head. *J Neurosci Res.* 2001;64:523–532.
35. Morrison JC, Johnson EC, Cepurna W, Jia L. Understanding mechanisms of pressure-induced optic nerve damage. *Prog Retinal Eye Res.* 2005;24:217–240.
36. Schlamp CL, Li Y, Dietz JA, Janssen KT, Nickells RW. Progressive ganglion cell loss and optic nerve degeneration in DBA/2J mice is variable and asymmetric. *BMC Neurosci.* 2006;7:66.
37. Levkovitch-Verbin H, Quigley HA, Martin KR, Valenta D, Baumrind LA, Pease ME. Translimbal laser photocoagulation to the trabecular meshwork as a model of glaucoma in rats. *Invest Ophthalmol Vis Sci.* 2002;43:402–410.
38. Chauhan BC, Levatte TL, Garnier KL, et al. Semiquantitative optic nerve grading scheme for determining axonal loss in experimental optic neuropathy. *Invest Ophthalmol Vis Sci.* 2006;47:634–640.
39. Ruifrok AC, Johnston DA. Quantification of histochemical staining by color deconvolution. *Anal Quant Cytol Histol.* 2001;23:291–299.
40. Chan HC, Chang RC, Koon-Ching Ip A, et al. Neuroprotective effects of *Lycium barbarum Lynn* on protecting retinal ganglion cells in an ocular hypertension model of glaucoma. *Exp Neurol.* 2007;203:269–273.
41. Li RS, Chen BY, Tay DK, Chan HH, Pu ML, So KF. Melanopsin-expressing retinal ganglion cells are more injury-resistant in a chronic ocular hypertension model. *Invest Ophthalmol Vis Sci.* 2006;47:2951–2958.
42. Sappington RM, Carlson BJ, Crish SD, Calkins D. The microbead occlusion model: a paradigm for induced ocular hypertension in rats and mice. *Invest Ophthalmol Vis Sci.* 2010;51:207–216.
43. Quigley HA, Addicks EM, Green WR, Maumenee AE. Optic nerve damage in human glaucoma, II: the site of injury and susceptibility to damage. *Arch Ophthalmol.* 1981;99:635–649.
44. Ju KR, Kim HS, Kim JH, Lee NY, Park CK. Retinal glial cell responses and Fas/FasL activation in rats with chronic ocular hypertension. *Brain Res.* 2006;1122:209–221.
45. Martin KR, Quigley HA, Valenta D, Kielczewski J, Pease ME. Optic nerve dynein motor protein distribution changes with intraocular pressure elevation in a rat model of glaucoma. *Exp Eye Res.* 2006;83:255–262.
46. Salinas-Navarro M, Alarcon-Martinez L, Valiente-Soriano FJ, et al. Ocular hypertension impairs optic nerve axonal transport leading to progressive retinal ganglion cell degeneration. *Exp Eye Res.* 2010;90:168–183.
47. Neufeld AH. Microglia in the optic nerve head and the region of parapapillary chorioretinal atrophy in glaucoma. *Arch Ophthalmol.* 1999;117:1050–1056.
48. Bunt SM, Lund RD, Land PW. Prenatal development of the optic projection in albino and hooded rats. *Brain Res.* 1983;282:149–168.
49. Cowey A, Franzini C. The retinal origin of uncrossed optic nerve fibres in rats and their role in visual discrimination. *Exp Brain Res.* 1979;35:443–455.
50. Morrison JC, Moore CG, Deppmeier LM, Gold BG, Meshul CK, Johnson EC. A rat model of chronic pressure-induced optic nerve damage. *Exp Eye Res.* 1997;64:85–96.
51. WoldeMussie E, Ruiz G, Wijono M, Wheeler LA. Neuroprotection of retinal ganglion cells by brimonidine in rats with laser-induced chronic ocular hypertension. *Invest Ophthalmol Vis Sci.* 2001;42:2849–2855.
52. Ito D, Imai Y, Ohsawa K, Nakajima K, Fukuuchi Y, Kohsaka S. Microglia-specific localisation of a novel calcium binding protein, Iba1. *Brain Res Mol Brain Res.* 1998;57:1–9.
53. Ito D, Tanaka K, Suzuki S, Dembo T, Fukuuchi Y. Enhanced expression of Iba1, ionized calcium-binding adapter molecule 1, after transient focal cerebral ischemia in rat brain. *Stroke.* 2001;32:1208–1215.
54. Ohsawa K, Imai Y, Sasaki Y, Kohsaka S. Microglia/macrophage-specific protein Iba1 binds to fimbrin and enhances its actin-bundling activity. *J Neurochem.* 2004;88:844–856.
55. Domercq M, Etxebarria E, Perez-Samartin A, Matute C. Excitotoxic oligodendrocyte death and axonal damage induced by glutamate transporter inhibition. *Glia.* 2005;52:36–46.
56. Mancardi G, Hart B, Roccatagliata L, et al. Demyelination and axonal damage in a non-human primate model of multiple sclerosis. *J Neurol Sci.* 2001;184:41–49.
57. Zhang Z, Chopp M, Powers C. Temporal profile of microglial response following transient (2 h) middle cerebral artery occlusion. *Brain Res.* 1997;744:189–198.
58. Kato H, Kogure K, Araki T, Itoyama Y. Graded expression of immunomolecules on activated microglia in the hippocampus following ischemia in a rat model of ischemic tolerance. *Brain Res.* 1995;694:85–93.
59. Cho KO, La HO, Cho YJ, Sung KW, Kim SY. Minocycline attenuates white matter damage in a rat model of chronic cerebral hypoperfusion. *J Neurosci Res.* 2006;83:285–291.
60. Nakaji K, Ihara M, Takahashi C, et al. Matrix metalloproteinase-2 plays a critical role in the pathogenesis of white matter lesions after chronic cerebral hypoperfusion in rodents. *Stroke.* 2006;37:2816–2823.
61. Wakita H, Tomimoto H, Akiguchi I, Kimura J. Dose-dependent, protective effect of FK506 against white matter changes in the rat brain after chronic cerebral ischemia. *Brain Res.* 1998;792:105–113.
62. Stoll G, Trapp BD, Griffin JW. Macrophage function during Wallerian degeneration of rat optic nerve: clearance of degenerating myelin and Ia expression. *J Neurosci.* 1989;9:2327–2335.
63. Frank M, Wolburg H. Cellular reactions at the lesion site after crushing of the rat optic nerve. *Glia.* 1996;16:227–240.
64. Tso MO, Shih CY, McLean IW. Is there a blood-brain barrier at the optic nerve head? *Arch Ophthalmol.* 1975;93:815–825.
65. Neumann H, Kotter MR, Franklin RJ. Debris clearance by microglia: an essential link between degeneration and regeneration. *Brain.* 2009;132:288–295.
66. Vargas ME, Barres BA. Why is Wallerian degeneration in the CNS so slow? *Annu Rev Neurosci.* 2007;30:153–179.
67. Rao K, Lund RD. Optic nerve degeneration induces the expression of MHC antigens in the rat visual system. *J Comp Neurol.* 1993;336:613–627.
68. Zhang C, Tso MO. Characterization of activated retinal microglia following optic axotomy. *J Neurosci Res.* 2003;73:840–845.
69. Kaneko H, Nishiguchi KM, Nakamura M, Kachi S, Terasaki H. Characteristics of bone marrow-derived microglia in the normal and injured retina. *Invest Ophthalmol Vis Sci.* 2008;49:4162–4168.

6. The influence of hyperglycaemia in experimental glaucoma

The previous papers have characterized and validated an experimental model of glaucoma, and established appropriate methods to quantify optic nerve damage. With these tools in hand, it is now possible to embark on the central query, the effect of hyperglycaemia in ocular hypertension.

Hyperglycaemia has been shown to exacerbate ischemic brain injury.[215] Compromised optic nerve blood flow and oxygen supply is a possible contributor to glaucomatous optic neuropathy. Nevertheless, evidence regarding an epidemiological association between diabetes mellitus and glaucoma is controversial, despite large-scale clinical trials. In the Ocular Hypertension Treatment Study, diabetes even seemed to protect against the conversion to glaucoma.[31] Glucose has been shown to protect retinal neurons during both acute and prolonged periods of ischemia.[249, 285] The following paper aims to further elucidate the role of hyperglycaemia in experimental glaucoma.

I chose to use STZ-diabetic rats because this model produces consistent elevation of systemic glucose levels and is well established in diabetes research. It has been used for more than 20 years. This paradigm, to some extent, mimics human type 1 diabetes. However, it is important to bear in mind that it does not necessarily reproduce all the changes seen in humans and the complete lack of insulin is in striking contrast to the more common type 2 diabetes. Hence, the study set-up reproduces the conditions found in epidemiologic research incompletely, and the results of this experimental work most likely do not reflect the situation of humans with diabetes mellitus and POAG to the full extent and complexity.

Protection of Retinal Ganglion Cells and the Optic Nerve During Short-term Hyperglycemia in Experimental Glaucoma

Contribution of each author

Andreas Ebneter:

Conception and design
Animal experiments and immunohistochemistry
Acquisition of data
Analysis and interpretation of data
Drafting and finalization of the manuscript
Obtaining funding

Glyn Chidlow:

Conception and design
Analysis and interpretation of data
Critical revision of the manuscript for important intellectual content
Administrative, technical, or material support
Supervision

John Wood:

Analysis and interpretation of data
Critical revision of the manuscript for important intellectual content
Supervision

Robert Casson:

Conception and design
Analysis and interpretation of data
Critical revision of the manuscript for important intellectual content
Statistical expertise
Obtaining funding
Supervision

Ebneter, A., Chidlow, G., Wood, J.P. & Casson, R.J. (2011) Protection of retinal ganglion cells and the optic nerve during short-term hyperglycemia in experimental glaucoma
Archives of Ophthalmology, v. 129 (10), pp. 1337-1344

7. Conclusions and future directions

7.1. Overall significance and contribution to the current knowledge

The current body of work provides further evidence pointing towards the optic nerve head as the site of the primary insult in experimental models of ocular hypertension. Importantly, it has confirmed disruption of the anterograde transport at the optic nerve head by means of endogenous markers. Previous studies were mainly based on the use of exogenous agents that were injected into the vitreous cavity. The utilization of endogenous markers provides the advantage of reducing the occurrence of artefactual changes.

The concurrent spatio-temporal study of the antrograde transport of endogenous amyloid precursor protein and sensitive markers of cytoskeleton breakdown, namely SMI-32, suggests that functional failure precedes structural breakdown. This emphasizes the significance of axonal transport for neuronal homeostasis and could make a case for energy failure as a pivotal facet of glaucoma pathology. This study also found evidence of neuron driven presumptive neuroregeneration at the optic nerve head.

Microglial markers hitherto have been used to quantify brain injury. In their role as surveillance elements this population of cells monitors the environment, reacts quickly to disturbances and sensitively indicates noxious influences and homeostasis disruption. This work investigated microglial involvement in glaucomatous optic neuropathy and foreshadows the usefulness of microglial markers in optic nerve and retinal research.

Finally, this work added an element of evidence to findings from epidemiological studies and found attenuated neurodegeneration of RGCs and their axons in the presence of systemic hyperglycaemia. This result may help to explain the absent or weak association between POAG and diabetes mellitus, and encourages further research towards bioenergetic neuroprotection.

7.2. Limitations of the study

7.2.1. Quantification of RGC

Sectoral retinal nerve fibre loss is a hallmark of glaucomatous optic neuropathy in humans, and provides strong evidence for the optic nerve head being the site of the primary insult. Therefore, as highlighted earlier, an ideal animal model of glaucomatous axon degeneration should produce sectoral damage. Sectoral loss has repeatedly been demonstrated in the DBA/J2 mouse as well as in rat models of ocular hypertension.[146, 180, 305] These models have subsequently been widely used as surrogate models for human glaucoma. Since ganglion cell loss is not uniform across the entire retina and the severity of damage variable, depending on the location, the most accurate analysis of ganglion cell numbers would include the whole retina. On a practical note, flat mounts of the retina are most commonly used.

In the present study, I chose to count ganglion cells on sagittal sections instead. This comes with the advantage of being able to stain sections with a multitude of antibodies, representing different aspects of cellular function from diverse cell populations. However, the estimates for individual animals might vary depending on the location of the section with respect to the areas of different severity of damage. Nevertheless, provided that the number of animals and sections analysed is large enough, the variability should be acceptable. Moreover, estimated axon counts on optic nerve cross sections are likely to be related to RGC loss, unless there is a significant element of

compartmentalization in the neurodegenerative process,[306] and similar findings in the two compartments substantiated the validity of the retinal findings.

7.2.2. Estimation of axonal loss

Full axon count techniques represent the most accurate way of determining structural axonal damage. Manual counting on transmission electron microscopy is considered the gold standard. Nevertheless, only about 50% of the optic nerve cross section is amenable for analysis with transmission electron microscopy[301] because the mesh grid used occupies about half of the tissue area, and therefore total nerve counts must be extrapolated. Light microscopy techniques underestimate the number of axons by up to 40% because small axons under 0.5 μm diameter are not detected due to the limited resolution of light microscopy.[295] However, manual counting is extremely time consuming and not practical for larger numbers of samples. Methods for semi-automated counting have therefore been developed and are often used to evaluate light microscopy photographs of semi-thin resin sections. Different approaches are used: (1) Full semi-automated counting on montaged pictures,[164] (2) semi-automated counting on a certain number of pictures taken randomly (commonly about 10 pictures, representing approximately 10% of the whole optic nerve cross section),[307] and (3) semi-automated counting of images taken after targeted sampling.[308] All of these methods produce satisfactory counts, however, semi-automated targeted sampling methods have been claimed to be most practical and accurate.[301] In this approach, the optic nerve cross section is first divided into zones of approximately equal damage. A defined number of pictures is then taken from each zone of damage and quantified by semi-automated counting. The total axon count is then extrapolated by a weighted average calculation. For all methods based on partial sampling, axonal loss should ideally be estimated by comparing the estimated count of a particular nerve to the estimated count of the contralateral nerve, which serves as internal control, where the pictures have been taken from identical locations. The axon density varies within the optic nerve, damage is not uniform[309] and inter-animal variability of axon numbers between individual animals can be substantial, even within the same strain.[310]

Finally, each method has its advantages and disadvantages. In general, greater accuracy comes at the cost of more time consumption. In this present study, I used two methods for axon quantification to improve accuracy: the Chauhan method[311] and semi-automated counting after targeted sampling. Quantification of the former relies on qualitative visual grading, while the latter uses automated axon counting by software. Full semi-automated counting on montaged pictures might have been better, but not practical due to limitations in manpower and accessibility of technology. To overcome possible limitations, results were corroborated by evaluation of longitudinal optic nerve sections after immuno-staining for microglia, macroglia and neurofilament markers.

7.2.3. Time frame of the study

In the present study, axonal and ganglion cell degeneration was quantified two weeks after induction of ocular hypertension. It would, without any doubt, be of interest to consider later time points as well to determine whether the neuroprotective effect observed is sustained or neurodegeneration merely delayed. However, STZ-induced hyperglycaemia itself is associated with vascular damage and neurodegeneration in the longer term, possibly in part because of the complete insulin withdrawal. Neuronal cells begin to die soon after the onset of STZ-diabetes. The molecular pathways involved have not yet been elucidated completely, but oxidative stress,

excitotoxicity and inflammation seem to be implicated.[312] The rate of apoptosis in the retina after only 1 month of STZ-diabetes is 10 times higher than in controls and after 7.5 months of diabetes the thickness of the inner plexiform layer is reduced by 22%, the inner nuclear layer by 10%. The RGC density was reduced by 10%.[313, 314] The vascular changes in the STZ-diabetes model include blood vessel dilation, capillary degeneration with loss of endothelial cells and pericytes, and microaneurysma formation.[315] Blood-retina-barrier breakdown with increased vascular permeability starts 2 weeks after onset of diabetes and is accompanied by increased leukostasis, which leads to vascular occlusion and tissue ischemia.[314, 316, 317] Elevated concentrations of extracellular glutamate have been measured in the vitreous and the retina of rats with STZ-induced diabetes.[318, 319] Early functional changes have been documented by electroretinography, which showed altered retinal electrophysiological activity.[320, 321] Of note, the positive scotopic threshold response, reflecting ganglion cell activity, was most sensitive to STZ-diabetes and changes were found as early as 4 weeks after induction,[322, 323] before morphological changes became obvious. Qin *et al.* detected ganglion cell dendritic field abnormalities 12 weeks after induction of STZ-diabetes.[290] Another group found retrograde axonal transport impairment of large and medium type RGC as early as one month after induction of STZ-diabetes, which was prevented by aldose reductase inhibitor.[324, 325]

7.3. Speculations about mechanisms of neuroprotection

In the present study I have not addressed the issue of possible mechanisms by which hyperglycaemia protects RGCs. However, mitochondria potentially are important in this context.[286] Mitochondrial dysfunction has been repeatedly implicated in the pathogenesis of glaucoma.[244]

Mitochondria play a cardinal role in neuron homeostasis. They are central not only in energy production, but play a crucial role in the regulation of cellular processes. In particular, they are pivotal in regulating cell death,[326, 327] marking the point of no return in apoptosis and necrosis. Mitochondria can induce apoptotic cell death both through caspase-dependent and caspase-independent pathways.[328] Furthermore, transport disruption and lack of mitochondria in synaptic terminals can induce synaptic degeneration. If the disruption is significant, Wallerian degeneration occurs. In less severe injuries 'dying-back' results.[306]

Mitochondria are involved in the pathogenesis of many neurodegenerative diseases, which all show the following features: selective brain areas and/or neuronal populations undergo neurodegeneration (involving mitochondrial dysfunction), loss of intracellular calcium homeostasis, and excitotoxicity.[329] The energy requirements to maintain membrane gradients in neural tissue are high, and, in general, neurons are highly dependent on glucose for ATP generation through oxidative phosphorylation and therefore have high mitochondrial content. Oxidative phosphorylation always results in ROS as by-products.[330] ROS are a group of small oxygen-containing free radicals that are extremely reactive due to their unpaired valence electrons. Under normal conditions, these ROS are neutralised by several cellular anti-oxidant mechanisms, like superoxide dismutases, glutathione peroxidase and catalase. If there is an imbalance between ROS generation and antioxidants, oxidative stress occurs. Neural tissue is particularly susceptible to ROS-induced damage because it has a high consumption of oxygen and is relatively deficient in oxidative defences. In particular, oxygen-glucose deprivation results in reduced ATP generation, mitochondrial dysfunction, impaired calcium buffering and increased ROS production.[331] Oxygen-glucose deprivation also initiates activation of microglia.[332]

There are many alternative generators of cellular ROS, including nicotinamide adenine dinucleotide phosphate-oxidase,[333] xanthine oxidase[334] and endothelial nitric oxide synthase.[335] However, in the majority of cell types, the mitochondrion is the major source of ROS. Physiological concentrations of ROS regulate many intracellular processes and are vital for survival.[336] ROS induce hypoxia-inducible factors (HIF), which are the master transcription factors responsible for the adaptation to low oxygen. HIFs maintain oxygen and energy homeostasis by regulating genes involved in metabolism, proliferation and cell survival.[337] HIF plays a protective role in neurodegenerative diseases.[338] ROS also activate NF-κB, another pro-survival transcription factor.[339] Furthermore, ROS activates p53 tumour suppressor, which, depending on the stress level, inhibits the cell cycle and upregulates several antioxidants, or induces apoptosis at high stress levels.[340] P53 also induces the pentose phosphate shunt via TP53-induced glycolysis and apoptosis regulator and inhibits glycolysis. The pentose phosphate shunt produces nicotinamide adenine dinucleotide phosphate, an important reducing agent for control of intracellular ROS levels.[341] However, excessively high levels of ROS cause oxidative stress, mitochondrial dysfunction, as well as intra- and extracellular damage or even cell death.[342]

The optic nerve has one of the highest energy demands and oxygen consumption rate in the body.[343] Several lines of evidence suggest that mitochondria and mitochondrial dysfunction play a central role in glaucoma.[286, 287, 344] Mitochondrial dysfunction could be primary,[345] but might as well be secondary to chronic hypoperfusion, excitotoxicity, immune dysregulation and glial changes. Of particular interest, however, is the fact that both in primary mitochondrial optic neuropathies and glaucoma, the optic nerve head appears to be central in the pathogenesis and represents an early site of clinical manifestation. This zone where the nerve fibres pass through the lamina cribrosa and become myelinated seems to be a locus of minor resistance to a variety of stressors. The density of mitochondria is very high anterior to the lamina cribrosa in the unmyelinated part of the axons, but abruptly diminishes as the myelin sheath begins.[346]

Mitochondrial biogenesis occurs in the somata of RGC, from where they are transported in the axons to the locations where they are needed, particularly in the unmyelinated portions of the nerve, including the nodes of Ranvier, and the synaptic terminals.[347] Mitochondria make up the largest cargo transported via axonal transport. Adequate mitochondrial distribution is essential for maintenance of function and cellular health and involves structural cytoskeleton proteins as well as mitochondrial fission and fusion.[348]

IOP and age[204] are the most important risk factors for glaucoma progression and potentially affect mitochondria and energy production of ganglion cells in several ways. The likelihood of developing glaucoma increases nearly 7-fold after 55 years,[17] suggesting that age-related changes render the optic nerve more vulnerable. This observation is not limited to glaucoma, but is equally true for other age-related neurodegenerative central nervous system disorders such as Alzheimer's and Parkinson's. Experimental data has shown a reduced metabolic reserve and increased metabolic vulnerability of aged RGCs in glaucomatous degeneration. The metabolic reserve, ATP, decreased IOP-dependent and age-dependent in mouse optic nerves.[349] Oxidative stress is a prominent feature of aging as deoxyribonucleic acid, proteins and lipids become increasingly susceptible to oxidative damage because of decreased efficiency of antioxidant mechanisms and cellular repair.[350, 351]

Mechanical stress could impair mitochondrial and other axonal transport. Band *et al.* using a mathematical modelling has hypothesized that IOP related passive intracellular fluid shifts could result in ATP depletion and disruption of axonal transport in the periphery of the optic nerve head.[352] Furthermore, hydrostatic pressure has been shown to trigger mitochondrial fission and decreases cellular ATP.[353] IOP elevation also activates astrocytes, which produce anti-oxidants, provide trophic support and are metabolically coupled to RGC. Perturbation of astrocytes in the

optic nerve head might impact on lactate supply and mitochondrial energy generation. Glia has been shown to produce TNF-α,[354] that modulates the redox status and induces oxidative stress.

Evidence that hypoxia is significantly involved in glaucoma pathogenesis is controversial. Nevertheless, tissue hypoxia could theoretically modulate the susceptibility of the optic nerve to IOP-induced stress. HIF-1α, a master regulator of oxygen homeostasis has been shown to be upregulated in the nerve head of glaucomatous human eyes.[355] HIF-1α interacts with a broad variety of metabolic pathways, which increase oxygen delivery or facilitate the metabolic adaption to hypoxia. In particular, HIF decreases mitochondrial oxidative phosphorylation and activates the conversion of pyruvate to lactate through glycolysis. This should reduces ROS production, but ATP production is less efficient. Nevertheless, additional tissue glucose availability to increase oxygen-independent ATP generation via glycolysis might be beneficial under circumstances of oxygen shortage, compensate to some extent for mitochondrial dysfunction, and facilitate compromised axonal transport.

In summary, additional energy supply is a possible, and probably the most likely mechanism of protection in this study. It could, by opening up alternative, mitochondria-independent pathways to produce ATP increase the metabolic reserve and delay disruption of axonal transport at the optic nerve head. Reduction of oxidative stress through bypassing mitochondrial metabolism and increased production of reducing molecules might be another explanation.

7.4. Future directions

Therapies aimed at improving mitochondrial function seem to slow down neuronal cell loss in glaucoma and other age-related neurodegenerative disease, and hence represent a promising neuroprotective strategy. Energy supply to starving tissues and buffering intracellular energy is a possible way to reduce mitochondrial dysfunction.

Systemic glucose delivery certainly is not practical because of the disastrous long-term complications of hyperglycaemia. Nevertheless, to study the potentially beneficial effect of topical glucose administration, our group is planning to conduct a prospective, randomized pilot study testing the hypothesis that topical glucose acts as a neurorecoverant and improves contrast sensitivity in glaucoma patients. Measuring contrast sensitivity is appealing because it represents a functional parameter, which would rapidly reflect improved cellular function. Bose *et al.*[356] reported non-IOP related improvement in contrast sensitivity after administration of a calcium antagonist (Nimodipine) in patients suffering from normal-tension glaucoma. Contrast sensitivity is an inexpensive clinical screening tool to assess potential neuroprotectants before embarking on large, time-consuming randomised controlled trials focussing on progression of visual field defects.

Creatine, a nitrogenous guanidine compound involved in supplying energy to muscles and neural tissue, acts as an energy buffer and is another potentially neuroprotective agent. Oral administration of creatine produces dose-dependent effects and is well tolerated, safe, and bioavailable to the brain. It is taken up into neural cells by a sodium-dependent creatine transporter and becomes physiologically active when it is transformed into phosphocreatinine. This transformation is regulated by the mitochondrial creatine kinase. Oral creatine supplementation to rats was neuroprotective against intracerebral injection of NMDA.[357] Subcutaneous creatine has been shown to protect neonatal rats against ischemic brain injury after unilateral common carotid artery occlusion.[358] In mice, oral creatine increased the healthy life span and decreased serum markers for oxidative stress and cerebral lipofuscin deposits.[359]

8. REFERENCES

1. Weinreb RN, Khaw PT. Primary open-angle glaucoma. *Lancet* 2004; **363**(9422)**:** 1711-20.

2. Fechtner RD, Weinreb RN. Mechanisms of optic nerve damage in primary open angle glaucoma. *Survey of ophthalmology* 1994; **39**(1)**:** 23-42.

3. Quigley HA, Nickells RW, Kerrigan LA, Pease ME, Thibault DJ, Zack DJ. Retinal ganglion cell death in experimental glaucoma and after axotomy occurs by apoptosis. *Investigative ophthalmology & visual science* 1995; **36**(5)**:** 774-86.

4. Nicolela MT, Drance SM. Various glaucomatous optic nerve appearances: clinical correlations. *Ophthalmology* 1996; **103**(4)**:** 640-9.

5. Tielsch JM, Sommer A, Katz J, Royall RM, Quigley HA, Javitt J. Racial variations in the prevalence of primary open-angle glaucoma. The Baltimore Eye Survey. *Jama* 1991; **266**(3)**:** 369-74.

6. Sommer A, Tielsch JM, Katz J, Quigley HA, Gottsch JD, Javitt J *et al.* Relationship between intraocular pressure and primary open angle glaucoma among white and black Americans. The Baltimore Eye Survey. *Archives of ophthalmology* 1991; **109**(8)**:** 1090-5.

7. Society EG. *Terminology and guidelines for glaucoma.*, 2nd edn European Glaucoma Society: Savona, 2003.

8. Webers CA, Beckers HJ, Nuijts RM, Schouten JS. Pharmacological management of primary open-angle glaucoma: second-line options and beyond. *Drugs and aging* 2008; **25**(9)**:** 729-59.

9. Quigley HA. Glaucoma. *Lancet* 2011; **377**(9774)**:** 1367-77.

10. Coleman AL. Glaucoma. *Lancet* 1999; **354**(9192)**:** 1803-10.

11. Quigley HA, Dunkelberger GR, Green WR. Retinal ganglion cell atrophy correlated with automated perimetry in human eyes with glaucoma. *American journal of ophthalmolology* 1989; **107**(5)**:** 453-64.

12. Quigley HA, Katz J, Derick RJ, Gilbert D, Sommer A. An evaluation of optic disc and nerve fiber layer examinations in monitoring progression of early glaucoma damage. *Ophthalmology* 1992; **99**(1)**:** 19-28.

13. Sample PA. Short-wavelength automated perimetry: it's role in the clinic and for understanding ganglion cell function. *Progress in retinal and eye research* 2000; **19**(4)**:** 369-83.

14. Polo V, Larrosa JM, Pinilla I, Perez S, Gonzalvo F, Honrubia FM. Predictive value of short-wavelength automated perimetry: a 3-year follow-up study. *Ophthalmology* 2002; **109**(4)**:** 761-5.

15. Landers J, Goldberg I, Graham S. A comparison of short wavelength automated perimetry with frequency doubling perimetry for the early detection of visual field loss in ocular hypertension. *Clinical and experimental ophthalmology* 2000; **28**(4)**:** 248-52.

16. Quigley HA. Number of people with glaucoma worldwide. *The British journal of ophthalmology* 1996; **80**(5)**:** 389-93.

17. Quigley H, Broman AT. The number of people with glaucoma worldwide in 2010 and 2020. *The British journal of ophthalmology* 2006; **90**(3)**:** 262-7.

18. Dielemans I, Vingerling JR, Wolfs RC, Hofman A, Grobbee DE, de Jong PT. The prevalence of primary open-angle glaucoma in a population-based study in The Netherlands. The Rotterdam Study. *Ophthalmology* 1994; **101**(11)**:** 1851-5.

19. Sommer A, Katz J, Quigley HA, Miller NR, Robin AL, Richter RC *et al.* Clinically detectable nerve fiber atrophy precedes the onset of glaucomatous field loss. *Archives of ophthalmology* 1991; **109**(1)**:** 77-83.

20. Leske MC, Heijl A, Hussein M, Bengtsson B, Hyman L, Komaroff E. Factors for glaucoma progression and the effect of treatment: the early manifest glaucoma trial. *Archives of ophthalmology* 2003; **121**(1)**:** 48-56.

21. Bengtsson B, Heijl A. A long-term prospective study of risk factors for glaucomatous visual field loss in patients with ocular hypertension. *Journal of glaucoma* 2005; **14**(2)**:** 135-8.

22. Shiose Y, Kitazawa Y, Tsukahara S, Akamatsu T, Mizokami K, Futa R *et al.* Epidemiology of glaucoma in Japan--a nationwide glaucoma survey. *Japanese journal of ophthalmology* 1991; **35**(2)**:** 133-55.

23. Mitchell P, Smith W, Attebo K, Healey PR. Prevalence of open-angle glaucoma in Australia. The Blue Mountains Eye Study. *Ophthalmology* 1996; **103**(10)**:** 1661-9.

24. Klein BE, Klein R, Sponsel WE, Franke T, Cantor LB, Martone J *et al.* Prevalence of glaucoma. The Beaver Dam Eye Study. *Ophthalmology* 1992; **99**(10)**:** 1499-504.

25. Heijl A, Leske MC, Bengtsson B, Hyman L, Bengtsson B, Hussein M. Reduction of intraocular pressure and glaucoma progression: results from the Early Manifest Glaucoma Trial. *Archives of ophthalmology* 2002; **120**(10)**:** 1268-79.

26. Anderson DR, Drance SM, Schulzer M. Natural history of normal-tension glaucoma. *Ophthalmology* 2001; **108**(2)**:** 247-53.

27. The Advanced Glaucoma Intervention Study (AGIS): 7. The relationship between control of intraocular pressure and visual field deterioration.The AGIS Investigators. *American journal of ophthalmology* 2000; **130**(4)**:** 429-40.

28. Mason RP, Kosoko O, Wilson MR, Martone JF, Cowan CL, Jr., Gear JC *et al.* National survey of the prevalence and risk factors of glaucoma in St. Lucia, West Indies. Part I. Prevalence findings. *Ophthalmology* 1989; **96**(9)**:** 1363-8.

29. Leske MC, Connell AM, Schachat AP, Hyman L. The Barbados Eye Study. Prevalence of open angle glaucoma. *Archives of ophthalmology* 1994; **112**(6)**:** 821-9.

30. Tielsch JM, Katz J, Sommer A, Quigley HA, Javitt JC. Family history and risk of primary open angle glaucoma. The Baltimore Eye Survey. *Archives of ophthalmology* 1994; **112**(1)**:** 69-73.

31. Kass MA, Heuer DK, Higginbotham EJ, Johnson CA, Keltner JL, Miller JP *et al.* The Ocular Hypertension Treatment Study: a randomized trial determines that topical ocular hypotensive medication delays or prevents the onset of primary open-angle glaucoma. *Archives of ophthalmology* 2002; **120**(6)**:** 701-13.

32. Gordon MO, Beiser JA, Brandt JD, Heuer DK, Higginbotham EJ, Johnson CA *et al.* The Ocular Hypertension Treatment Study: baseline factors that predict the onset of primary open-angle glaucoma. *Archives of ophthalmology* 2002; **120**(6)**:** 714-20.

33. Fingert JH, Stone EM, Sheffield VC, Alward WLM. Myocilin glaucoma. *Survey of ophthalmology* 2002; **47**(6)**:** 547-61.

34. Stewart WC, Kolker AE, Sharpe ED, Day DG, Holmes KT, Leech JN *et al.* Factors associated with long-term progression or stability in primary open-angle glaucoma. *American journal of ophthalmolology* 2000; **130**(3)**:** 274-9.

35. Neelakantan A, Vaishnav HD, Iyer SA, Sherwood MB. Is addition of a third or fourth antiglaucoma medication effective? *Journal of glaucoma* 2004; **13**(2)**:** 130-6.

36. Brubaker RF. Flow of aqueous humor in humans [The Friedenwald Lecture]. *Investigative ophthalmology & visual science* 1991; **32**(13)**:** 3145-66.

37. Nilsson SF. The uveoscleral outflow routes. *Eye* 1997; **11**(Pt 2)**:** 149-54.

38. Weinreb RN, Toris CB, Gabelt BT, Lindsey JD, Kaufman PL. Effects of prostaglandins on the aqueous humor outflow pathways. *Survey of ophthalmology* 2002; **47**(Suppl 1)**:** S53-64.

39. Hylton C, Robin AL. Update on prostaglandin analogs. *Current opinion in ophthalmology* 2003; **14**(2)**:** 65-9.

40. Toris CB, Camras CB, Yablonski ME. Acute versus chronic effects of brimonidine on aqueous humor dynamics in ocular hypertensive patients. *American journal of ophthalmolology* 1999; **128**(1)**:** 8-14.

41. Lambert WS, Ruiz L, Crish SD, Wheeler LA, Calkins DJ. Brimonidine prevents axonal and somatic degeneration of retinal ganglion cell neurons. *Molecular neurodegeneration* 2011; **6**(1)**:** 4.

42. Krupin T, Liebmann JM, Greenfield DS, Ritch R, Gardiner S. A randomized trial of brimonidine versus timolol in preserving visual function: results from the Low-Pressure Glaucoma Treatment Study. *American journal of ophthalmolology* 2011; **151**(4)**:** 671-81.

43. Rahman MQ, Ramaesh K, Montgomery DM. Brimonidine for glaucoma. *Expert opinion on drug safety* 2010; **9**(3)**:** 483-91.

44. Sugrue MF. Pharmacological and ocular hypotensive properties of topical carbonic anhydrase inhibitors. *Progress in retinal and eye research* 2000; **19**(1)**:** 87-112.

45. Herkel U, Pfeiffer N. Update on topical carbonic anhydrase inhibitors. *Current opinion in ophthalmology* 2001; **12**(2)**:** 88-93.

46. Hoyng PF, van Beek LM. Pharmacological therapy for glaucoma: a review. *Drugs* 2000; **59**(3)**:** 411-34.

47. Boger WP. Shortterm "escape" and longterm "drift." The dissipation effects of the beta adrenergic blocking agents. *Survey of ophthalmology* 1983; **28**(Suppl)**:** 235-42.

48. Schuman JS. Effects of systemic beta-blocker therapy on the efficacy and safety of topical brimonidine and timolol. *Ophthalmology* 2000; **107**(6)**:** 1171-7.

49. Rolim de Moura C, Paranhos A, Jr., Wormald R. Laser trabeculoplasty for open angle glaucoma. *Cochrane database of systemic reviews* 2007; (4)**:** CD003919.

50. Van Buskirk EM. Pathophysiology of laser trabeculoplasty. *Survey of ophthalmology* 1989; **33**(4)**:** 264-72.

51. Damji KF, Shah KC, Rock WJ, Bains HS, Hodge WG. Selective laser trabeculoplasty v argon laser trabeculoplasty: a prospective randomised clinical trial. *The British journal of ophthalmology* 1999; **83**(6)**:** 718-22.

52. Latina MA, Tumbocon JA. Selective laser trabeculoplasty: a new treatment option for open angle glaucoma. *Current opinion in ophthalmology* 2002; **13**(2)**:** 94-6.

53. Barkana Y, Belkin M. Selective laser trabeculoplasty. *Survey of ophthalmology* 2007; **52**(6)**:** 634-54.

54. Sharaawy T, Bhartiya S. Surgical management of glaucoma: evolving paradigms. *Indian journal of ophthalmology* 2011; **59**(Suppl)**:** S123-30.

55. Fankhauser F, Kwasniewska S, Van der Zypen E. Cyclodestructive procedures. I. Clinical and morphological aspects: a review. *Ophthalmologica* 2004; **218**(2)**:** 77-95.

56. Van Buskirk EM, Cioffi GA. Glaucomatous optic neuropathy. *American journal of ophthalmology* 1992; **113**(4)**:** 447-52.

57. Burgoyne CF, Crawford Downs J, Bellezza AJ, Francis Suh JK, Hart RT. The optic nerve head as a biomechanical structure: A new paradigm for understanding the role of IOP-related stress and strain in the pathophysiology of glaucomatous optic nerve head damage. *Progress in retinal and eye research* 2005; **24**(1)**:** 39-73.

58. Bellezza AJ, Hart RT, Burgoyne CF. The optic nerve head as a biomechanical structure: Initial finite element modeling. *Investigative ophthalmology & visual science* 2000; **41**(10)**:** 2991-3000.

59. Yan DB, Coloma FM, Metheetrairut A, Trope GE, Heathcote JG, Ethier CR. Deformation of the lamina cribrosa by elevated intraocular pressure. *The British journal of ophthalmology* 1994; **78**(8)**:** 643-8.

60. Sultan MB, Mansberger SL, Lee PP. Understanding the importance of IOP variables in glaucoma: a systematic review. *Survey of ophthalmology* 2009; **54**(6)**:** 643-62.

61. Kaufmann C, Bachmann LM, Robert YC, Thiel MA. Ocular pulse amplitude in healthy subjects as measured by dynamic contour tonometry. *Archives of ophthalmology* 2006; **124**(8)**:** 1104-8.

62. Sigal IA, Ethier CR. Biomechanics of the optic nerve head. *Experimental eye research* 2009; **88**(4)**:** 799-807.

63. Kerr J, Nelson P, O'Brien C. A comparison of ocular blood flow in untreated primary open-angle glaucoma and ocular hypertension. *American journal of ophthalmology* 1998; **126**(1)**:** 42-51.

64. Bagga H, Liu JH, Weinreb RN. Intraocular pressure measurements throughout the 24 h. *Current opinion in ophthalmology* 2009; **20**(2)**:** 79-83.

65. Watson PG, Young RD. Scleral structure, organisation and disease. A review. *Experimental eye research* 2004; **78**(3)**:** 609-23.

66. Anderson DR. Ultrastructure of human and monkey lamina cribrosa and optic nerve head. *Archives of ophthalmology* 1969; **82**(6)**:** 800-14.

67. Hernandez MR. The optic nerve head in glaucoma: Role of astrocytes in tissue remodeling. *Progress in retinal and eye research* 2000; **19**(3)**:** 297-321.

68. Gelman S, Cone FE, Pease ME, Nguyen TD, Myers K, Quigley HA. The presence and distribution of elastin in the posterior and retrobulbar regions of the mouse eye. *Experimental eye research* 2010; **90**(2)**:** 210-5.

69. Kielty CM, Sherratt MJ, Shuttleworth CA. Elastic fibres. *Journal of cell science* 2002; **115**(Pt 14)**:** 2817-28.

70. Hernandez MR. Ultrastructural immunocytochemical analysis of elastin in the human lamina cribrosa: Changes in elastic fibers in primary open-angle glaucoma. *Investigative ophthalmology & visual science* 1992; **33**(10)**:** 2891-903.

71. Hernandez MR, Luo XX, Andrzejewske W, Neufeld AH. Age-related changes in the extracellular matrix of the human optic nerve head. *American journal of ophthalmology* 1989; **107**(5)**:** 476-84.

72. Pena JDO, Netland PA, Vidal I, Dorr DA, Rasky A, Hernandez MR. Elastosis of the lamina cribrosa in glaucomatous optic neuropathy. *Experimental eye research* 1998; **67**(5)**:** 517-24.

73. Quigley EN, Quigley HA, Pease ME, Kerrigan LA. Quantitative studies of elastin in the optic nerve heads of persons with primary open-angle glaucoma. *Ophthalmology* 1996; **103**(10)**:** 1680-5.

74. Quigley HA, Brown A, Dorman-Pease ME. Alterations in elastin of the optic nerve head in human and experimental glaucoma. *The British journal of ophthalmology* 1991; **75**(9)**:** 552-7.

75. Quigley HA, Dorman-Pease ME, Brown AE. Quantitative study of collagen and elastin of the optic nerve head and sclera in human and experimental monkey glaucoma. *Current eye research* 1991; **10**(9)**:** 877-88.

76. Thorleifsson G, Magnusson KP, Sulem P, Walters GB, Gudbjartsson DF, Stefansson H *et al.* Common sequence variants in the LOXL1 gene confer susceptibility to exfoliation glaucoma. *Science* 2007; **317**(5843)**:** 1397-400.

77. Sigal IA, Flanagan JG, Tertinegg I, Ethier CR. Finite element modeling of optic nerve head biomechanics. *Investigative ophthalmology & visual science* 2004; **45**(12)**:** 4378-87.

78. Sigal IA, Flanagan JG, Tertinegg I, Ethier CR. Reconstruction of human optic nerve heads for finite element modeling. *Technology and health care* 2005; **13**(4)**:** 313-29.

79. Downs JC, Suh JKF, Thomas KA, Bellezza AJ, Burgoyne CF, Hart RT. Viscoelastic characterization of peripapillary sclera: Material properties by quadrant in rabbit and monkey eyes. *Journal of biomechanical engineering* 2003; **125**(1)**:** 124-31.

80. Downs JC, Suh JKF, Thomas KA, Bellezza AJ, Hart RT, Burgoyne CF. Viscoelastic material properties of the peripapillary sclera in normal and early-glaucoma monkey eyes. *Investigative ophthalmology & visual science* 2005; **46**(2)**:** 540-6.

81. Meredith SP, Swift L, Eke T, Broadway DC. The acute morphologic changes that occur at the optic nerve head induced by medical reduction of intraocular pressure. *Journal of glaucoma* 2007; **16**(6)**:** 556-61.

82. Wells AP, Garway-Heath DF, Poostchi A, Wong T, Chan KCY, Sachdev N. Corneal hysteresis but not corneal thickness correlates with optic nerve surface compliance in glaucoma patients. *Investigative ophthalmology & visual science* 2008; **49**(8)**:** 3262-8.

83. Greene PR. Closed-form ametropic pressure-volume and ocular rigidity solutions. *American journal of optometry and physiological optics* 1985; **62**(12)**:** 870-8.

84. Silver DM, Geyer O. Pressure-volume relation for the living human eye. *Current eye research* 2000; **20**(2)**:** 115-20.

85. Sigal IA, Flanagan JG, Tertinegg I, Ethier CR. Modeling individual-specific human optic nerve head biomechanics. Part I: IOP-induced deformations and influence of geometry. *Biomechanics and modeling in mechanobiology* 2009; **8**(2)**:** 85-98.

86. Sigal IA, Flanagan JG, Tertinegg I, Ethier CR. Modeling individual-specific human optic nerve head biomechanics. Part II: Influence of material properties. *Biomechanics and modeling in mechanobiology* 2009; **8**(2)**:** 99-109.

87. Sigal IA, Flanagan JG, Ethier CR. Factors influencing optic nerve head biomechanics. *Investigative ophthalmology & visual science* 2005; **46**(11)**:** 4189-99.

88. Morgan WH, Yu DY, Balaratnasingam C. The role of cerebrospinal fluid pressure in glaucoma pathophysiology: The dark side of the optic disc. *Journal of glaucoma* 2008; **17**(5)**:** 408-13.

89. Morgan WH, Yu DY, Cooper RL, Alder VA, Cringle SJ, Constable IJ. The influence of cerebrospinal fluid pressure on the lamina cribrosa tissue pressure gradient. *Investigative ophthalmology & visual science* 1995; **36**(6)**:** 1163-72.

90. Morgan WH, Yu DY, Alder VA, Cringle SJ, Cooper RL, House PH *et al.* The correlation between cerebrospinal fluid pressure and retrolaminar tissue pressure. *Investigative ophthalmology & visual science* 1998; **39**(8)**:** 1419-28.

91. Quigley HA, Hohman RM, Addicks EM. Morphologic changes in the lamina cribrosa correlated with neural loss in open-angle glaucoma. *American journal of ophthalmology* 1983; **95**(5)**:** 673-91.

92. Quigley HA, Addicks EM, Green WR, Maumenee AE. Optic nerve damage in human glaucoma. II. The site of injury and susceptibility to damage. *Archives of ophthalmology* 1981; **99**(4)**:** 635-49.

93. Quigley HA. Neuronal death in glaucoma. *Progress in retinal and eye research* 1999; **18**(1)**:** 39-57.

94. Radius RL, Gonzales M. Anatomy of the lamina cribrosa in human eyes. *Archives of ophthalmology* 1981; **99**(12)**:** 2159-62.

95. Jonas JB, Mardin CY, Schlotzer-Schrehardt U, Naumann GOH. Morphometry of the human lamina cribrosa surface. *Investigative ophthalmology & visual science* 1991; **32**(2)**:** 401-5.

96. Quigley HA, Addicks EM. Regional differences in the structure of the lamina cribrosa and their relation to glaucomatous optic nerve damage. *Archives of ophthalmology* 1981; **99**(1)**:** 137-43.

97. Miller KM, Quigley HA. The clinical appearance of the lamina cribrosa as a function of the extent of glaucomatous optic nerve damage. *Ophthalmology* 1988; **95**(1)**:** 135-8.

98. Susanna Jr R. The lamina cribrosa and visual field defects in open-angle glaucoma. *Canadian journal of ophthalmology* 1983; **18**(3)**:** 124-6.

99. Burgoyne CF, Morrison JC. The anatomy and pathophysiology of the optic nerve head in glaucoma. *Journal of glaucoma* 2001; **10**(5 Suppl 1)**:** S16-8.

100. Yablonski ME, Asamoto A. Hypothesis concerning the pathophysiology of optic nerve damage in open angle glaucoma. *Journal of glaucoma* 1993; **2**(2)**:** 119-27.

101. Huang H, Kamm RD, Lee RT. Cell mechanics and mechanotransduction: Pathways, probes, and physiology. *American journal of physiology. Cell physiology* 2004; **287**(1)**:** C1-11.

102. Kirwan RP, Fenerty CH, Crean J, Wordinger RJ, Clark AF, O'Brien CJ. Influence of cyclical mechanical strain on extracellular matrix gene expression in human lamina cribrosa cells in vitro. *Molecular vision* 2005; **11:** 798-810.

103. Edwards ME, Good TA. Use of a mathematical model to estimate stress and strain during elevated pressure induced lamina cribrosa deformation. *Current eye research* 2001; **23**(3)**:** 215-25.

104. Wang HB, Dembo M, Wang YL. Substrate flexibility regulates growth and apoptosis of normal but not transformed cells. *American journal of physiology. Cell physiology* 2000; **279**(5)**:** C1345-50.

105. Collin O, Na S, Chowdhury F, Hong M, Shin ME, Wang F *et al.* Self-Organized Podosomes Are Dynamic Mechanosensors. *Current biology* 2008; **18**(17)**:** 1288-94.

106. Morrison JC, Dorman-Pease ME, Dunkelberger GR, Quigley HA. Optic nerve head extracellular matrix in primary optic atrophy and experimental glaucoma. *Archives of ophthalmology* 1990; **108**(7)**:** 1020-4.

107. Yang H, Downs JC, Bellezza A, Thompson H, Burgoyne CF. 3-D histomorphometry of the normal and early glaucomatous monkey optic nerve head: Prelaminar neural tissues and cupping. *Investigative ophthalmology & visual science* 2007; **48**(11)**:** 5068-84.

108. Yang H, Downs JC, Girkin C, Sakata L, Bellezza A, Thompson H *et al.* 3-D histomorphometry of the normal and early glaucomatous monkey optic nerve head: Lamina cribrosa and peripapillary scleral position and thickness. *Investigative ophthalmology & visual science* 2007; **48**(10)**:** 4597-607.

109. Roberts MD, Grau V, Grimm J, Reynaud J, Bellezza AJ, Burgoyne CF *et al.* Remodeling of the connective tissue microarchitecture of the lamina cribrosa in early experimental glaucoma. *Investigative ophthalmology & visual science* 2009; **50**(2)**:** 681-90.

110. Quigley HA, McKinnon SJ, Zack DJ, Pease ME, Kerrigan-Baumrind LA, Kerrigan DF *et al.* Retrograde axonal transport of BDNF in retinal ganglion cells is blocked by acute IOP elevation in rats. *Investigative ophthalmology & visual science* 2000; **41**(11)**:** 3460-6.

111. Tezel G, Hernandez MR, Wax MB. In vitro evaluation of reactive astrocyte migration, a component of tissue remodeling in glaucomatous optic nerve head. *Glia* 2001; **34**(3)**:** 178-89.

112. Nakazawa T, Nakazawa C, Matsubara A, Noda K, Hisatomi T, She H *et al.* Tumor necrosis factor-alpha mediates oligodendrocyte death and delayed retinal ganglion cell loss in a mouse model of glaucoma. *The Journal of neuroscience* 2006; **26**(49)**:** 12633-41.

113. Lichter PR. Expectations from clinical trials: results of the Early Manifest Glaucoma Trial. *Archives of ophthalmology* 2002; **120**(10)**:** 1371-2.

114. Osborne NN, Chidlow G, Layton CJ, Wood JP, Casson RJ, Melena J. Optic nerve and neuroprotection strategies. *Eye* 2004; **18**(11)**:** 1075-84.

115. Hayreh SS. Blood flow in the optic nerve head and factors that may influence it. *Progress in retinal and eye research* 2001; **20**(5)**:** 595-624.

116. Hofman P, Hoyng P, vanderWerf F, Vrensen GF, Schlingemann RO. Lack of blood-brain barrier properties in microvessels of the prelaminar optic nerve head. *Investigative ophthalmology & visual science* 2001; **42**(5)**:** 895-901.

117. Pournaras CJ, Rungger-Brandle E, Riva CE, Hardarson SH, Stefansson E. Regulation of retinal blood flow in health and disease. *Progress in retinal and eye research* 2008; **27**(3)**:** 284-330.

118. Riva CE, Hero M, Titze P, Petrig B. Autoregulation of human optic nerve head blood flow in response to acute changes in ocular perfusion pressure. *Graefe's archive for clinical and experimental ophthalmology* 1997; **235**(10)**:** 618-26.

119. Flammer J, Orgul S. Optic nerve blood-flow abnormalities in glaucoma. *Progress in retinal and eye research* 1998; **17**(2)**:** 267-89.

120. Evans DW, Harris A, Garrett M, Chung HS, Kagemann L. Glaucoma patients demonstrate faulty autoregulation of ocular blood flow during posture change. *The British journal of ophthalmology* 1999; **83**(7)**:** 809-13.

121. Broadway DC, Drance SM. Glaucoma and vasospasm. *The British journal of ophthalmology* 1998; **82**(8)**:** 862-70.

122. Buckley C, Hadoke PWF, Henry E, O'Brien C. Systemic vascular endothelial cell dysfunction in normal pressure glaucoma. *The British journal of ophthalmology* 2002; **86**(2)**:** 227-32.

123. Flammer J, Pache M, Resink T. Vasospasm, its role in the pathogenesis of diseases with particular reference to the eye. *Progress in retinal and eye research* 2001; **20**(3)**:** 319-49.

124. Orgül S. An endothelin-1-induced model of chronic optic nerve ischemia in rhesus monkeys. *Journal of glaucoma* 1996; **5**(2)**:** 135-8.

125. Orgül S, Cioffi GA, Wilson DJ, Bacon DR, Van Buskirk EM. An endothelin-1 induced model of optic nerve ischemia in the rabbit. *Investigative ophthalmology & visual science* 1996; **37**(9)**:** 1860-9.

126. Gherghel D, Orgül S, Gugleta K, Gekkieva M, Flammer J. Relationship between ocular perfusion pressure and retrobulbar blood flow in patients with glaucoma with progressive damage. *American journal of ophthalmology* 2000; **130**(5)**:** 597-605.

127. Schulzer M, Drance SM, Carter CJ, Brooks DE, Douglas GR, Lau W. Biostatistical evidence for two distinct chronic open angle glaucoma populations. *The British journal of ophthalmology* 1990; **74**(4)**:** 196-200.

128. Buchi ER, Suivaizdis I, Fu J. Pressure-induced retinal ischemia in rats: An experimental model for quantitative study. *Ophthalmologica* 1991; **203**(3)**:** 138-47.

129. Selles-Navarro I, Villegas-Perez MP, Salvador-Silva M, Ruiz-Gomez JM, Vidal-Sanz M. Retinal ganglion cell death after different transient periods of pressure-induced ischemia and survival intervals: A quantitative in vivo study. *Investigative ophthalmology & visual science* 1996; **37**(10)**:** 2002-14.

130. Adachi M, Takahashi K, Nishikawa M, Miki H, Uyama M. High intraocular pressure-induced ischemia and reperfusion injury in the optic nerve and retina in rats. *Graefe's archive for clinical and experimental ophthalmology* 1996; **234**(7)**:** 445-51.

131. Rosenbaum DM, Rosenbaum PS, Gupta H, Singh M, Aggarwal A, Hall DH *et al.* The role of the p53 protein in the selective vulnerability of the inner retina to transient ischemia. *Investigative ophthalmology & visual science* 1998; **39**(11)**:** 2132-9.

132. Katai N, Yoshimura N. Apoptotic retinal neuronal death by ischemia-reperfusion is executed by two distinct caspase family proteases. *Investigative ophthalmology & visual science* 1999; **40**(11)**:** 2697-705.

133. Lam TT, Abler AS, Tso MOM. Apoptosis and caspases after ischemia-reperfusion injury in rat retina. *Investigative ophthalmology & visual science* 1999; **40**(5)**:** 967-75.

134. Hangai M, Yoshimura N, Hiroi K, Mandai M, Honda Y. Inducible nitric oxide synthase in retinal ischemia-reperfusion injury. *Experimental eye research* 1996; **63**(5)**:** 501-9.

135. Perlman JI, McCole SM, Pulluru P, Chang CJ, Lam TT, Tso MOM. Disturbances in the distribution of neurotransmitters in the rat retina after ischemia. *Current eye research* 1996; **15**(6)**:** 589-96.

136. Cone FE, Gelman SE, Son JL, Pease ME, Quigley HA. Differential susceptibility to experimental glaucoma among 3 mouse strains using bead and viscoelastic injection. *Experimental eye research* 2010; **91**(3)**:** 415-24.

137. Gaasterland D, Kupfer C. Experimental glaucoma in the rhesus monkey. *Investigative ophthalmology & visual science* 1974; **13**(6)**:** 455-7.

138. Ueda J, Sawaguchi S, Hanyu T, Yaoeda K, Fukuchi T, Abe H *et al.* Experimental glaucoma model in the rat induced by laser trabecular photocoagulation after an intracameral injection of india ink. *Japanese journal of ophthalmology* 1998; **42**(5)**:** 337-44.

139. Morrison JC, Johnson E, Cepurna WO. Rat models for glaucoma research. *Progress in brain research* 2008; **173:** 285-301.

140. WoldeMussie E, Ruiz G, Wijono M, Wheeler LA. Neuroprotection of retinal ganglion cells by brimonidine in rats with laser-induced chronic ocular hypertension. *Investigative ophthalmology & visual science* 2001; **42**(12)**:** 2849-55.

141. Levkovitch-Verbin H, Quigley HA, Martin KRG, Valenta D, Baumrind LA, Pease ME. Translimbal laser photocoagulation to the trabecular meshwork as a model of glaucoma in rats. *Investigative ophthalmology & visual science* 2002; **43**(2)**:** 402-10.

142. Aihara M, Lindsey JD, Weinreb RN. Experimental mouse ocular hypertension: establishment of the model. *Investigative ophthalmology & visual science* 2003; **44**(10)**:** 4314-20.

143. Gross RL, Ji J, Chang P, Pennesi ME, Yang Z, Zhang J *et al.* A mouse model of elevated intraocular pressure: retina and optic nerve findings. *Transactions of the American Ophthalmological Society* 2003; **101:** 163-9.

144. Grozdanic SD, Betts DM, Sakaguchi DS, Allbaugh RA, Kwon YH, Kardon RH. Laser-induced mouse model of chronic ocular hypertension. *Investigative ophthalmology & visual science* 2003; **44**(10)**:** 4337-46.

145. Morrison JC, Fraunfelder FW, Milne ST, Moore CG. Limbal microvasculature of the rat eye. *Investigative ophthalmology & visual science* 1995; **36**(3)**:** 751-6.

146. Morrison JC, Moore CG, Deppmeier LMH, Gold BG, Meshul CK, Johnson EC. A rat model of chronic pressure-induced optic nerve damage. *Experimental eye research* 1997; **64**(1)**:** 85-96.

147. Chauhan BC, Pan J, Archibald ML, LeVatte TL, Kelly MEM, Tremblay F. Effect of intraocular pressure on optic disc topography, electroretinography, and axonal loss in a chronic pressure-induced rat model of optic nerve damage. *Investigative ophthalmology & visual science* 2002; **43**(9)**:** 2969-76.

148. McKinnon SJ, Lehman DM, Kerrigan-Baumrind LA, Merges CA, Pease ME, Kerrigan DF *et al.* Caspase activation and amyloid precursor protein cleavage in rat ocular hypertension. *Investigative ophthalmology & visual science* 2002; **43**(4)**:** 1077-87.

149. Johnson EC, Jia L, Cepurna WO, Doser TA, Morrison JC. Global changes in optic nerve head gene expression after exposure to elevated intraocular pressure in a rat glaucoma model. *Investigative ophthalmology & visual science* 2007; **48**(7)**:** 3161-77.

150. Ahmed F, Brown KM, Stephan DA, Morrison JC, Johnson EC, Tomarev SI. Microarray analysis of changes in mRNA levels in the rat retina after experimental elevation of intraocular pressure. *Investigative ophthalmology & visual science* 2004; **45**(4)**:** 1247-58.

151. Kipfer-Kauer A, McKinnon SJ, Frueh BE, Goldblum D. Distribution of amyloid precursor protein and amyloid-beta in ocular hypertensive C57BL/6 mouse eyes. *Current eye research* 2010; **35**(9)**:** 828-34.

152. Shareef SR, Garcia-Valenzuela E, Salierno A, Walsh J, Sharma SC. Chronic ocular hypertension following episcleral venous occlusion in rats. *Experimental eye research* 1995; **61**(3)**:** 379-82.

153. Mittag TW, Danias J, Pohorenec G, Yuan HM, Burakgazi E, Chalmers-Redman R *et al.* Retinal damage after 3 to 4 months of elevated intraocular pressure in a rat glaucoma model. *Investigative ophthalmology & visual science* 2000; **41**(11)**:** 3451-9.

154. Neufeld AH, Das S, Vora S, Gachie E, Kawai S, Manning PT *et al.* A prodrug of a selective inhibitor of inducible nitric oxide synthase is neuroprotective in the rat model of glaucoma. *Journal of glaucoma* 2002; **11**(3)**:** 221-5.

155. Ahmed FAKM, Chaudhary P, Sharma SC. Effects of increased intraocular pressure on rat retinal ganglion cells. *International journal of developmental neuroscience* 2001; **19**(2)**:** 209-18.

156. Grozdanic SD, Betts DM, Sakaguchi DS, Kwon YH, Kardon RH, Sonea IM. Temporary elevation of the intraocular pressure by cauterization of vortex and episcleral veins in rats causes functional deficits in the retina and optic nerve. *Experimental eye research* 2003; **77**(1)**:** 27-33.

157. Morrison JC, Johnson EC, Cepurna WO, Funk RHW. Microvasculature of the rat optic nerve head. *Investigative ophthalmology & visual science* 1999; **40**(8)**:** 1702-9.

158. Morrison JC, DeFrank MP, Van Buskirk EM. Comparative microvascular anatomy of mammalian ciliary processes. *Investigative ophthalmology & visual science* 1987; **28**(8)**:** 1325-40.

159. Sawada A, Neufeld AH. Confirmation of the rat model of chronic, moderately elevated intraocular pressure. *Experimental eye research* 1999; **69**(5)**:** 525-31.

160. Danias J, Shen F, Kavalarakis M, Chen B, Goldblum D, Lee K *et al.* Characterization of retinal damage in the episcleral vein cauterization rat glaucoma model. *Experimental eye research* 2006; **82**(2)**:** 219-28.

161. Ruiz-Ederra J, Verkman AS. Mouse model of sustained elevation in intraocular pressure produced by episcleral vein occlusion. *Experimental eye research* 2006; **82**(5)**:** 879-84.

162. Chen H, Wei X, Cho KS, Chen G, Sappington R, Calkins DJ *et al.* Optic neuropathy due to microbead-induced elevated intraocular pressure in the mouse. *Investigative ophthalmology & visual science* 2011; **52**(1)**:** 36-44.

163. Samsel PA, Kisiswa L, Erichsen JT, Cross SD, Morgan JE. A novel method for the induction of experimental glaucoma using magnetic microspheres. *Investigative ophthalmology & visual science* 2011; **52**(3)**:** 1671-5.

164. Sappington RM, Carlson BJ, Crish SD, Calkins DJ. The microbead occlusion model: a paradigm for induced ocular hypertension in rats and mice. *Investigative ophthalmology & visual science* 2010; **51**(1)**:** 207-16.

165. Urcola JH, Hernández M, Vecino E. Three experimental glaucoma models in rats: Comparison of the effects of intraocular pressure elevation on retinal ganglion cell size and death. *Experimental eye research* 2006; **83**(2)**:** 429-37.

166. Weber AJ, Zelenak D. Experimental glaucoma in the primate induced by latex microspheres. *Journal of neuroscience methods* 2001; **111**(1)**:** 39-48.

167. Chan HC, Chang RC, Koon-Ching Ip A, Chiu K, Yuen WH, Zee SY *et al.* Neuroprotective effects of Lycium barbarum Lynn on protecting retinal ganglion cells in an ocular hypertension model of glaucoma. *Experimental neurology* 2007; **203**(1)**:** 269-73.

168. Mermoud A, Baerveldt G, Mickler DS, Wu GS, Rao NA. Animal model for uveitic glaucoma. *Graefe's archive for clinical and experimental ophthalmology* 1994; **232**(9)**:** 553-60.

169. John SWM, Anderson MG, Smith RS. Mouse genetics: A tool to help unlock the mechanisms of glaucoma. *Journal of glaucoma* 1999; **8**(6)**:** 400-12.

170. Harada T, Harada C, Nakamura K, Quah HMA, Okumura A, Namekata K *et al.* The potential role of glutamate transporters in the pathogenesis of normal tension glaucoma. *The Journal of clinical investigation* 2007; **117**(7)**:** 1763-70.

171. Libby RT, Smith RS, Savinova OV, Zabaleta A, Martin JE, Gonzalez FJ *et al.* Modification of ocular defects in mouse developmental glaucoma models by tyrosinase. *Science* 2003; **299**(5612)**:** 1578-81.

172. Anderson MG, Smith RS, Savinova OV, Hawes NL, Chang B, Zabaleta A *et al.* Genetic modification of glaucoma associated phenotypes between AKXD-28/Ty and DBA/2J mice. *BMC genetics* 2001; **2:** 1.

173. John SWM, Smith RS, Savinova OV, Hawes NL, Chang B, Turnbull D *et al.* Essential iris atrophy, pigment dispersion, and glaucoma in DBA/2J mice. *Investigative ophthalmology & visual science* 1998; **39**(6)**:** 951-62.

174. Sheldon WG, Warbritton AR, Bucci TJ, Turturro A. Glaucoma in food-restricted and ad libitum-fed DBA/2NNia mice. *Laboratory animal science* 1995; **45**(5)**:** 508-18.

175. Libby RT, Li Y, Savinova OV, Barter J, Smith RS, Nickells RW *et al.* Susceptibility to neurodegeneration in a glaucoma is modified by bax gene dosage. *PLoS genetics* 2005; **1**(1)**:** 17-26.

176. Anderson MG, Smith RS, Hawes NL, Zabaleta A, Chang B, Wiggs JL *et al.* Mutations in genes encoding melanosomal proteins cause pigmentary glaucoma in DBA/2J mice. *Nature genetics* 2002; **30**(1)**:** 81-5.

177. Schlamp CL, Li Y, Dietz JA, Janssen KT, Nickells RW. Progressive ganglion cell loss and optic nerve degeneration in DBA/2J mice is variable and asymmetric. *BMC neuroscience* 2006; **7:** 66.

178. May CA, Lutjen-Drecoll E. Morphology of the murine optic nerve. *Investigative ophthalmology & visual science* 2002; **43**(7)**:** 2206-12.

179. Howell GR, Libby RT, Jakobs TC, Smith RS, Phalan FC, Barter JW *et al.* Axons of retinal ganglion cells are insulted in the optic nerve early in DBA/2J glaucoma. *The Journal of cell biology* 2007; **179**(7)**:** 1523-37.

180. Jakobs TC, Libby RT, Ben Y, John SWM, Masland RH. Retinal ganglion cell degeneration is topological but not cell type specific in DBA/2J mice. *The Journal of cell biology* 2005; **171**(2)**:** 313-25.

181. Buckingham BP, Inman DM, Lambert W, Oglesby E, Calkins DJ, Steele MR *et al.* Progressive ganglion cell degeneration precedes neuronal loss in a mouse model of glaucoma. *The Journal of neuroscience* 2008; **28**(11)**:** 2735-44.

182. Zhou Y, Grinchuk O, Tomarev SI. Transgenic mice expressing the Tyr437His mutant of human myocilin protein develop glaucoma. *Investigative ophthalmology & visual science* 2008; **49**(5)**:** 1932-9.

183. Senatorov V, Malyukova I, Fariss R, Wawrousek EF, Swaminathan S, Sharan SK *et al.* Expression of mutated mouse myocilin induces open-angle glaucoma in transgenic mice. *The Journal of neuroscience* 2006; **26**(46)**:** 11903-14.

184. Mabuchi F, Lindsey JD, Aihara M, Mackey MR, Weinreb RN. Optic nerve damage in mice with a targeted type I collage mutation. *Investigative ophthalmology & visual science* 2004; **45**(6)**:** 1841-5.

185. Ittner LM, Schwerdtfeger K, Kunz TH, Muff R, Husmann K, Grimm C *et al.* Transgenic mice with ocular overexpression of an adrenomedullin receptor reflect human acute angle-closure glaucoma. *Clinical science* 2008; **114**(1-2)**:** 49-58.

186. Solomon AS, Lavie V, Hauben U, Monsonego A, Yoles E, Schwartz M. Complete transection of rat optic nerve while sparing the meninges and the vasculature: An experimental model for optic nerve neuropathy and trauma. *Journal of neuroscience methods* 1996; **70**(1)**:** 21-5.

187. Yoles E, Schwartz M. Degeneration of spared axons following partial white matter lesion: Implications for optic nerve neuropathies. *Experimental neurology* 1998; **153**(1)**:** 1-7.

188. Yoles E, Schwartz M. Elevation of intraocular glutamate levels in rats with partial lesion of the optic nerve. *Archives of ophthalmology* 1998; **116**(7)**:** 906-10.

189. Dreyer EB, Zurakowski D, Schumer RA, Podos SM, Lipton SA. Elevated glutamate levels in the vitreous body of humans and monkeys with glaucoma. *Archives of ophthalmology* 1996; **114**(3)**:** 299-305.

190. Lotery AJ. Glutamate excitotoxicity in glaucoma: truth or fiction? *Eye* 2005; **19**(4)**:** 369-70.

191. Sisk DR, Kuwabara T. Histologic changes in the inner retina of albino rats following intravitreal injection of monosodium L-glutamate. *Graefe's archive for clinical and experimental ophthalmology* 1985; **223**(5)**:** 250-8.

192. Lam TT, Abler AS, Kwong JMK, Tso MOM. N-methyl-D-aspartate (NMDA)-induced apoptosis in rat retina. *Investigative ophthalmology & visual science* 1999; **40**(10)**:** 2391-7.

193. Ellis JD, Morris AD, MacEwen CJ. Should diabetic patients be screened for glaucoma? *The British journal of ophthalmology* 1999; **83**(3)**:** 369-72.

194. Armstrong JR, Daily RK, Dobson HL, Girard LJ. The incidence of glaucoma in diabetes mellitus. A comparison with the incidence of glaucoma in the general population. *American journal of ophthalmology* 1960; **50**(1)**:** 55-63.

195. Armaly MF, Krueger DE, Maunder L. Biostatistical analysis of the collaborative glaucoma study. I. Summary report of the risk factors for glaucomatous visual-field defects. *Archives of ophthalmology* 1980; **98**(12)**:** 2163-71.

196. Becker B. Diabetes mellitus and primary open-angle glaucoma. The XXVII Edward Jackson Memorial Lecture. *American journal of ophthalmology* 1971; **71**(1 Pt 1)**:** 1-16.

197. Bouzas AG, Gragoudas ES, Balodimos MC, Brinegar CH, Aiello LM. Intraocular pressure in diabetes. Relationship to retinopathy and blood glucose level. *Archives of ophthalmology* 1971; **85**(4)**:** 423-7.

198. Mapstone R, Clark CV. Prevalence of diabetes in glaucoma. *British medical journal* 1985; **291**(6488)**:** 93-5.

199. Morgan RW, Drance SM. Chronic open angle glaucoma and ocular hypertension. An epidemiological study. *The British journal of ophthalmology* 1975; **59**(4)**:** 211-5.

200. Reynolds DC. Relative risk factors in chronic open-angle glaucoma: An epidemiological study. *American journal of optometry and physiological optics* 1977; **54**(2)**:** 116-20.

201. Kahn HA, Milton RC. Alternative definitions of open-angle glaucoma. Effect on prevalence and associations in the Framingham Eye Study. *Archives of ophthalmology* 1980; **98**(12)**:** 2172-7.

202. Klein BEK, Klein R, Jensen SC. Open-angle glaucoma and older-onset diabetes: The Beaver Dam Eye Study. *Ophthalmology* 1994; **101**(7)**:** 1173-7.

203. Tielsch JM, Katz J, Quigley HA, Javitt JC, Sommer A. Diabetes, intraocular pressure, and primary open-angle glaucoma in the Baltimore Eye Survey. *Ophthalmology* 1995; **102**(1)**:** 48-53.

204. Leske MC, Connell AM, Wu SY, Hyman LG, Schachat AP. Risk factors for open-angle glaucoma. The Barbados Eye Study. *Archives of ophthalmology* 1995; **113**(7)**:** 918-24.

205. Leske MC, Wu SY, Hennis A, Honkanen R, Nemesure B. Risk factors for incident open-angle glaucoma: the Barbados Eye Studies. *Ophthalmology* 2008; **115**(1)**:** 85-93.

206. de Voogd S, Ikram MK, Wolfs RCW, Jansonius NM, Witteman JCM, Hofman A *et al.* Is Diabetes Mellitus a Risk Factor for Open-Angle Glaucoma? The Rotterdam Study. *Ophthalmology* 2006; **113**(10)**:** 1827-31.

207. Dielemans I, De Jong PTVM, Stolk R, Vingerling JR, Grobbee DE, Hofman A. Primary open-angle glaucoma, intraocular pressure, and diabetes mellitus in the general elderly population: The Rotterdam study. *Ophthalmology* 1996; **103**(8)**:** 1271-5.

208. Mitchell P, Smith W, Chey T, Healey PR. Open-angle glaucoma and diabetes: The Blue Mountains Eye Study, Australia. *Ophthalmology* 1997; **104**(4)**:** 712-8.

209. Quigley HA, West SK, Rodriguez J, Munoz B, Klein R, Snyder R. The prevalence of glaucoma in a population-based study of Hispanic subjects: Proyecto VER. *Archives of ophthalmology* 2001; **119**(12)**:** 1819-26.

210. Pasquale LR, Kang JH, Manson JE, Willett WC, Rosner BA, Hankinson SE. Prospective Study of Type 2 Diabetes Mellitus and Risk of Primary Open-Angle Glaucoma in Women. *Ophthalmology* 2006; **113**(7)**:** 1081-6.

211. Chopra V, Varma R, Francis BA, Wu J, Torres M, Azen SP. Type 2 diabetes mellitus and the risk of open-angle glaucoma the Los Angeles Latino Eye Study. *Ophthalmology* 2008; **115**(2)**:** 227-32.

212. Ellis JD, Evans JMM, Ruta DA, Baines PS, Leese G, MacDonald TM *et al.* Glaucoma incidence in an unselected cohort of diabetic patients: Is diabetes mellitus a risk factor for glaucoma? *The British journal of ophthalmology* 2000; **84**(11)**:** 1218-24.

213. Le A, Mukesh BN, McCarty CA, Taylor HR. Risk factors associated with the incidence of open-angle glaucoma: The visual impairment project. *Investigative ophthalmology & visual science* 2003; **44**(9)**:** 3783-9.

214. Qureshi AI, Giles WH, Croft JB. Impaired glucose tolerance and the likelihood of nonfatal stroke and myocardial infarction: The third national health and nutrition examination survey. *Stroke* 1998; **29**(7)**:** 1329-32.

215. Heuschmann PU, Kolominsky-Rabas PL, Misselwitz B, Hermanek P, Leffmann C, Janzen RWC *et al.* Predictors of in-hospital mortality and attributable risks of death after ischemic stroke: The German Stroke Registers Study Group. *Archives of internal medicine* 2004; **164**(16)**:** 1761-8.

216. Capes SE, Hunt D, Malmberg K, Pathak P, Gerstein HC. Stress hyperglycemia and prognosis of stroke in nondiabetic and diabetic patients: A systematic overview. *Stroke* 2001; **32**(10)**:** 2426-32.

217. Tanne D. Impaired glucose metabolism and cerebrovascular diseases. *Advances in cardiology* 2008; **45:** 107-13.

218. Melamed E. Reactive hyperglycaemia in patients with acute stroke. *Journal of the neurological sciences* 1976; **29**(2-4)**:** 267-75.

219. Tracey F, Crawford VLS, Lawson JT, Buchanan KD, Stout RW. Hyperglycaemia and mortality from acute stroke. *Quarterly journal of medicine* 1993; **86**(7)**:** 439-46.

220. Van Kooten F, Hoogerbrugge N, Naarding P, Koudstaal PJ. Hyperglycemia in the acute phase of stroke is not caused by stress. *Stroke* 1993; **24**(8)**:** 1129-32.

221. Hamilton MG, Tranmer BI, Auer RN. Insulin reduction of cerebral infarction due to transient focal ischemia. *Journal of neurosurgery* 1995; **82**(2)**:** 262-8.

222. Bruno A, Kent TA, Coull BM, Shankar RR, Saha C, Becker KJ *et al.* Treatment of hyperglycemia in ischemic stroke (THIS): a randomized pilot trial. *Stroke* 2008; **39**(2)**:** 384-9.

223. Bruno A. Management of hyperglycemia during acute stroke. *Current cardiology reports* 2009; **11**(1)**:** 36-41.

224. Voll CL, Auer RN. Insulin attenuates ischemic brain damage independent of its hypoglycemic effect. *Journal of cerebral blood flow and metabolism* 1991; **11**(6)**:** 1006-14.

225. Duckrow RB, Beard DC, Brennan RW. Regional cerebral blood flow decreases during hyperglycemia. *Annals of neurology* 1985; **17**(3)**:** 267-72.

226. Li PA, Shuaib A, Miyashita H, He QP, Siesjö BK. Hyperglycemia enhances extracellular glutamate accumulation in rats subjected to forebrain ischemia. *Stroke* 2000; **31**(1)**:** 183-92.

227. Berger L, Hakim AM. The association of hyperglycemia with cerebral edema in stroke. *Stroke* 1986; **17**(5)**:** 865-71.

228. Mohanty P, Hamouda W, Garg R, Aljada A, Ghanim H, Dandona P. Glucose challenge stimulates reactive oxygen species (ROS) generation by leucocytes. *Journal of clinical endocrinology and metabolism* 2000; **85**(8)**:** 2970-3.

229. Folbergrova J, Memezawa H, Smith ML, Siesjo BK. Focal and perifocal changes in tissue energy state during middle cerebral artery occlusion in normo- and hyperglycemic rats. *Journal of cerebral blood flow and metabolism* 1992; **12**(1)**:** 25-33.

230. Wagner KR, Kleinholz M, De Courten-Myers GM, Myers RE. Hyperglycemic versus normoglycemic stroke: Topography of brain metabolites, intracellular pH, and infarct size. *Journal of cerebral blood flow and metabolism* 1992; **12**(2)**:** 213-22.

231. Haefliger IO, Flammer J, Beny JL, Luscher TF. Endothelium-dependent vasoactive modulation in the ophthalmic circulation. *Progress in retinal and eye research* 2001; **20**(2)**:** 209-25.

232. Rassam SM, Patel V, Chen HC, Kohner EM. Regional retinal blood flow and vascular autoregulation. *Eye* 1996; **10**(Pt 3)**:** 331-7.

233. Toda N, Nakanishi-Toda M. Nitric oxide: ocular blood flow, glaucoma, and diabetic retinopathy. *Progress in retinal and eye research* 2007; **26**(3)**:** 205-38.

234. Dandona P, James IM, Newbury PA. Cerebral blood flow in diabetes mellitus: evidence of abnormal cerebrovascular reactivity. *British medical journal* 1978; **2**(6133)**:** 325-6.

235. Giacco F, Brownlee M. Oxidative stress and diabetic complications. *Circulation research* 2010; **107**(9)**:** 1058-70.

236. Yancey CM, Linsenmeier RA. Oxygen distribution and consumption in the cat retina at increased intraocular pressure. *Investigative ophthalmology & visual science* 1989; **30**(4)**:** 600-11.

237. Ahmed J, Linsenmeier RA, Dunn R, Jr. The oxygen distribution in the prelaminar optic nerve head of the cat. *Experimental eye research* 1994; **59**(4)**:** 457-65.

238. Vorwerk CK, Gorla MS, Dreyer EB. An experimental basis for implicating excitotoxicity in glaucomatous optic neuropathy. *Survey of ophthalmology* 1999; **43**(Suppl 1)**:** S142-50.

239. Neufeld AH. Nitric oxide: a potential mediator of retinal ganglion cell damage in glaucoma. *Survey of ophthalmology* 1999; **43**(Suppl 1)**:** S129-35.

240. Li Q, Puro DG. Diabetes-induced dysfunction of the glutamate transporter in retinal Müller cells. *Investigative ophthalmology & visual science* 2002; **43**(9)**:** 3109-16.

241. Hartnett ME. The effects of oxygen stresses on the development of features of severe retinopathy of prematurity: knowledge from the 50/10 OIR model. *Documenta ophthalmologica* 2010; **120**(1)**:** 25-39.

242. Khandhadia S, Lotery A. Oxidation and age-related macular degeneration: insights from molecular biology. *Expert reviews in molecular medicine* 2010; **12:** e34.

243. Kowluru RA, Chan PS. Oxidative stress and diabetic retinopathy. *Experimental diabetes research* 2007; **2007:** 43603.

244. Tezel G. Oxidative stress in glaucomatous neurodegeneration: mechanisms and consequences. *Progress in retinal and eye research* 2006; **25**(5)**:** 490-513.

245. Winkler BS. A quantitative assessment of glucose metabolism in the isolated rat retina. In: Christen Y, Doly M, Droy-Lefaix MT (eds). *Les Séminaires Ophtalmologiques d'IPSEN: Vision et Adaptation*, vol. 6. Elsevier: Amsterdam, 1995, pp 78-96.

246. Winkler BS. Glycolytic and oxidative metabolism in relation to retinal function. *Journal of general physiology* 1981; **77**(6)**:** 667-92.

247. Linsenmeier RA, Braun RD. Oxygen distribution and consumption in the cat retina during normoxia and hypoxemia. *Journal of general physiology* 1992; **99**(2)**:** 177-97.

248. Winkler BS, Sauer MW, Starnes CA. Modulation of the Pasteur effect in retinal cells: implications for understanding compensatory metabolic mechanisms. *Experimental eye research* 2003; **76**(6)**:** 715-23.

249. Casson RJ, Chidlow G, Wood JP, Osborne NN. The effect of hyperglycemia on experimental retinal ischemia. *Archives of ophthalmology* 2004; **122**(3)**:** 361-6.

250. Lundquist O, Osterlin S. Glucose concentration in the vitreous of nondiabetic and diabetic human eyes. *Graefe's archive for clinical and experimental ophthalmology* 1994; **232**(2)**:** 71-4.

251. Winkler BS. The electroretinogram of the isolated rat retina. *Vision research* 1972; **12**(6)**:** 1183-98.

252. McRipley MA, Ahmed J, Chen EP, Linsenmeier RA. Effects of adaptation level and hypoglycemia on function of the cat retina during hypoxemia. *Visual neuroscience* 1997; **14**(2)**:** 339-50.

253. Emery M, Schorderet DF, Roduit R. Acute hypoglycemia induces retinal cell death in mouse. *PLoS one* 2011; **6**(6)**:** e21586.

254. Wang L, Kondo M, Bill A. Glucose metabolism in cat outer retina. Effects of light and hyperoxia. *Investigative ophthalmology & visual science* 1997; **38**(1)**:** 48-55.

255. Wang L, Tornquist P, Bill A. Glucose metabolism in pig outer retina in light and darkness. *Acta physiologica Scandinavica* 1997; **160**(1)**:** 75-81.

256. Wang L, Tornquist P, Bill A. Glucose metabolism of the inner retina in pigs in darkness and light. *Acta physiologica Scandinavica* 1997; **160**(1)**:** 71-4.

257. Padnick-Silver L, Linsenmeier RA. Effect of acute hyperglycemia on oxygen and oxidative metabolism in the intact cat retina. *Investigative ophthalmology & visual science* 2003; **44**(2)**:** 745-50.

258. Atherton A, Hill DW, Keen H, Young S, Edwards EJ. The effect of acute hyperglycaemia on the retinal circulation of the normal cat. *Diabetologia* 1980; **18**(3)**:** 233-7.

259. Illing EK, Gray CH. Retinal metabolism in diabetes; the metabolism of retinae of normal and alloxandiabetic rabbits. *The Journal of endocrinology* 1951; **7**(3)**:** 242-7.

260. Sponsel WE, DePaul KL, Zetlan SR. Retinal hemodynamic effects of carbon dioxide, hyperoxia, and mild hypoxia. *Investigative ophthalmology & visual science* 1992; **33**(6)**:** 1864-9.

261. Berkowitz BA, Kowluru RA, Frank RN, Kern TS, Hohman TC, Prakash M. Subnormal retinal oxygenation response precedes diabetic-like retinopathy. *Investigative ophthalmology & visual science* 1999; **40**(9)**:** 2100-5.

262. Alder VA, Yu DY, Cringle SJ, Su EN. Changes in vitreal oxygen tension distribution in the streptozotocin diabetic rat. *Diabetologia* 1991; **34**(7)**:** 469-76.

263. Bursell SE, Clermont AC, Kinsley BT, Simonson DC, Aiello LM, Wolpert HA. Retinal blood flow changes in patients with insulin-dependent diabetes mellitus and no diabetic retinopathy. *Investigative ophthalmology & visual science* 1996; **37**(5)**:** 886-97.

264. Feke GT, Buzney SM, Ogasawara H, Fujio N, Goger DG, Spack NP *et al.* Retinal circulatory abnormalities in type 1 diabetes. *Investigative ophthalmology & visual science* 1994; **35**(7)**:** 2968-75.

265. Linsenmeier RA, Braun RD, McRipley MA, Padnick LB, Ahmed J, Hatchell DL *et al.* Retinal hypoxia in long-term diabetic cats. *Investigative ophthalmology & visual science* 1998; **39**(9)**:** 1647-57.

266. Takata K, Hirano H, Kasahara M. Transport of glucose across the blood-tissue barriers. *International review of cytology* 1997; **172:** 1-53.

267. Takata K, Kasahara T, Kasahara M, Ezaki O, Hirano H. Ultracytochemical localization of the erythrocyte/HepG2-type glucose transporter (GLUT1) in cells of the blood-retinal barrier in the rat. *Investigative ophthalmology & visual science* 1992; **33**(2)**:** 377-83.

268. Poulsom R, Prockop DJ, Boot-Handford RP. Effects of long-term diabetes and galactosaemia upon lens and retinal mRNA levels in the rat. *Experimental eye research* 1990; **51**(1)**:** 27-32.

269. Kumagai AK, Vinores SA, Pardridge WM. Pathological upregulation of inner blood-retinal barrier Glut1 glucose transporter expression in diabetes mellitus. *Brain research* 1996; **706**(2)**:** 313-7.

270. Kumagai AK. Glucose transport in brain and retina: implications in the management and complications of diabetes. *Diabetes/metabolism research and reviews* 1999; **15**(4)**:** 261-73.

271. Kumagai AK, Glasgow BJ, Pardridge WM. GLUT1 glucose transporter expression in the diabetic and nondiabetic human eye. *Investigative ophthalmology & visual science* 1994; **35**(6)**:** 2887-94.

272. Mantych GJ, Hageman GS, Devaskar SU. Characterization of glucose transporter isoforms in the adult and developing human eye. *Endocrinology* 1993; **133**(2)**:** 600-7.

273. Watanabe T, Mio Y, Hoshino FB, Nagamatsu S, Hirosawa K, Nakahara K. GLUT2 expression in the rat retina: localization at the apical ends of Müller cells. *Brain Research* 1994; **655**(1-2)**:** 128-34.

274. Watanabe T, Matsushima S, Okazaki M, Nagamatsu S, Hirosawa K, Uchimura H *et al.* Localization and ontogeny of GLUT3 expression in the rat retina. *Brain research. Developmental brain research* 1996; **94**(1)**:** 60-6.

275. Watanabe T, Nagamatsu S, Matsushima S, Kirino T, Uchimura H. Colocalization of GLUT3 and choline acetyltransferase immunoreactivity in the rat retina. *Biochemical and biophysical research communications* 1999; **256**(3)**:** 505-11.

276. Knott RM, Robertson M, Muckersie E, Forrester JV. Regulation of glucose transporters (GLUT-1 and GLUT-3) in human retinal endothelial cells. *The Biochemical journal* 1996; **318**(Pt 1)**:** 313-7.

277. Takagi H, King GL, Aiello LP. Hypoxia upregulates glucose transport activity through an adenosine-mediated increase of GLUT1 expression in retinal capillary endothelial cells. *Diabetes* 1998; **47**(9)**:** 1480-8.

278. Takagi H, Tanihara H, Seino Y, Yoshimura N. Characterization of glucose transporter in cultured human retinal pigment epithelial cells: gene expression and effect of growth factors. *Investigative ophthalmology & visual science* 1994; **35**(1)**:** 170-7.

279. Sena DF, Ramchand K, Lindsley K. Neuroprotection for treatment of glaucoma in adults. *Cochrane database of systematic reviews* 2010; (2)**:** CD006539.

280. Lagreze WA, Knorle R, Bach M, Feuerstein TJ. Memantine is neuroprotective in a rat model of pressure-induced retinal ischemia. *Investigative ophthalmology & visual science* 1998; **39**(6)**:** 1063-6.

281. Danesh-Meyer HV. Neuroprotection in glaucoma: recent and future directions. *Current opinion in ophthalmology* 2011; **22**(2)**:** 78-86.

282. Bakalash S, Shlomo GB, Aloni E, Shaked I, Wheeler L, Ofri R *et al.* T-cell-based vaccination for morphological and functional neuroprotection in a rat model of chronically elevated intraocular pressure. *Journal of molecular medicine* 2005; **83**(11)**:** 904-16.

283. Kipnis J, Yoles E, Porat Z, Cohen A, Mor F, Sela M *et al.* T cell immunity to copolymer 1 confers neuroprotection on the damaged optic nerve: possible therapy for optic neuropathies. *Proceedings of the National Academy of Sciences of the United States of America* 2000; **97**(13)**:** 7446-51.

284. Lichter PR, Musch DC, Gillespie BW, Guire KE, Janz NK, Wren PA *et al.* Interim clinical outcomes in the Collaborative Initial Glaucoma Treatment Study comparing initial treatment randomized to medications or surgery. *Ophthalmology* 2001; **108**(11)**:** 1943-53.

285. Holman MC, Chidlow G, Wood JP, Casson RJ. The effect of hyperglycemia on hypoperfusion-induced injury. *Investigative ophthalmology & visual science* 2010; **51**(4)**:** 2197-207.

286. Kong GY, Van Bergen NJ, Trounce IA, Crowston JG. Mitochondrial dysfunction and glaucoma. *Journal of glaucoma* 2009; **18**(2)**:** 93-100.

287. Lee S, Van Bergen NJ, Kong GY, Chrysostomou V, Waugh HS, O'Neill EC *et al.* Mitochondrial dysfunction in glaucoma and emerging bioenergetic therapies. *Experimental eye research* 2010; **93**(2)**:** 204-12.

288. Correia SC, Carvalho C, Cardoso S, Santos RX, Santos MS, Oliveira CR *et al.* Mitochondrial preconditioning: a potential neuroprotective strategy. *Frontiers in aging neuroscience* 2010; **2:** 138.

289. Gastinger MJ, Singh RS, Barber AJ. Loss of cholinergic and dopaminergic amacrine cells in streptozotocin-diabetic rat and Ins2Akita-diabetic mouse retinas. *Investigative ophthalmology & visual science* 2006; **47**(7)**:** 3143-50.

290. Qin Y, Xu G, Wang W. Dendritic abnormalities in retinal ganglion cells of three-month diabetic rats. *Current eye research* 2006; **31**(11)**:** 967-74.

291. Crish SD, Calkins DJ. Neurodegeneration in glaucoma: progression and calcium-dependent intracellular mechanisms. *Neuroscience* 2011; **176:** 1-11.

292. Morrison J, Farrell S, Johnson E, Deppmeier L, Moore CG, Grossmann E. Structure and composition of the rodent lamina cribrosa. *Experimental eye research* 1995; **60**(2)**:** 127-35.

293. Martin KR, Quigley HA, Valenta D, Kielczewski J, Pease ME. Optic nerve dynein motor protein distribution changes with intraocular pressure elevation in a rat model of glaucoma. *Experimental eye research* 2006; **83**(2)**:** 255-62.

294. Son JL, Soto I, Oglesby E, Lopez-Roca T, Pease ME, Quigley HA *et al.* Glaucomatous optic nerve injury involves early astrocyte reactivity and late oligodendrocyte loss. *Glia* 2010; **58**(7)**:** 780-9.

295. Morrison JC, Johnson EC, Cepurna W, Jia L. Understanding mechanisms of pressure-induced optic nerve damage. *Progress in retinal and eye research* 2005; **24**(2)**:** 217-40.

296. Inman DM, Sappington RM, Horner PJ, Calkins DJ. Quantitative correlation of optic nerve pathology with ocular pressure and corneal thickness in the DBA/2 mouse model of glaucoma. *Investigative ophthalmology & visual science* 2006; **47**(3)**:** 986-96.

297. Pease ME, Zack DJ, Berlinicke C, Bloom K, Cone F, Wang Y *et al.* Effect of CNTF on retinal ganglion cell survival in experimental glaucoma. *Investigative ophthalmology & visual science* 2009; **50**(5)**:** 2194-200.

298. Anderson MG, Libby RT, Gould DB, Smith RS, John SW. High-dose radiation with bone marrow transfer prevents neurodegeneration in an inherited glaucoma. *Proceedings of the National Academy of Sciences of the United States of America* 2005; **102**(12)**:** 4566-71.

299. Chauhan BC, Levatte TL, Garnier KL, Tremblay F, Pang IH, Clark AF *et al.* Semiquantitative optic nerve grading scheme for determining axonal loss in experimental optic neuropathy. *Investigative ophthalmology & visual science* 2006; **47**(2)**:** 634-40.

300. Jia L, Cepurna WO, Johnson EC, Morrison JC. Effect of general anesthetics on IOP in rats with experimental aqueous outflow obstruction. *Investigative ophthalmology & visual science* 2000; **41**(11)**:** 3415-3419.

301. Marina N, Bull ND, Martin KR. A semiautomated targeted sampling method to assess optic nerve axonal loss in a rat model of glaucoma. *Nature protocols* 2010; **5**(10)**:** 1642-51.

302. Hernandez MR, Miao H, Lukas T. Astrocytes in glaucomatous optic neuropathy. *Progress in retinal and eye research* 2008; **173:** 353-73.

303. Butt AM, Pugh M, Hubbard P, James G. Functions of optic nerve glia: axoglial signalling in physiology and pathology. *Eye* 2004; **18**(11)**:** 1110-21.

304. Naskar R, Wissing M, Thanos S. Detection of early neuron degeneration and accompanying microglial responses in the retina of a rat model of glaucoma. *Investigative ophthalmology & visual science* 2002; **43**(9)**:** 2962-8.

305. Salinas-Navarro M, Alarcon-Martinez L, Valiente-Soriano FJ, Jimenez-Lopez M, Mayor-Torroglosa S, Aviles-Trigueros M *et al.* Ocular hypertension impairs optic nerve axonal transport leading to progressive retinal ganglion cell degeneration. *Experimental eye research* 2010; **90**(1)**:** 168-83.

306. Whitmore AV, Libby RT, John SWM. Glaucoma: Thinking in new ways - A rôle for autonomous axonal self-destruction and other compartmentalised processes? *Progress in retinal and eye research* 2005; **24**(6)**:** 639-62.

307. Pease ME, Zack DJ, Berlinicke C, Bloom K, Cone F, Wang Y *et al.* Effect of CNTF on retinal ganglion cell survival in experimental glaucoma. *Investigative ophthalmology & visual science* 2009; **50**(5)**:** 2194-200.

308. Bull ND, Irvine KA, Franklin RJ, Martin KR. Transplanted oligodendrocyte precursor cells reduce neurodegeneration in a model of glaucoma. *Investigative ophthalmology & visual science* 2009; **50**(9)**:** 4244-53.

309. Soto I, Pease ME, Son JL, Shi X, Quigley HA, Marsh-Armstrong N. Retinal ganglion cell loss in a rat ocular hypertension model is sectorial and involves early optic nerve axon loss. *Investigative ophthalmology & visual science* 2011; **52**(1)**:** 434-41.

310. Cepurna WO, Kayton RJ, Johnson EC, Morrison JC. Age related optic nerve axonal loss in adult Brown Norway rats. *Experimental eye research* 2005; **80**(6)**:** 877-84.

311. Chauhan BC, LeVatte TL, Garnier KL, Tremblay F, Pang IH, Clark AF *et al.* Semiquantitative optic nerve grading scheme for determining axonal loss in experimental optic neuropathy. *Investigative ophthalmology & visual science* 2006; **47**(2)**:** 634-40.

312. Kern TS, Barber AJ. Retinal ganglion cells in diabetes. *The Journal of physiology* 2008; **586**(Pt 18)**:** 4401-8.

313. Barber AJ, Lieth E, Khin SA, Antonetti DA, Buchanan AG, Gardner TW. Neural apoptosis in the retina during experimental and human diabetes. Early onset and effect of insulin. *The Journal of clinical investigation* 1998; **102**(4)**:** 783-91.

314. El-Remessy AB, Al-Shabrawey M, Khalifa Y, Tsai NT, Caldwell RB, Liou GI. Neuroprotective and blood-retinal barrier-preserving effects of cannabidiol in experimental diabetes. *The American journal of pathology* 2006; **168**(1)**:** 235-44.

315. Alder VA, Su EN, Yu DY, Cringle S, Yu P. Overview of studies on metabolic and vascular regulatory changes in early diabetic retinopathy. *Australian and New Zealand journal of ophthalmology* 1998; **26**(2)**:** 141-8.

316. Joussen AM, Murata T, Tsujikawa A, Kirchhof B, Bursell SE, Adamis AP. Leukocyte-mediated endothelial cell injury and death in the diabetic retina. *The American journal of pathology* 2001; **158**(1)**:** 147-52.

317. Honjo M, Tanihara H, Nishijima K, Kiryu J, Honda Y, Yue BY *et al.* Statin inhibits leukocyte-endothelial interaction and prevents neuronal death induced by ischemia-reperfusion injury in the rat retina. *Archives of ophthalmology* 2002; **120**(12)**:** 1707-13.

318. Kowluru RA, Engerman RL, Case GL, Kern TS. Retinal glutamate in diabetes and effect of antioxidants. *Neurochemistry international* 2001; **38**(5)**:** 385-90.

319. Lieth E, Barber AJ, Xu B, Dice C, Ratz MJ, Tanase D *et al.* Glial reactivity and impaired glutamate metabolism in short-term experimental diabetic retinopathy. *Diabetes* 1998; **47**(5)**:** 815-20.

320. Zhu B, Wang W, Gu Q, Xu X. Erythropoietin protects retinal neurons and glial cells in early-stage streptozotocin-induced diabetic rats. *Experimental eye research* 2008; **86**(2)**:** 375-82.

321. Kusari J, Zhou S, Padillo E, Clarke KG, Gil DW. Effect of memantine on neuroretinal function and retinal vascular changes of streptozotocin-induced diabetic rats. *Investigative ophthalmology & visual science* 2007; **48**(11)**:** 5152-9.

322. Kohzaki K, Vingrys AJ, Bui BV. Early inner retinal dysfunction in streptozotocin-induced diabetic rats. *Investigative ophthalmology & visual science* 2008; **49**(8)**:** 3595-604.

323. Bui BV, Loeliger M, Thomas M, Vingrys AJ, Rees SM, Nguyen CT *et al.* Investigating structural and biochemical correlates of ganglion cell dysfunction in streptozotocin-induced diabetic rats. *Experimental eye research* 2009; **88**(6)**:** 1076-83.

324. Ino-Ue M, Zhang L, Naka H, Kuriyama H, Yamamoto M. Polyol metabolism of retrograde axonal transport in diabetic rat large optic nerve fiber. *Investigative ophthalmology & visual science* 2000; **41**(13)**:** 4055-8.

325. Zhang L, Ino-ue M, Dong K, Yamamoto M. Retrograde axonal transport impairment of large- and medium-sized retinal ganglion cells in diabetic rat. *Current eye research* 2000; **20**(2)**:** 131-6.

326. Orrenius S. Reactive oxygen species in mitochondria-mediated cell death. *Drug metabolism reviews* 2007; **39**(2-3)**:** 443-55.

327. Kroemer G, Reed JC. Mitochondrial control of cell death. *Nature medicine* 2000; **6**(5)**:** 513-9.

328. Krantic S, Mechawar N, Reix S, Quirion R. Apoptosis-inducing factor: a matter of neuron life and death. *Progress in neurobiology* 2007; **81**(3)**:** 179-96.

329. Beal MF. Mitochondria, free radicals, and neurodegeneration. *Current opinion in neurobiology* 1996; **6**(5)**:** 661-6.

330. Andreyev AY, Kushnareva YE, Starkov AA. Mitochondrial metabolism of reactive oxygen species. *Biochemistry* 2005; **70**(2)**:** 200-14.

331. Halliwell B. Reactive oxygen species and the central nervous system. *Journal of neurochemistry* 1992; **59**(5)**:** 1609-23.

332. Kaushal V, Schlichter LC. Mechanisms of microglia-mediated neurotoxicity in a new model of the stroke penumbra. *The Journal of neuroscience* 2008; **28**(9)**:** 2221-30.

333. Babior BM. The NADPH oxidase of endothelial cells. *IUBMB Life* 2000; **50**(4-5)**:** 267-9.

334. Yokoyama Y, Beckman JS, Beckman TK, Wheat JK, Cash TG, Freeman BA *et al.* Circulating xanthine oxidase: Potential mediator of ischemic injury. *American journal of physiology. Gastrointestinal and liver physiology* 1990; **258**(4 Pt 1)**:** G564-70.

335. Dijkstra G, Moshage H, Van Dullemen HM, De Jager-Krikken A, Tiebosch ATMG, Kleibeuker JH *et al.* Expression of nitric oxide synthases and formation of nitrotyrosine and reactive oxygen species in inflammatory bowel disease. *The Journal of pathology* 1998; **186**(4)**:** 416-21.

336. Valko M, Leibfritz D, Moncol J, Cronin MTD, Mazur M, Telser J. Free radicals and antioxidants in normal physiological functions and human disease. *International journal of biochemistry and cell biology* 2007; **39**(1)**:** 44-84.

337. Semenza GL. Targeting HIF-1 for cancer therapy. *Nature reviews. Cancer* 2003; **3**(10)**:** 721-32.

338. Correia SC, Moreira PI. Hypoxia-inducible factor 1: A new hope to counteract neurodegeneration? *Journal of neurochemistry* 2010; **112**(1)**:** 1-12.

339. Kamata H, Manabe T, Oka SI, Kamata K, Hirata H. Hydrogen peroxide activates IkappaB kinases through phosphorylation of serine residues in the activation loops. *FEBS Letters* 2002; **519**(1-3)**:** 231-7.

340. Vousden KH, Lane DP. p53 in health and disease. *Nature reviews. Molecular cell biology* 2007; **8**(4)**:** 275-83.

341. Bensaad K, Tsuruta A, Selak MA, Vidal MNC, Nakano K, Bartrons R *et al.* TIGAR, a p53-Inducible Regulator of Glycolysis and Apoptosis. *Cell* 2006; **126**(1)**:** 107-20.

342. Rego AC, Oliveira CR. Mitochondrial dysfunction and reactive oxygen species in excitotoxicity and apoptosis: implications for the pathogenesis of neurodegenerative diseases. *Neurochemical research* 2003; **28**(10)**:** 1563-74.

343. Yu DY, Cringle SJ. Oxygen distribution and consumption within the retina in vascularised and avascular retinas and in animal models of retinal disease. *Progress in retinal and eye research* 2001; **20**(2)**:** 175-208.

344. Munemasa Y, Kitaoka Y, Kuribayashi J, Ueno S. Modulation of mitochondria in the axon and soma of retinal ganglion cells in a rat glaucoma model. *Journal of neurochemistry* 2010; **115**(6)**:** 1508-19.

345. Abu-Amero KK, Morales J, Bosley TM. Mitochondrial abnormalities in patients with primary open-angle glaucoma. *Investigative ophthalmology & visual science* 2006; **47**(6)**:** 2533-41.

346. Barron MJ, Griffiths P, Turnbull DM, Bates D, Nichols P. The distributions of mitochondria and sodium channels reflect the specific energy requirements and conduction properties of the human optic nerve head. *The British journal of ophthalmology* 2004; **88**(2)**:** 286-90.

347. Carelli V, Ross-Cisneros FN, Sadun AA. Mitochondrial dysfunction as a cause of optic neuropathies. *Progress in retinal and eye research* 2004; **23**(1)**:** 53-89.

348. Chen H, Chan DC. Critical dependence of neurons on mitochondrial dynamics. *Current opinion in cell biology* 2006; **18**(4)**:** 453-9.

349. Baltan S, Inman DM, Danilov CA, Morrison RS, Calkins DJ, Horner PJ. Metabolic vulnerability disposes retinal ganglion cell axons to dysfunction in a model of glaucomatous degeneration. *The Journal of neuroscience* 2010; **30**(16)**:** 5644-52.

350. Wei YH, Lu CY, Lee HC, Pang CY, Ma YS. Oxidative damage and mutation to mitochondrial DNA and age-dependent decline of mitochondrial respiratory function. *Annals of the New York academy of sciences* 1998; **854:** 155-70.

351. Navarro A, Boveris A. The mitochondrial energy transduction system and the aging process. *American journal of physiology. Cell physiology* 2007; **292**(2)**:** C670-86.

352. Band LR, Hall CL, Richardson G, Jensen OE, Siggers JH, Foss AJ. Intracellular flow in optic nerve axons: a mechanism for cell death in glaucoma. *Investigative ophthalmology & visual science* 2009; **50**(8)**:** 3750-8.

353. Ju WK, Liu Q, Kim KY, Crowston JG, Lindsey JD, Agarwal N *et al.* Elevated hydrostatic pressure triggers mitochondrial fission and decreases cellular ATP in differentiated RGC-5 cells. *Investigative ophthalmology & visual science* 2007; **48**(5)**:** 2145-51.

354. Tezel G, Yang X. Caspase-independent component of retinal ganglion cell death, in vitro. *Investigative ophthalmology & visual science* 2004; **45**(11)**:** 4049-59.

355. Tezel G, Wax MB. Hypoxia-inducible factor 1alpha in the glaucomatous retina and optic nerve head. *Archives of ophthalmology* 2004; **122**(9)**:** 1348-56.

356. Bose S, Piltz JR, Breton ME. Nimodipine, a centrally active calcium antagonist, exerts a beneficial effect on contrast sensitivity in patients with normal-tension glaucoma and in control subjects. *Ophthalmology* 1995; **102**(8)**:** 1236-41.

357. Malcon C, Kaddurah-Daouk R, Beal MF. Neuroprotective effects of creatine administration against NMDA and malonate toxicity. *Brain research* 2000; **860**(1-2)**:** 195-8.

358. Adcock KH, Nedelcu J, Loenneker T, Martin E, Wallimann T, Wagner BP. Neuroprotection of creatine supplementation in neonatal rats with transient cerebral hypoxia-ischemia. *Developmental neuroscience* 2002; **24**(5)**:** 382-8.

359. Bender A, Beckers J, Schneider I, Holter SM, Haack T, Ruthsatz T. Creatine improves health and survival of mice. *Neurobiology of aging* 2008; **29**(9)**:** 1404-11.